

Design, Synthesis, and Biological Evaluation of a Series of Oxazolone Carboxamides as a Novel Class of Acid Ceramidase Inhibitors

Samantha Caputo,[¶] Simona Di Martino,[¶] Vincenzo Cilibrasi, Piero Tardia, Marco Mazzonna, Debora Russo, Ilaria Penna, Maria Summa, Sine Mandrup Bertozzi, Natalia Realini, Natasha Margaroli, Marco Migliore, Giuliana Ottonello, Min Liu, Peter Lansbury, Andrea Armirotti, Rosalia Bertorelli, Soumya S. Ray, Renato Skerlj,* and Rita Scarpelli*Cite This: *J. Med. Chem.* 2020, 63, 15821–15851

Read Online

ACCESS |



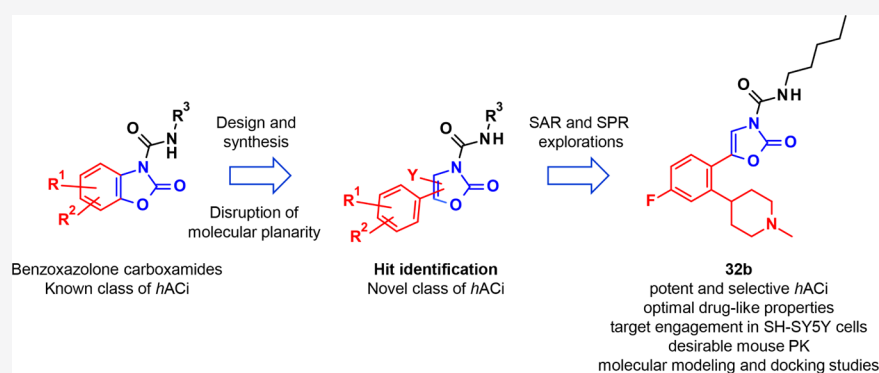
Metrics & More



Article Recommendations



Supporting Information



ABSTRACT: Acid ceramidase (AC) is a cysteine hydrolase that plays a crucial role in the metabolism of lysosomal ceramides, important members of the sphingolipid family, a diversified class of bioactive molecules that mediate many biological processes ranging from cell structural integrity, signaling, and cell proliferation to cell death. In the effort to expand the structural diversity of the existing collection of AC inhibitors, a novel class of substituted oxazol-2-one-3-carboxamides were designed and synthesized. Herein, we present the chemical optimization of our initial hits, 2-oxo-4-phenyl-*N*-(4-phenylbutyl)oxazole-3-carboxamide **8a** and 2-oxo-5-phenyl-*N*-(4-phenylbutyl)oxazole-3-carboxamide **12a**, which resulted in the identification of 5-[4-fluoro-2-(1-methyl-4-piperidyl)phenyl]-2-oxo-*N*-pentyl-oxazole-3-carboxamide **32b** as a potent AC inhibitor with optimal physicochemical and metabolic properties, showing target engagement in human neuroblastoma SH-SY5Y cells and a desirable pharmacokinetic profile in mice, following intravenous and oral administration. **32b** enriches the arsenal of promising lead compounds that may therefore act as useful pharmacological tools for investigating the potential therapeutic effects of AC inhibition in relevant sphingolipid-mediated disorders.

INTRODUCTION

Ceramides (Cer) and their metabolites are members of the sphingolipid (SL) family that play important roles as integral components of the eukaryotic cell membranes and signaling molecules in apoptosis, cell growth, differentiation, senescence, diabetes, insulin resistance, inflammation, neurodegenerative disorders, and atherosclerosis.^{1–4} The proper regulation of ceramide biosynthesis and metabolism is controlled by a complex, highly compartmentalized, and interconnected network of enzymatic pathways essential to maintaining the cellular homeostasis and development.¹ Although a detailed analysis of this complex network is beyond the scope of this paper, a simplified representation of the ceramide metabolism is shown in Figure 1. Cer are the centerpiece of the SL metabolism,

produced in response to stressful stimuli via two major pathways: the *de novo* pathway from serine and palmitoyl-CoA in the endoplasmic reticulum and the *salvage* pathway from the recycling of sphingosine (So), bypassing the formation of dihydroceramide. The generated Cer can be transported to distinct cellular compartments and further modified to more complex SLs, for example, glycosylated to hexosylceramides

Received: September 7, 2020

Published: December 8, 2020



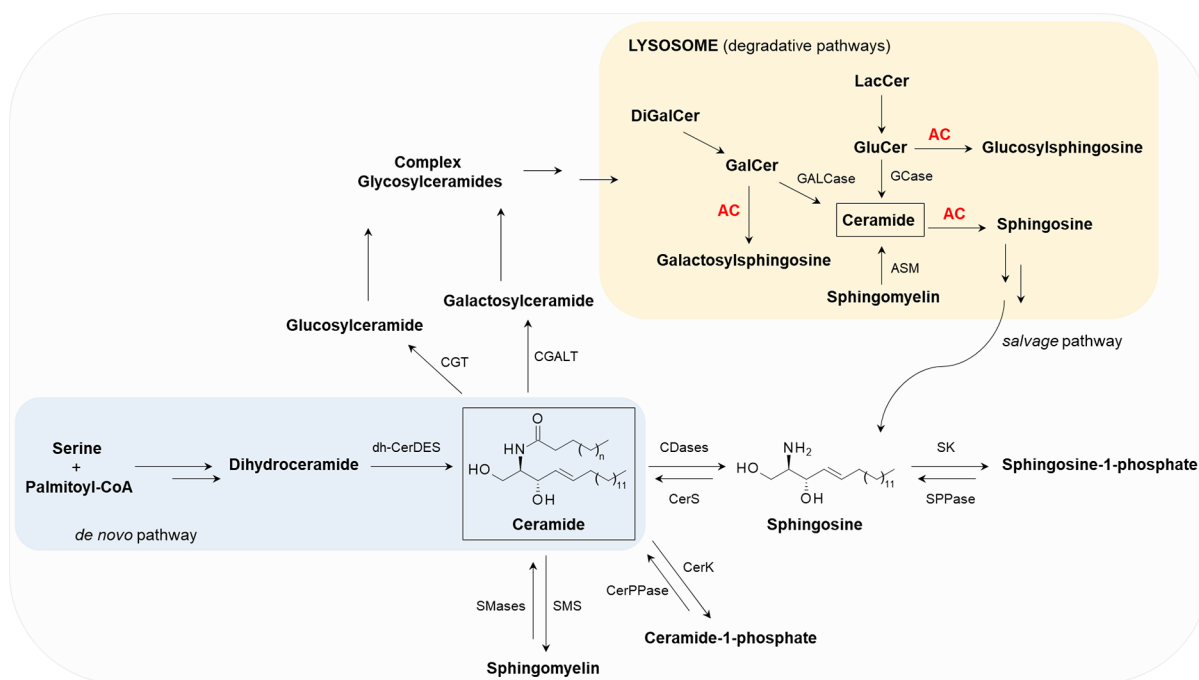


Figure 1. Overview of the ceramide metabolism and some related enzymes.

(HexCer) and, in turn, to more complex glycosylceramides; metabolized into sphingomyelin (SM) and ceramide-1-phosphate (Cer-1P); and catabolized to produce So, which is further phosphorylated to sphingosine-1-phosphate (So-1P). Cellular Cer can also be generated through *catabolic* pathways in distinct sub-cellular compartments. In the lysosomes, for example, SM and HexCer (glucosylceramide and galactosylceramide) participate in distinct degradative pathways that contribute to the formation of lysosomal Cer. In the same compartment, HexCer can be hydrolyzed through distinct pathways to generate the corresponding lysosomal glycosylsphingosines.⁵ Evidence to date suggests that imbalances in this complex network because of an altered expression and/or regulation of SL-modifying enzymes can lead to dysregulated cell signaling responses that contribute to the initiation and progression of several SL-related disorders.^{3,4} During the past years, aided by the impressive advances of the modern biological and analytical technologies, the scientific community has focused much attention on improving the understanding of the functional roles of some basic components of this metabolic network, under physiological and pathological conditions.⁶

Ceramidases (CDases) have attracted particular attention as key SL-metabolizing enzymes that regulate the levels and functions of different bioactive lipids, especially, Cer and So.⁷ Thus far, five human CDases (*h*CDase) have been identified, which can be characterized by their different optimal pH for catalytic activity and localization in cells: acid ceramidase (AC), neutral ceramidase (NC), alkaline ceramidase 1 (ACER1), alkaline ceramidase 2 (ACER2), and alkaline ceramidase 3 (ACER3).^{7,8} Because of differences in tissue distribution and expression level, cellular localization, optimum pH, and substrate specificity, these CDases appear to play distinct physiological roles in cellular responses.⁸ The overexpression of NC has been implicated in colon carcinogenesis⁹ and, therefore, it has emerged as a potential new therapeutic target for cancer therapy.¹⁰ Recent reports have shown the implication of ACER1 in keratinocyte differentiation^{11,12} and that of ACER2 in

programmed cell death in response to DNA damage.¹³ ACER3 has been reported to control both cell proliferation and apoptosis¹⁴ and to be involved in motor coordination-associated Purkinje cell degeneration.^{15,16} Despite these fundamental studies on the functional roles of NC and ACER1-3 in certain biological processes, further investigations are still on going to better clarify their implications in human diseases.⁸ By contrast, a growing body of evidence describes the important role of AC in the development and progression of different human pathological conditions, suggesting human AC (*h*AC) as a potential target for promising therapeutic applications. *h*AC (also known as *N*-acylsphingosine amidohydrolase-1, *ASA*H-1) is a lysosomal cysteine amidase that, at an optimal pH of 4.5, hydrolyzes Cer into So and fatty acids (Figure 1).^{17,18} Because the phosphorylation of So is the only pathway for the formation of So-1P, cellular So-1P is highly dependent on the availability of So; hence, *h*AC is a critical enzyme in regulating not only the hydrolysis of Cer but also the generation of both So and So-1P in cells. Cer and So-1P have opposing effects in the control of cell fate.¹⁹ While Cer favor cell-cycle arrest²⁰ and apoptosis,^{21,22} So-1P promotes angiogenesis, cell survival, and proliferation.^{23–26} Hence, the altered Cer/So balance determines the shifting of cell fate toward apoptosis and proliferation, respectively, and contributes to the pathogenesis of some human diseases. For example, various common diseases, including inflammation, pain, and several pulmonary disorders, have been associated with aberrant *h*AC activities.²⁷ *h*AC is also deficient in two rare inherited disorders: spinal muscular atrophy with myoclonic epilepsy and Farber's disease.²⁸ By contrast, collected evidence has shown that *h*AC is abnormally expressed in various types of human cancer, for example, prostate,²⁹ melanoma,³⁰ head and neck,³¹ colon,³² and glioblastoma.³³ It has been observed that the overexpression of *h*AC renders the cells more resistant to pharmacological induction of apoptosis.^{29,34} Therefore, the inhibition of *h*AC has been proposed as a potential strategy to enhance the therapeutic efficacy of standard antineoplastic agents and radiation.^{34,35} Relevant evidence has

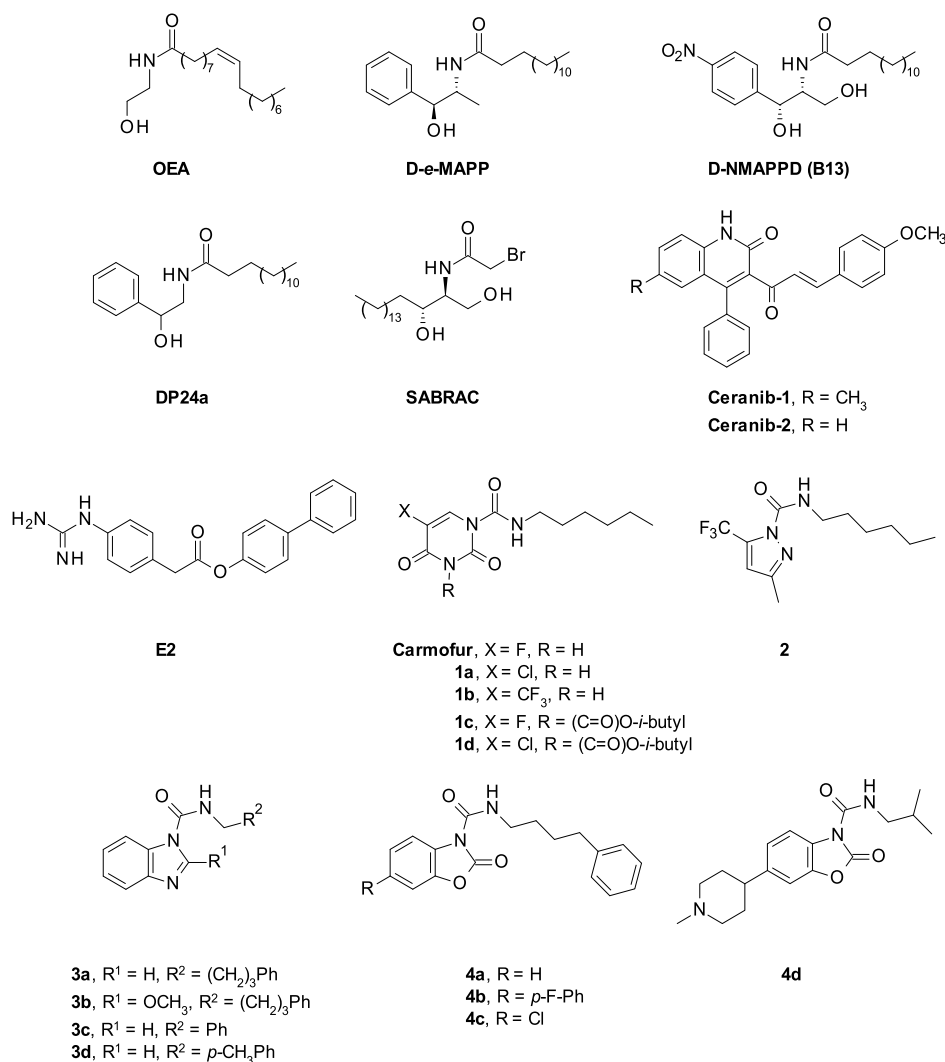


Figure 2. Representative known and structurally diversified AC inhibitors.

shown that Alzheimer's disease (AD) brains exhibit elevated level and activity of *hAC*, suggesting a potential role of AC in controlling neuronal apoptosis and in the molecular mechanism of AD.³⁶ Notably, recent reports are proposing the role of *hAC* inhibition as an emerging strategy for treating some types of rare inherited metabolic disorders called lysosomal storage diseases (LSDs),^{37–39} in particular, some severe neuropathic conditions related to Gaucher's⁴⁰ disease (GD) and Krabbe's⁴¹ disease (KD). GD and KD are caused by the defective functions of some specific lysosomal proteins, acid β -glucocerebrosidase (GCCase, β -glucosyl ceramidase) for GD and β -galactocerebrosidase (GALCase, β -galactosyl ceramidase) for KD. In GD patients, recent evidence suggests an active role of *hAC* in the catabolism of the lysosomal glucosylceramide, which is responsible for the accumulation of toxic glucosylsphingosine (Figure 1).⁴² In KD patients, deficiency of GALCase activity results in the buildup of the galactosylceramide and the galactosylsphingosine (psychosine) in nervous tissues, especially in the brain. Notably, a recent report suggests that genetic ablation or pharmacological inhibition of AC could eliminate the accumulation of the neurotoxic psychosine and prolong the life span of the KD mouse model.⁴³ There are no approved treatments for neuropathic GD and KD; targeting the inhibition of *hAC* may

provide an innovative approach for treating these severe diseases.

Although many efforts in the past decade have been made to identify new classes of *hAC* inhibitors, to date, these activities have resulted in limited success and a very limited number of suitable candidates for in vivo experiments are currently available. In a recent study, Gebai and co-workers reported the crystal structure analysis of mammalian AC (PDB code: 5U7Z),⁴⁴ which may assist future structure-guided drug discovery programs. First generation *hAC* inhibitors were designed on the basis of substrate (Cer)-based structures, for example, *N*-oleylethanolamine (OEA, median inhibitory concentration (IC₅₀) \sim 500 μ M,⁴⁵ Figure 2). Despite being the first Cer-mimicking inhibitor to be described, the ability of OEA to inhibit *hAC* was not always reproducible.^{45–47} Further representative examples are *D*-erithro-2-(*N*-myristoylamino)-1-phenyl-1-propanol (*D*-*e*-MAPP, IC₅₀ > 500 μ M in HL-60 cell lysates⁴⁵ and IC₅₀ = 500 μ M in HaCaT cell lysates,⁴⁸ Figure 2) and its more water soluble derivative *N*-NMAPPD (B13, IC₅₀ \sim 10 μ M in HaCaT cell lysates,⁴⁸ Figure 2). Efforts to ameliorate these Cer-mimicking molecules led to several structurally varied analogues of B13, as compounds DP24a (IC₅₀ = 1.287 μ M,⁴⁹ Figure 2) and the potent irreversible AC inhibitor SABRAC

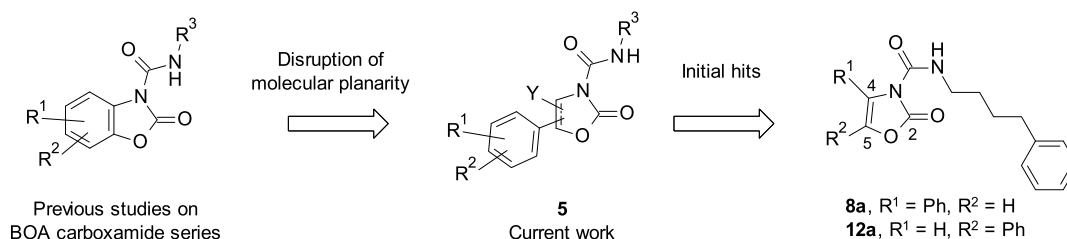
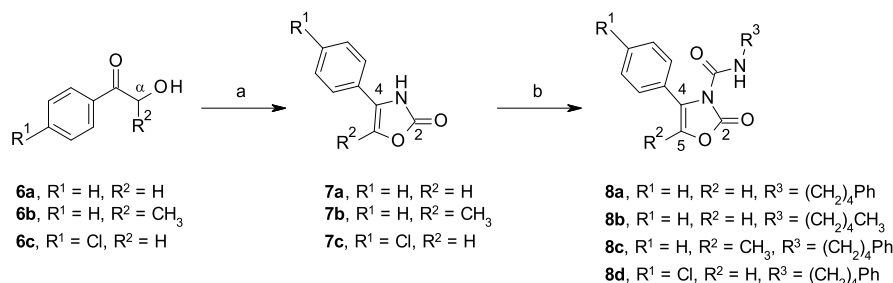


Figure 3. Rational design of the novel class of AC inhibitors and hit identification.

Scheme 1. Synthesis of 8a–d^a

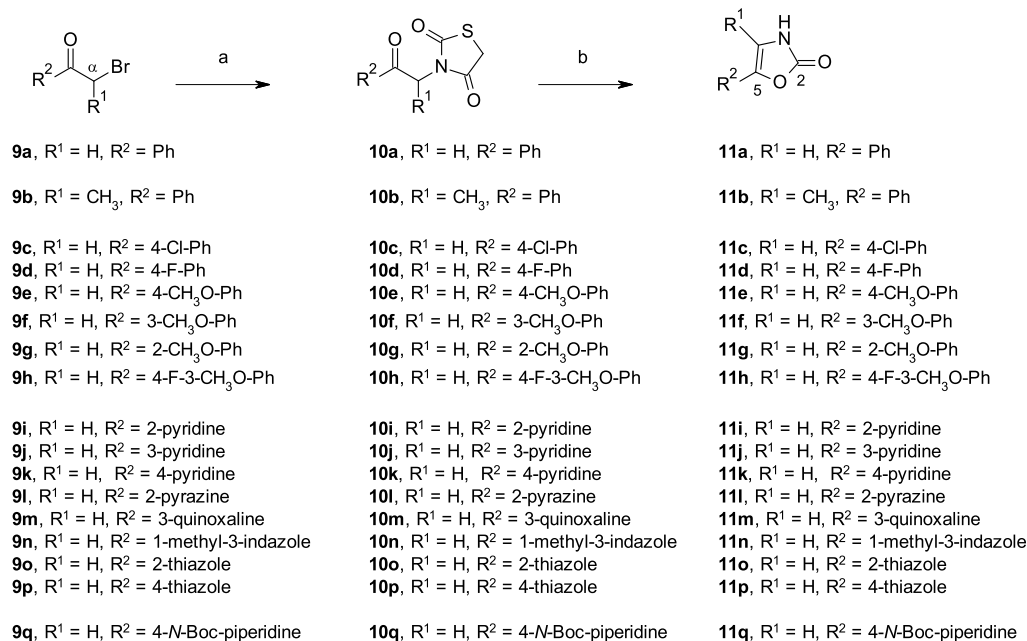


^aReagents and conditions: (a) KNCO, AcOH, and *i*-PrOH, 70 °C, 3 h (36–53%) and (b) RNCO and DMAP, CH₃CN, rt, 3–16 h (15–82%).

(IC₅₀ = 0.052 μM,^{50,51} Figure 2). By contrast, the quinolinone-based compounds, Ceranib-1 and its optimized analogue Ceranib-2, represent the first class of non-Cer-mimicking inhibitors of *h*CDase identified by Draper and co-workers by screening a chemical library (*h*CDase IC₅₀ = 55 μM and 28 μM in SKOV3 cells, respectively,⁵² Figure 2). In another study by Yildiz-Oze and co-workers, Ceranib-2 was found to inhibit *h*AC activity by 44% at 25 μM in H460 cells.⁵³ More recently, Cho and co-workers reported the identification of the hit compound [1,1'-biphenyl]-4-yl-2-(4-guanidinophenyl)acetate (E2, IC₅₀ = 52 μM,⁵⁴ Figure 2) from 68 guanidine-based derivatives tested for the discovery of new antiangiogenic inhibitors and determined the role of *h*AC as the E2-binding protein. Although a comparative analysis of the AC inhibitory activities of these different molecules is limited by the fact that the reported pharmacological data have been collected using different assay conditions and protein sources (Table S1),^{45–50,52–54} overall, these AC inhibitors are characterized by low inhibitory potency (as those with IC₅₀ values in the μM range)^{45–49,52–54} and poor drug-likeness (as those with, e.g., long lipophilic carbon chains).^{45–50}

A significant breakthrough was made by Realini and co-workers with the identification of carmofur [rat AC (*r*AC) IC₅₀ = 29 nM,⁵⁵ Figure 2 and Table S1] and some close uracil analogues, for example, compounds 1a–d, as nanomolar inhibitors of AC activity (1a, *r*AC IC₅₀ = 67 nM;⁵⁵ 1b, *r*AC IC₅₀ = 12 nM;⁵⁵ 1c, *r*AC IC₅₀ = 16 nM⁵⁶ and *h*AC IC₅₀ = 7.7 nM;³⁰ and 1d, *h*AC IC₅₀ = 12.8 nM,³⁰ Figure 2 and Table S1). Despite being potent AC inhibitors with some potential applications as chemo-sensitizing agents, the uracil derivatives showed low chemical and metabolic stability. Successively, using a ligand-based virtual screening approach, with carmofur as the template, Diamanti and co-workers identified a new class of potent *h*AC inhibitors, exemplified by the pyrazole carboxamide 2 (IC₅₀ = 14 nM,⁵⁷ Figure 2 and Table S1). However, these molecules exhibited low metabolic stability (2, mouse plasma half-life, *t*_{1/2} = 9 min),⁵⁷ limiting their therapeutic potential. Through a systematic computational investigation, Ortega and

co-workers reported the identification of benzimidazole derivatives 3a–d (3a, IC₅₀ = 2.5 nM; 3b, IC₅₀ = 13.9 nM; 3c, IC₅₀ = 22.5 nM; and 3d, IC₅₀ = 14.8 nM,⁵⁸ Figure 2 and Table S1) with promising AC inhibitory activity in different melanoma cell lines.⁵⁸ A screening campaign of a small compound library was exploited by Pizzirani and co-workers resulting in the identification of the benzoxazolone (abbreviated as BOA, hereafter) carboxamide series, exemplified by the initial hit 4a (IC₅₀ = 64 nM,⁵⁹ Figure 2 and Table S1).⁵⁹ Preliminary studies led to the more advanced and systematically active analogues 4b (IC₅₀ = 79 nM,⁵⁹ Figure 2 and Table S1) and 4c (IC₅₀ = 33 nM,⁶⁰ Figure 2 and Table S1).^{59,60} Although these molecules showed potent inhibitory effects on *h*AC activity, they generally suffered from low aqueous solubility and moderate metabolic stability, which impede their further development as oral drugs. During recent years, we directed the scope of our research work to solve these limitations. As part of our continued efforts in the optimization of the BOA carboxamide series, we recently reported the discovery of the piperidine 4d (IC₅₀ = 166 nM,⁶¹ Figure 2 and Table S1) as a lead compound with good oral bioavailability, excellent brain penetration, and target engagement in two animal models of neuropathic GD and KD.⁶¹ As an extension of this work while adopting a different strategy, we started an exploratory drug discovery program directed to the search for a novel class of *h*AC inhibitors with optimal drug-like properties, suitable for investigational studies in cellular and *in vivo* model systems. In the present study, we describe our strategies for the design and synthesis of a novel chemotype of *h*AC inhibitors (general structure, compound 5, Figure 3). The disruption of the molecular planarity of the fused bicyclic BOA moiety resulted in the identification of two initial hits, 2-oxo-4-phenyl-*N*-(4-phenylbutyl)oxazole-3-carboxamide 8a and 2-oxo-5-phenyl-*N*-(4-phenylbutyl)oxazole-3-carboxamide 12a (Figure 3). Herein, we present the structure–activity relationship (SAR) exploration of this novel series of substituted oxazol-2-one-3-carboxamides and the chemical optimization which resulted in the identification of 5-[4-fluoro-2-(1-methyl-4-piperidyl)-phenyl]-2-oxo-*N*-pentyl-oxazole-3-carboxamide 32b as a potent

Scheme 2. Synthesis of 11a–q^a

^aReagents and conditions: (a) TZD, K₂CO₃, and DMF, rt, 1–2 h. (b) LiOH and THF, rt, 30 min–1 h (6%–quant. over two steps for 11a, 11c–p) or *t*-BuOK and THF, rt, 30 min (for 11b and 11q; 10 and 38% over two steps; respectively).

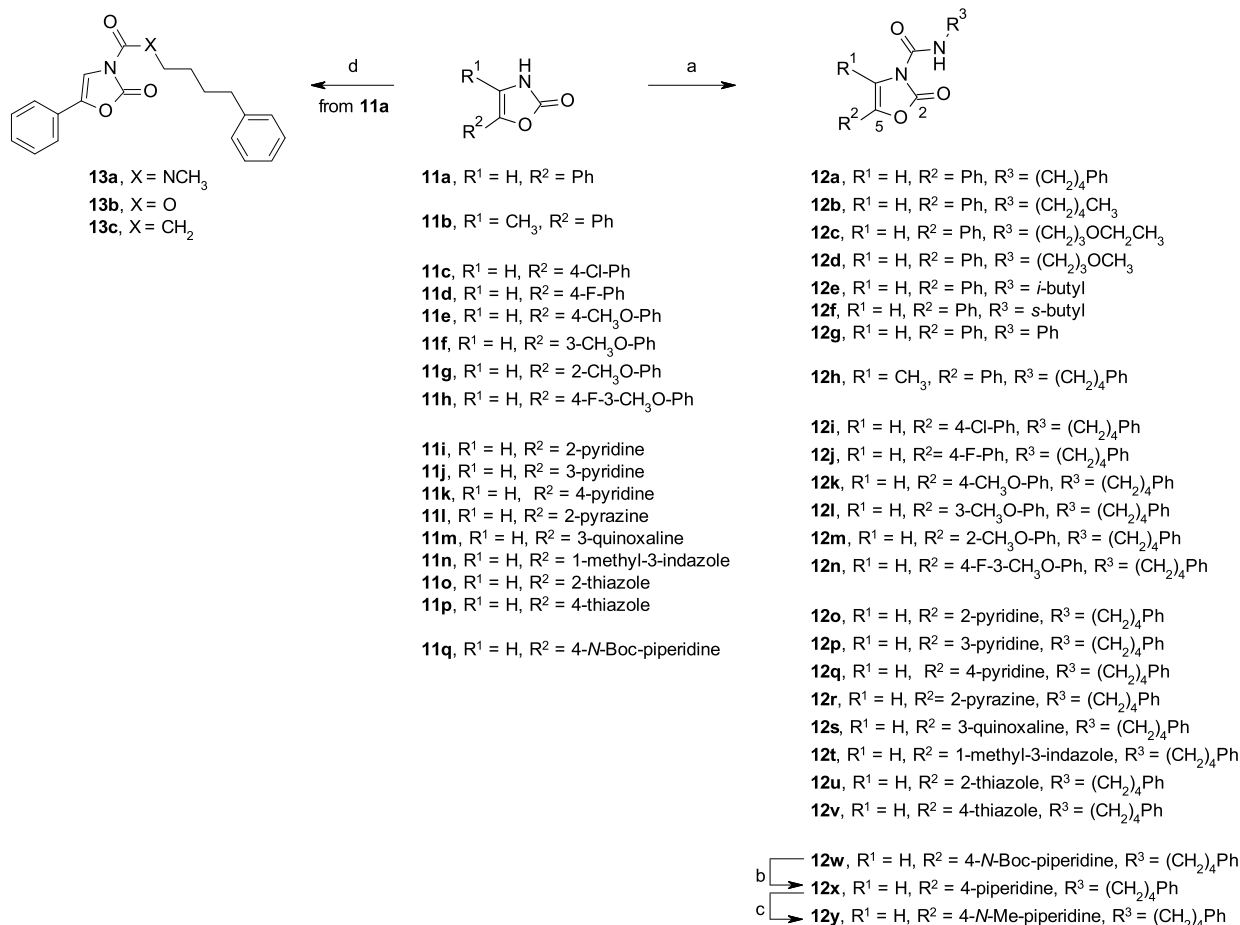
and drug-like *h*AC inhibitor—structurally differentiated from previously reported series.

CHEMISTRY

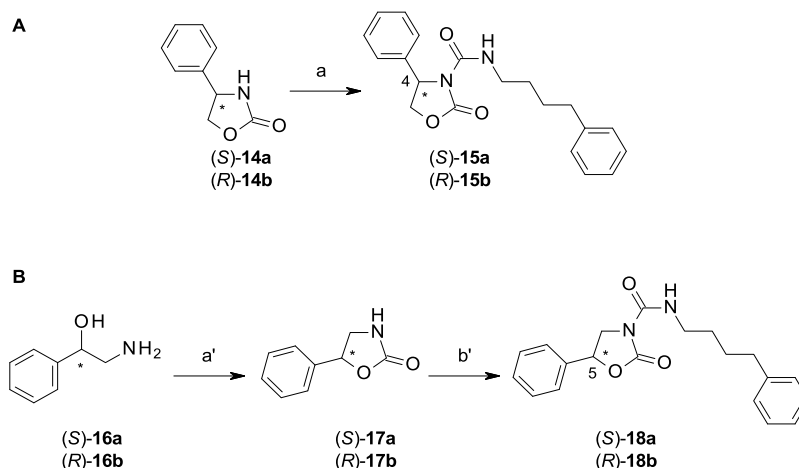
The synthetic routes for the preparation of all target compounds are described in Schemes 1–6. We introduced different substituents at the C(4)- and C(5)-positions of the 2-oxazolone core scaffold by exploring the synthetic pathways depicted in Schemes 1 and 2. The substituted 4-phenyl-oxazol-2-one derivatives 7a–c were obtained starting from the corresponding α -hydroxy ketones 6a–c, through the condensation reaction with potassium cyanate and in situ intramolecular cyclization under acidic conditions (Scheme 1).⁶² A series of substituted 5-phenyl- and 5-heteroaryl-oxazol-2-one derivatives 11a–q were synthesized starting from the commercially available α -bromo ketones 9a–q by condensation with 2,4-thiazolidinedione (TZD), followed by intramolecular cyclization of the intermediates 10a–q under basic conditions (LiOH or *t*-BuOK) (Scheme 2).⁶³ We introduced the carboxamide functionalities using standard conditions, by reacting intermediates 7a–c or 11a–q with the corresponding commercially available isocyanates, as in the synthesis of 8a–d (Scheme 1) or 12a–b, g–w (Scheme 3). Alternatively, the isocyanates were generated in situ, through the activation of the corresponding amines by reaction with Boc₂O in the presence of 4-(dimethylamino)-pyridine (DMAP)⁶⁴ (12c–d, Scheme 3) or by reaction with triphosgene in the presence of *N,N*-diisopropylethylamine (DIPEA) or Et₃N⁶⁵ (12e–f, Scheme 3). The *N*-methylated analogue 13a and the carbamate 13b were prepared upon the activation of 11a with triphosgene in the presence of DIPEA, followed by the addition of *N*-methyl-4-phenylbutylamine and 4-phenyl-1-butanol, respectively (Scheme 3). On the other hand, 11a was converted to the corresponding amide 13c by reaction with the corresponding freshly prepared 6-phenylhexanoic chloride. The oxazolidin-2-one analogues 15a–b were prepared starting from the

commercially available chiral (4*S*)-14a- and (4*R*)-14b-phenyl-oxazolidin-2-ones by carboxamide formation under standard conditions (Scheme 4A). A similar synthetic strategy was adopted for the preparation of analogues 18a–b upon the formation of the enantiomers (5*S*)-17a- and (5*R*)-17b-phenyl-oxazolidin-2-ones starting from the enantiomerically pure 2-amino-1-phenylethanol 16a–b via 1,1'-carbonyldiimidazole (CDI)-mediated intramolecular cyclization (Scheme 4B).

Similar procedures were exploited for the preparation of the targeted oxazolone carboxamides 25c–f and 32a–c, bearing a 4-methylpiperidine moiety at the C(3')- and C(2')-positions of the phenyl ring, respectively (Schemes 5 and 6). The methyl ketones 22a–b and 28 were prepared in two steps, starting from the corresponding bromophenyls 20a–b and 26, using Pd-catalyzed cross-coupling reactions, in the presence of the commercially available boronic pinacol ester 19, followed by hydrogenation in EtOH at 60 °C in the presence of 10% Pd/C and cyclohexene (as in the synthesis of 22a–b), or using Pd(OH)₂ and ammonium formate in MeOH at reflux (as in the synthesis of 28). The resulting methyl ketones 22a–b and 28 were transformed into the corresponding α -bromo ketones 22c–d and 29, through a slightly modified reported procedure,⁶⁶ consisting of an in situ addition of *N*-bromosuccinimide (NBS) to the corresponding silyl enol ethers in the presence of Et₃N at a controlled low temperature (Schemes 5 and 6). The α -bromo ketones 22c–d and 29 were directly reacted with TZD to afford the corresponding intermediates 23a–b and 30 and then converted, through an intramolecular cyclization, to the 2-oxazolones 24a–b and 31a, respectively, as described above. Standard reaction conditions were exploited to convert the piperidines 24b and 31a to the corresponding 4-methylpiperidines 24d and 31c, which involved *N*-Boc removal and reductive amination in the presence of NaBH(OAc)₃ and 37% aqueous solution of HCHO. Alternatively, as in the synthesis of 25c, these synthetic steps were performed on the corresponding carboxamide

Scheme 3. Synthesis of 12a–y and 13a–c^a

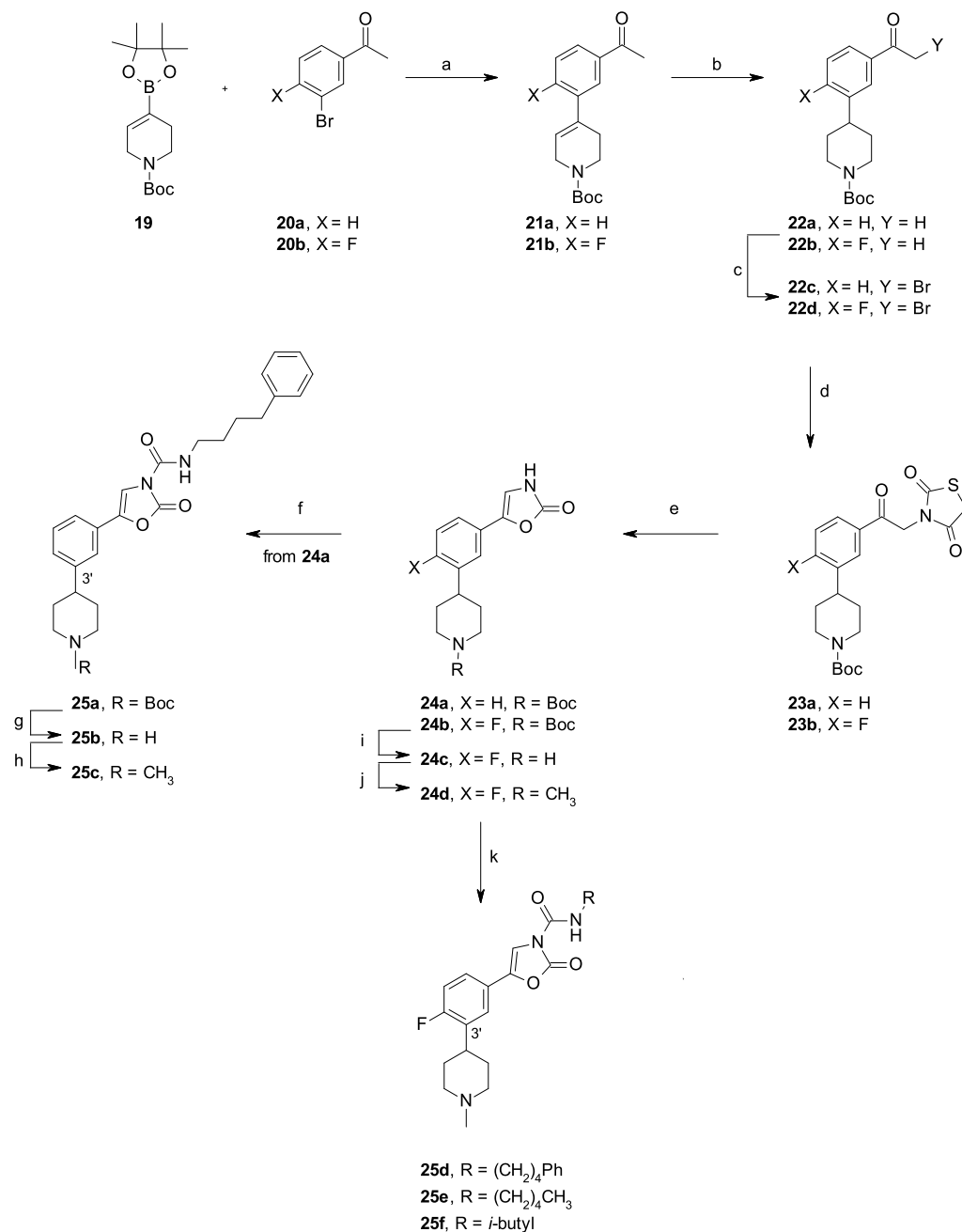
^aReagents and conditions: (a) RNCO and DMAP (10–83% for **12a–b, h–w**) or Et₃N (78% for **12g**) and CH₃CN, rt, 3–16 h or RNH₂, Boc₂O, DMAP and CH₃CN, rt, 1–3 h (48–80% for **12c–d**) or RNH₂, triphosgene, and DIPEA (76% for **12e**) or Et₃N (24% for **12f**) and DCM, rt, 3–12 h; (b) 4 M HCl, 1,4-dioxane, rt, 2 h; (c) HCHO, AcOH, NaBH(OAc)₃, and CH₃CN, rt, 1 h (34% over two steps); (d) for **13a**: *N*-methyl-4-phenylbutylamine, triphosgene, DIPEA, and DCM, 0 °C to rt, 3 h (98%); for **13b**: 4-phenyl-1-butanol, triphosgene, DIPEA, and DCM, 0 °C to rt, 3 h (53%); for **13c**: 6-phenylhexanoic acid, SOCl₂, and DCM, rt, 6 h; then **11a**, Et₃N and THF, 0 °C to rt, 16 h (55%).

Scheme 4. Synthesis of 15a–b and 18a–b^a

^aReagents and conditions: for the synthesis of **15a–b**: (a) 4-phenylbutyl isocyanate, DMAP, DMF, 50 °C, 2 h, (47–81%); for the synthesis of **18a–b**: (a') CDI, imidazole, DCM, rt, 16 h (86–92%); (b') 4-phenylbutyl isocyanate, DMAP, DMF, 50 °C, 4 h (68–79%).

derivative **25a**, obtained by reacting **24a** with 4-phenylbutyl isocyanate (Scheme 5). Finally, the carboxamide functionality of

the targeted compounds **25d–f** and **32a–c** was introduced using standard reaction conditions, as described above.

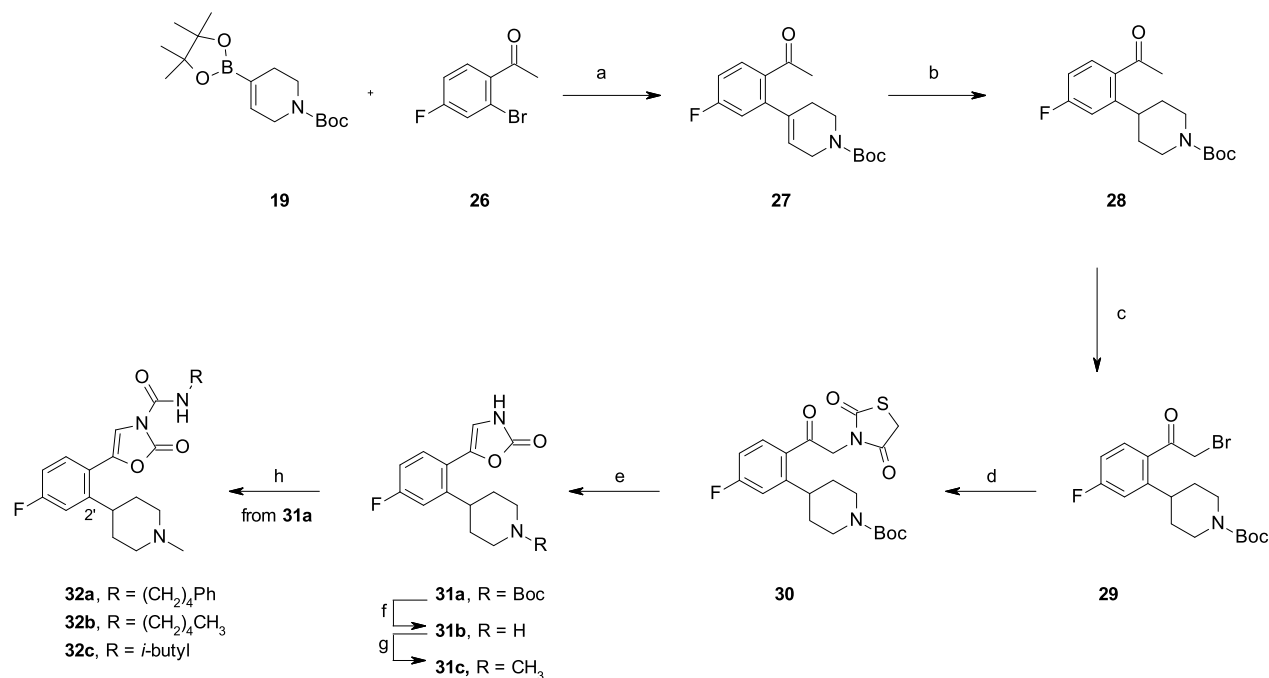
Scheme 5. Synthesis of 25c–f^a

^aReagents and conditions: (a) Pd(PPh₃)₄, 2 M Na₂CO₃, and 1,4-dioxane, reflux, 16 h (77–87%); (b) 10% Pd/C, cyclohexene, and EtOH, 60 °C, 24 h (65%); (c) TMSOTf, Et₃N, and THF, –78 to –50 °C, 4 h; then, NBS and THF, –40 to –20 °C, 30 min; (d) TZD, K₂CO₃, and DMF, rt, 1–2 h (93% over three steps for **23b**); (e) *t*-BuOK and THF, rt, 1 h (29% over 4 steps for **24a**) or LiOH and THF, rt, 30 min (72% for **24b**); (f) 4-phenylbutyl isocyanate, DMAP, and pyridine, rt, 16 h (69%); (g) 4 M HCl and 1,4-dioxane, rt, 2 h (46%); (h) HCHO, AcOH, NaBH(OAc)₃, and CH₃CN, rt, 1 h (60%) (i) 4 M HCl and 1,4-dioxane, rt, 2 h; (j) HCHO, AcOH, NaBH(OAc)₃, and CH₃CN, rt, 1 h (71% over two steps); and (k) RNCO, DMAP, and pyridine, rt, 16 h (25–36% for **25d–e**) or *i*-BuNH₂, triphosgene, Et₃N, and DCM, rt, 3 h (82% for **25f**).

RESULTS AND DISCUSSION

A common characteristic of some classes of known AC inhibitors is the presence of a cysteine (Cys)-targeting warhead as the α -bromo acetyl moiety or the urea-like functionality that can undergo a chemical reaction with the thiol group of the catalytic Cys143 of *h*AC to produce a covalent bond,⁴⁴ as reported for 2-bromoacetamide SABRAC⁵¹ and the carboxamides **3a–b**⁵⁸ and **4a**⁵⁹ (Figure 2). This evidence has been supported by recent studies, reported by Dementiev and co-

workers, on the crystal structure analysis of carmofur covalently bound to Cys143 at a 2.7 Å resolution.⁶⁷ While potent and, in certain cases, systemically active, for example, analogues **4b–c**,^{59,60} these potent *h*AC inhibitors share two characteristics that hamper their applications as oral drugs. First, the chemical warheads which, on the one hand, are responsible for the covalent binding mechanisms of these inhibitors and, on the other hand, can contribute to the poor chemical and plasma stability of these molecules (e.g., carmofur, **1a–d** and **2**);^{56,57} second, the hydrophobic linear side-chains, although funda-

Scheme 6. Synthesis of 32a–c^a

^aReagents and conditions: (a) Pd(PPh₃)₄, 2 M Na₂CO₃, and 1,4-dioxane, reflux, 16 h (85%); (b) HCO₂NH₄, 20% Pd(OH)₂, and MeOH, 60 °C, 4 h (69%); (c) TMSOTf, Et₃N, and THF, –78 to –50 °C, 4 h; then, NBS and THF, –40 to –20 °C, 30 min; (d) TZD, K₂CO₃, and DMF, rt, 2 h (66% over three steps); (e) *t*-BuOK and THF, rt, 30 min (67%); (f) 4 M HCl and 1,4-dioxane, rt, 2 h; (g) HCHO, AcOH, NaBH(OAc)₃, and CH₃CN, rt, 1 h and (h) RNCO, DMAP, and pyridine, rt, 16 h (62% for **32a**; 64% for **32b**) or *i*-BuNH₂, triphosgene, Et₃N, and DCM, rt, 3 h (20% for **32c**).

mental for target recognition and some degree of specificity, negatively affect the drug-like properties of these molecules (e.g., SABRAC and **4a**).^{51,59} Thus, there is a strong need for novel and optimized *h*AC inhibitors. In this respect, our continued efforts dedicated to the chemical optimization of the BOA carboxamide series, exemplified by **4a–c**,^{59,60} have recently led to the identification of the lead **4d** as a potent and orally bioavailable *h*AC inhibitor with excellent brain penetration in mice and target engagement in two animal models of LSDs (Figure 2).⁶¹ As part of our more exploratory research program, our medicinal chemistry strategies were also focused on expanding the chemical diversity of the existing *h*AC inhibitors for the identification of new chemotypes with optimal physicochemical and metabolic properties suitable for cellular and in vivo studies. In this regard, by the disruption of the molecular planarity of the fused bicyclic aromatic BOA system, we designed a series of compounds with the general structure **5** and synthesized a few initial molecules, for example, the 2-oxo-4-phenyl-*N*-(4-phenylbutyl)oxazole-3-carboxamide **8a** and 2-oxo-5-phenyl-*N*-(4-phenylbutyl)oxazole-3-carboxamide **12a** (Figure 3). In particular, we were interested in studying the substituted-oxazolone ring system as a potential and attractive strategy for the BOA bioisosteric replacement. In addition, we envisaged that the insertion of this relatively unexplored heterocycle system, by reducing the molecular planarity of the core scaffold and, therefore, varying the nature of the leaving group at the reactive electrophilic functionality, might be a valuable strategy for the subsequent optimization of our targeted molecules.⁶⁸ By contrast, in order to somehow preserve the *h*AC recognition, we initially designed scaffolds that bear a lipophilic group on the lateral chain of the urea-like functionality, as the butyl phenyl group of **8a** and **12a**, already described in other series of known

inhibitors (e.g., **3a–b** and **4a–c**, Figure 1) to be suitable for chemical optimization. Compounds **8a** and **12a** were screened against *h*AC using a fluorogenic assay and were able to inhibit the enzymatic activity with IC₅₀ values equal to 0.007 and 0.090 μM, respectively (Table 1). These initial results encouraged us to start a preliminary SAR exploration around these new scaffolds in the three main Regions A, B, and C, as depicted in Figure 4, with the objective of identifying the pharmacophore necessary for target inhibition.

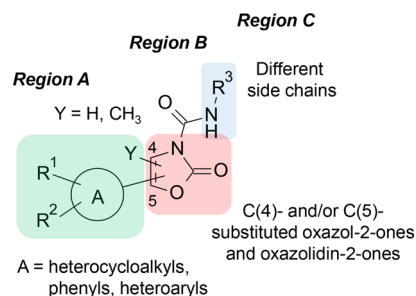
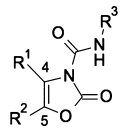


Figure 4. Planned SAR exploration.

In this regard, to first validate our initial hits, we prepared a set of representative analogues around the 4-phenyl-oxazol-2-one (4-POA) and 5-phenyl-oxazol-2-one (5-POA) carboxamide compounds **8a** and **12a** (Table 1). Interestingly, in the 4-POA carboxamide series, although a slight drop in potency was detected with the removal of the terminal aromatic ring, as in the *n*-pentyl analogue **8b** (*h*AC IC₅₀ = 0.025 μM), the insertion of a Cl atom at the *para* phenyl position was tolerated, with compound **8d** (*h*AC IC₅₀ = 0.005 μM) being equipotent to the

Table 1. Inhibitory Potencies of Compounds **8a–d** and **12a–n** and **12y** on the Activity of *hAC*



Compound	R ¹	R ²	R ³	<i>hAC</i> IC ₅₀ (μM)±SD ^{a, b}
8a		H		0.007 ± 0.001
8b		H		0.025 ± 0.001
8c		CH ₃		0.042 ± 0.010
8d		H		0.005 ± 0.0002
12a	H			0.090 ± 0.048
12b	H			0.039 ± 0.013
12c	H			2.04 ± 0.540
12d	H			53% inh at 10μM
12e	H			1.70 ± 0.202
12f	H			21% inh at 10μM ^c
12g	H			20% inh. at 5μM
12h	CH ₃			0.069 ± 0.001
12i	H			0.083 ± 0.003
12j	H			0.185 ± 0.070
12k	H			0.400 ± 0.019
12l	H			0.341 ± 0.006
12m	H			0.177 ± 0.092
12n	H			0.080 ± 0.003
12y	H			1.40 ± 0.094

^aIC₅₀ values are the mean of at least three independent experiments performed in three technical replicates. ^bIC₅₀ values were not determined for compounds showing less than 50% inhibition at concentrations of 10 μM for *hAC*. ^cPartial degradation was observed in the 10 mM DMSO solution.

parent **8a** (*hAC* IC₅₀ = 0.007 μM) (Table 1). In contrast, the insertion of a methyl group on the C(5)-position of the oxazolone ring, as in the di-substituted analogue **8c**, resulted in a 6-fold loss of potency (*hAC* IC₅₀ = 0.042 μM). A slightly different trend was observed in the 5-POA carboxamide series; the removal of the terminal phenyl ring, as in the *n*-pentyl analogue **12b** (*hAC* IC₅₀ = 0.039 μM), resulted in a weak improvement in potency compared to the parent compound **12a** (*hAC* IC₅₀ = 0.090 μM). Both the insertion of a Cl atom at the *para* phenyl position, as in **12i**, and the insertion of a methyl group at the C(4)-position of the oxazolone ring, as in **12h**, afforded analogues (*hAC* IC₅₀ = 0.083 and 0.069 μM, respectively) with similar potency compared to **12a** (Table 1).

These encouraging preliminary results confirmed that both the 4- and 5-(POA) carboxamide series were promising scaffolds and warranted further exploration. Nevertheless, a head-to-head comparison of the two hit series directed future investigations toward the 5-POA carboxamide series. Specifically, although being very potent *hAC* inhibitors, the 4-POA carboxamide series suffered from significantly poorer chemical stability compared to the 5-POA carboxamide series, as measured by performing the stability assay in aqueous media [**8a**, *t*_{1/2} = 10 min, in phosphate buffered saline (PBS), pH 7.4; **12a**, *t*_{1/2} = >12 h, in PBS, pH 7.4].

First, we demonstrated the importance of the reactive carboxamide functionality of **12a** because the corresponding unsubstituted analogue **11a** was not active against *hAC* at the concentrations tested (Scheme 3 and Figure 5A), suggesting that inhibition by **12a** could occur through covalent AC modification. Preliminary kinetic studies on *hAC*-enriched lysates showed that **12a** causes a concentration-dependent reduction in the maximal catalytic velocity of AC (*V*_{max}) without

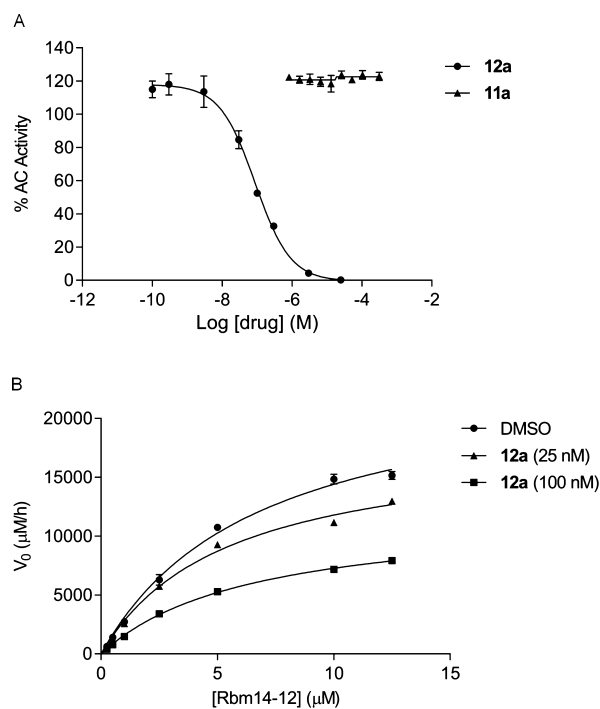
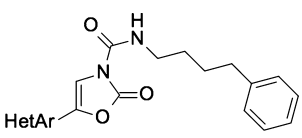
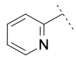
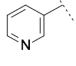
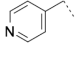
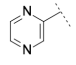
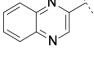
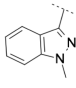
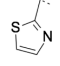
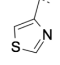


Figure 5. (A) Concentration–response curve for the inhibition of *hAC* activity by **11a** and **12a**; (B) Michaelis–Menten analysis of the reaction of *hAC* in the presence of vehicle (DMSO 1%, ●) or **12a** (25 nM, ▲; 100 nM, ■). Rbm14-12: fluorogenic substrate of *hAC*. The graph is representative of two independent experiments, each performed in three technical replicates.

Table 2. Inhibitory Potencies of Compounds 12o–v on the Activity of hAC


Compound	HetAr	hAC IC ₅₀ (μM)±SD ^a
12o		0.025 ± 0.001
12p		0.070 ± 0.017
12q		0.018 ± 0.009
12r		0.032 ± 0.011
12s		0.037 ± 0.018
12t		0.092 ± 0.060
12u		0.059 ± 0.001
12v		0.044 ± 0.012

^aIC₅₀ values are the mean of at least three independent experiments performed in three technical replicates.

Table 3. Aqueous Kinetic Solubility and In Vitro Metabolism of Some Selected Compounds

compound	solubility (μM) ^a (PBS, pH 7.4)	<i>m</i> -plasma ^b <i>t</i> _{1/2} (min) [% at 120 min]	<i>m</i> -LM ^c <i>t</i> _{1/2} (min) [% at 60 min]
12a	<1	<5	40
12b	<1	>120 [60%]	<5
12c	20	80	<5
12e	<1	>120 [70%]	50
12j	<1	90	60
12l	<1	>120 [64%]	30
12n	<1	>120 [64%]	>60 [74%]
12o	<1	40	10
12p	<1	60	>60 [55%]
12q	<1	30	>60 [75%]
12r	<1	40	60

^aAqueous kinetic solubility in PBS. ^bMouse plasma. ^cMouse liver microsomes. ^{a,b,c}Values are reported as the mean of at least two independent experiments performed in two technical replicates.

influencing the Michaelis–Menten constant (*K_M*) (Figure S5B and Table S2) supporting irreversible binding. In addition, the

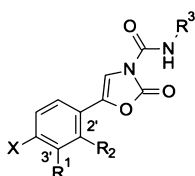
replacement of the *N*–H of the urea-like functionality of 12a with a *N*–Me (13a), with an oxygen (13b) or with a methylene (13c) were detrimental to activity (Scheme 3), as these analogues were not active against hAC at the concentrations tested (1 and 10 μM). Moreover, we demonstrated that the presence of the oxazol-2-one ring of 12a was essential to maintaining inhibitory potency, since the corresponding chiral 1,3-oxazolidinone carboxamide analogues 18a–b were not active against hAC at the concentrations tested (1 and 10 μM) (Scheme 3). A similar outcome was also observed with the chiral 1,3-oxazolidinone carboxamide analogues of the more potent 8a, compounds 15a–b (Scheme 3).⁵⁷

Therefore, based on these results, we continued with a more focused SAR exploration, by targeting additional analogues bearing small linear and branched alkyl substituents on the side-chain at the *N*-terminal urea moiety of 12a series (Region C, Figure 4). Replacement of one methylene unit with an oxygen in the *n*-pentyl chain of 12b (as ethers 12c–d) significantly affected the inhibitory potency; specifically, 12c showed an hAC IC₅₀ = 2.04 μM, while a complete loss in potency was observed for 12d (Table 1). These results suggested that the lipophilic side-chains at region C were very likely occupying a hydrophobic channel of the enzyme. Our SAR exploration continued with the insertion of branched alkyl groups, the *i*-butyl 12e inhibited AC with an IC₅₀ of 1.70 μM, while the *s*-butyl analogue 12f was not active up to 10 μM. No improvement was also observed with the aryl urea 12g.

In parallel, our medicinal chemistry efforts were also focused on the exploration of region A by introducing different substituents on the phenyl ring of the 12a series. Besides, the *p*-Cl atom of 12i, both electron-withdrawing (F) and electron-donating (OCH₃) groups at different positions of the phenyl ring were tolerated, resulting in compounds, such as 12j (*p*-F) and 12k–m (*p*-, *m*- and *o*-OCH₃), with hAC IC₅₀ values in the submicromolar ranges (Table 1). In addition, the di-substituted derivative 12n (*p*-F, *m*-OCH₃) was almost equipotent (hAC IC₅₀ = 0.080 μM) to 12a.

With these results in hand, we explored the replacement of the substituted phenyl rings at the C(5)-position of the oxazol-2-one moiety with a series of heteroaryl groups by preparing compounds 12o–v (Table 2). Different 5- and 6-membered-, 6 + 5-, and 6 + 6-fused heteroaryl groups were introduced on Region A. Interestingly, we identified potent AC inhibitors, for example, the 2- and 4-pyridyl analogues 12o and 12q, showing hAC IC₅₀ = 0.025 and 0.018 μM, respectively; whereas, the 3-pyridyl isomer 12p (hAC IC₅₀ = 0.070 μM) was almost equipotent to 12a (Table 2). A similar improvement of inhibitory potency was also observed with other nitrogen containing heteroaryl derivatives, for example, the pyrazine (12r) and quinoxaline (12s) analogues (hAC IC₅₀ = 0.032 and 0.037 μM, respectively). On the other hand, while the thiazole isomers 12u and 12v showed a moderately improved inhibitory activity (hAC IC₅₀ = 0.059 and 0.044 μM, respectively), the 1-methylindazole 12t (hAC IC₅₀ = 0.092 μM) was equipotent to the parent 12a.

A comparison of several of these analogues in terms of aqueous kinetic solubility (PBS, pH 7.4) and in vitro metabolism (*t*_{1/2} in mouse plasma and mouse liver microsomes) underlined some important differences (Table 3), which informed the next steps of the SAR exploration. In general, these compounds showed poor aqueous solubility, which was not ameliorated by the removal of the terminal lipophilic phenyl group (e.g., *n*-pentyl analogue 12b), or by the introduction of more polar

Table 4. Inhibitory Potencies of Compounds 25c–f and 32a–c on the Activity of *hAC*

Compound	X	R ¹	R ²	R ³	<i>hAC</i> IC ₅₀ (μM) ± SD ^a
25c	H		H		0.153 ± 0.066
25d	F		H		0.341 ± 0.050
25e	F		H		1.923 ± 0.531
25f	F		H		26% inh at 10 μM ^b
32a	F	H			0.337 ± 0.074
32b	F	H			0.129 ± 0.026
32c	F	H			38% inh at 10 μM ^b

^aIC₅₀ values are the mean of at least three independent experiments performed in three technical replicates. ^bIC₅₀ values were not determined for compounds showing less than 50% inhibition at concentrations of 10 μM for *hAC*.

Table 5. Aqueous Kinetic Solubility and In Vitro Metabolism of Some Selected Compounds

compound	solubility (μM) ^a (PBS, pH 7.4)	<i>m</i> -plasma ^b <i>t</i> _{1/2} (min) [% at 120 min]	<i>m</i> -LM ^c <i>t</i> _{1/2} (min) [% at 60 min]
25c	70	>120 [73%]	30
25d	30	>120 [80%]	>60 [70%]
32a	60	>120 [54%]	>60 [51%]
32b	>250	110	>60 [74%]

^aAqueous kinetic solubility in PBS. ^bMouse plasma. ^cMouse liver microsomes. ^{a,b,c}Values are reported as the mean of at least two independent experiments performed in two technical replicates.

groups, such as an oxygen atom on the lateral chain (**12c**) or heteroaryl rings at the C(5)-position of the oxazol-2-one moiety (e.g., the pyridines **12o–q** and the pyrazine **12r**) (Table 3). On the contrary, more pronounced differences were observed by comparing the mouse plasma and mouse liver microsomal stability properties of these analogues. In general, except for the parent **12a** and the heteroaryls **12o** and **12q–r**, the selected compounds showed good mouse plasma stability. In contrast, poor mouse microsomal stabilities were observed within the phenyl derivatives, except when a F-atom was inserted in the phenyl ring, for example, *p*-F analogues **12j** (*m*-liver microsomal *t*_{1/2} = 60 min) and **12n** (*m*-liver microsomal *t*_{1/2} > 60 min, 74% compound remaining at 1 h). An improvement of the mouse

microsomal stability was also detected with the *i*-butyl analogue **12e** (*m*-liver microsomal *t*_{1/2} = 50 min). A similar effect of the F-atom was shown by some nitrogen containing heteroaryl analogues, bearing an “aza”-group in the phenyl ring, for example, the 4-pyridyl **12q** (*m*-liver microsomal *t*_{1/2} > 60 min, 75% compound remaining at 1 h) and the pyrazine **12r** (*m*-liver microsomal *t*_{1/2} = 60 min) (Table 3).

Based on these results, we continued the SAR exploration by modifying the scaffold with the insertion of some potential solubilizing groups. We specifically focused our attention on regions A and B due to the fact that, as mentioned above, our SAR study suggested region C to be more involved in lipophilic interactions with *hAC* (Table 1). In this respect, our preliminary exploration of this series showed that the insertion of an hydrophilic group, such as the *N*-methyl-piperidine ring at the C(5)-position of the oxazol-2-one moiety (**12y**, Table 1), although detrimental for the inhibitory potency (*hAC* IC₅₀ = 1.40 μM), was essential for significantly improving the aqueous solubility (**12y**, kinetic solubility = 248 μM). As a consequence, we decided to investigate the effect of inserting the *N*-methyl-piperidine group directly at the C(3')-position of the phenyl ring of the 5-POA carboxamide series by preparing analogues **25c** and **25d** (Table 4). Although a similar decrease in potency (*hAC* IC₅₀ = 0.153 and 0.341 μM, respectively) was observed compared to the corresponding parent compounds **12a** and **12j**, we were pleased to notice that, overall, these structural modifications were tolerated. Moreover, a similar trend was observed when the *N*-methyl-piperidine ring was moved to the C(2')-position of the phenyl ring, with **32a** (*hAC* IC₅₀ = 0.337 μM) being equipotent to **25d**. Notably, we observed that these targeted compounds showed moderately improved solubility (kinetic solubility > 30 μM, Table 5) compared to the parent compounds **12a** and **12j**.

These results prompted us to continue a more focused SAR study on the lateral chains of **25d** and **32a** scaffolds, selecting the optimal moieties previously identified in the exploration of region C (Tables 1 and 3) and, hence, synthesizing the corresponding *n*-pentyl analogues **25e** and **32b** and the *i*-butyl analogues **25f** and **32c**. Although, a complete loss in potency was observed with both *i*-butyl analogues **25f** and **32c**, the *n*-pentyl derivatives **25e** and **32b** gave unexpected results. While **25e** showed a *hAC* IC₅₀ of 1.9 μM, surprisingly, compound **32b** inhibited *hAC* with an IC₅₀ equal to 0.129 μM. In addition, compound **32b**, bearing both the *N*-methyl piperidine ring and the small linear alkyl chain, showed a high solubility value (kinetic solubility > 250 μM) (Table 5). Finally, the most promising compounds were evaluated for in vitro metabolism (Table 5). In general, we were pleased to observe that the selected compounds exhibited good mouse plasma stabilities with *t*_{1/2} values ≥ 2 h. On the other hand, the poor mouse liver microsomal stability observed for **25c** was ameliorated by the insertion of a F-atom at the *para*-position of the phenyl ring (**25d**, *m*-liver microsomal *t*_{1/2} > 60 min, 70% compound remaining at 1 h). A similar trend was observed with the other fluorinated analogues, compound **32a–b**. Furthermore, additional in vitro metabolism studies were performed on **32b** which showed acceptable *h*-plasma (*t*_{1/2} = 40 min) and good *h*-liver microsomal stability (*t*_{1/2} > 60 min, 80% compound remaining at 1 h).

Based on its inhibitory potency and good overall drug-like properties, compound **32b** was selected for further biological and pharmacological characterizations. As previously anticipated for the initial hit **12a** and based on our previous work with

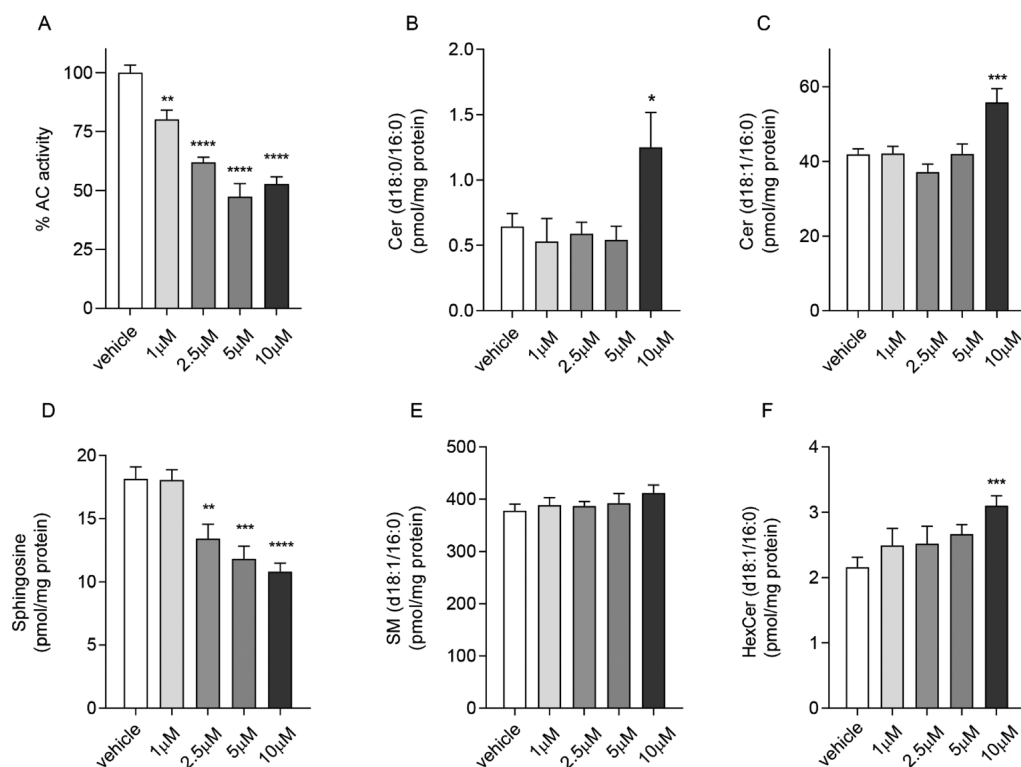


Figure 6. Concentration dependence of the effects of 32b in SH-SY5Y cells on *hAC* activity after a 3 h incubation (A) and SL levels (B–F). GraphPad Prism software (GraphPad Software, Inc., USA) was used for statistical analysis. Data were analyzed using the Student *t*-test or 1-way ANOVA followed by the Bonferroni post hoc test for multiple comparisons. Differences between groups were considered statistically significant at values of $p < 0.05$. Values are expressed as means SEM of at least six determinations. Experiments were repeated twice with similar results.

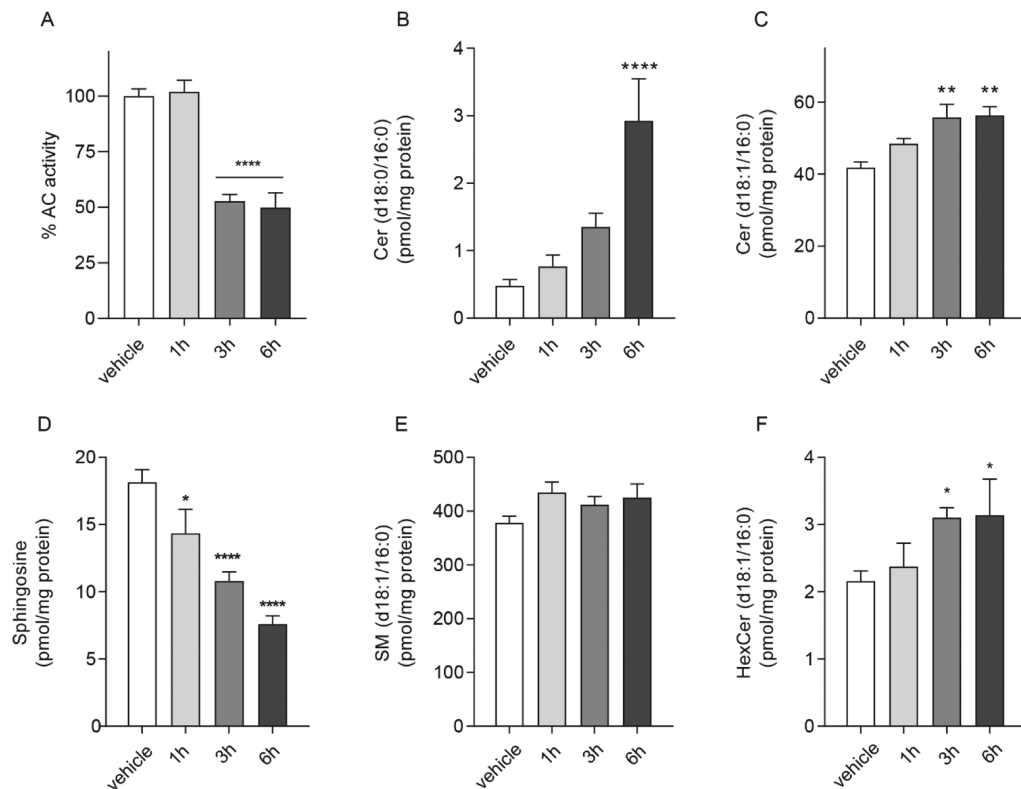


Figure 7. Time course of the effects of 32b (10 μM) in SH-SY5Y cells on *hAC* activity (A) and SL levels (B–F). GraphPad Prism software (GraphPad Software, Inc., USA) was used for statistical analysis. Data were analyzed using the Student *t*-test or 1-way ANOVA followed by the Bonferroni post hoc test for multiple comparisons. Differences between groups were considered statistically significant at values of $p < 0.05$. Values are expressed as means SEM of at least six determinations. Experiments were repeated twice with similar results.

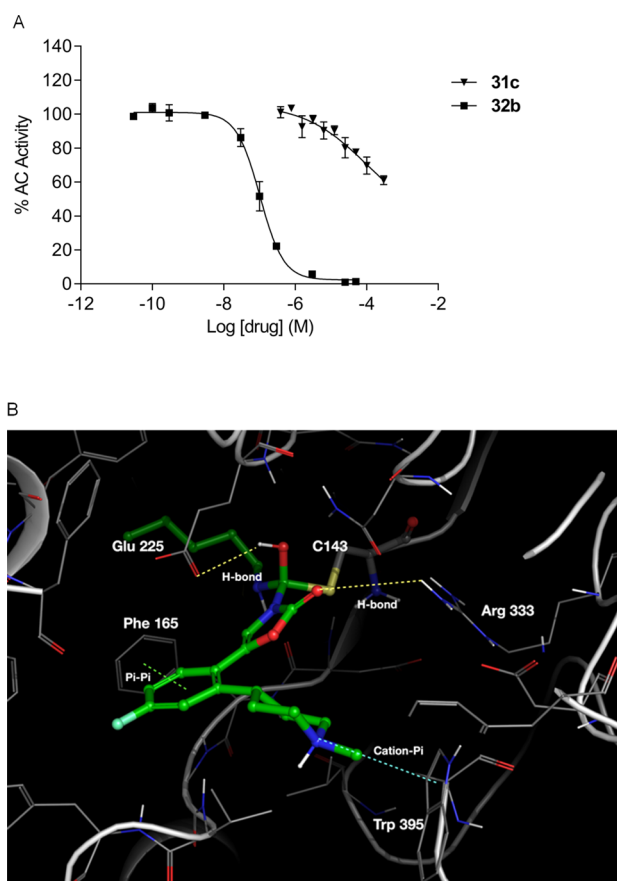


Figure 8. Concentration–response curve for the inhibition of *hAC* activity by **31c** and **32b** (A) and putative docking pose of compound **32b** in *hAC* (PDB code: 6MHM) (B).

4d,⁶¹ the mechanism of inhibition of **32b** occurs through covalent *hAC* modification. This was further supported by the corresponding analogue **31c**, lacking the reactive urea-like functionality of **32b**, which was not active against *hAC* (Figure 8A). Based on these considerations, we prioritized the selectivity evaluation of **32b** against human *N*-acylethanolamine acid amidase (*hNAAA*), a lysosomal cysteine amidase that shares 33–34% sequence identity and a very similar reactive site with *hAC*.⁶⁹ Notably, **32b** showed no effect at up to 125 μ M against *hNAAA* under our assay conditions. In an effort to gain insights

into the structural bases of these biological results, we then performed molecular modeling and docking studies using the X-ray crystal structures of *hAC* (PDB code: 6MHM)⁶⁷ and *hNAAA* (PDB code: 6DXX).⁶⁹ The protein (*hAC*)–ligand (targeted compound) binding site was prepared by adding hydrogen atoms, optimizing hydrogen bonds, and verifying the protonation states of His, Gln, and Asn. The energy minimization was carried out using a default constraint of 0.3 Å rmsd and OPLS 3e force field. The SiteMap tool was used to identify binding pockets of *hAC*. The docking calculation on the SAR series was carried out using Schrödinger covalent docking program CovDock. The docking procedure used the distance cutoffs (8 Å *C β* to the ligand, 5 Å to the ligand reactive carbonyl group) to decide if the covalent reaction can indeed happen or a molecule pose should be kept for further consideration. Cys143 was used as the reactive nucleophile in the calculations. While under experimental conditions, the leaving group would in fact cleave from the molecule and only a part of the molecule would remain attached to Cys143; the docking calculation actually captures the binding pose quality of the tetrahedral intermediate (reaction intermediate). The binding strength and quality of the pose for this is likely to have an impact on the overall ligand potency. A series of compounds from the described SAR studies were analyzed using this docking model. We observed that, while the docking model could account for the large changes in potency and the scores were well correlated with the experimental potency, it was hard to account for the smaller incremental changes in the SAR data. Nevertheless, these computational analyses gave useful insights in our experimental results. In particular, in silico docking studies of **32b** to *hAC* suggests a binding mode of the corresponding tetrahedral intermediate (reaction intermediate, docking score = -7.3), as depicted in Figure 8B. The docking pose suggests the alkyl side-chain (*n*-pentyl) of **32b** sharing the same binding mode of the *n*-hexyl chain of carmofur (Figure 2) within the *hAC* binding pocket,⁶⁷ where lipophilic residues, such as Phe163, Tyr137, Leu211, and Meth161, are localized. In addition, hydrogen bonding interaction stabilizes the transition state around the catalytic Cys143 residue between the side-chain carboxyl group of Glu225 (2.77 Å) and the hydroxy group (tetrahedral intermediate) on the alpha carbon of the reaction center. The ligand pose itself is stabilized by a cation–pi interaction between the protonated *N*-methyl amino group of the piperidine ring and Trp395 and a second edge to face the pi–pi interaction between the fluorophenyl group of the ligand and Phe165 (4.56 and 3.43

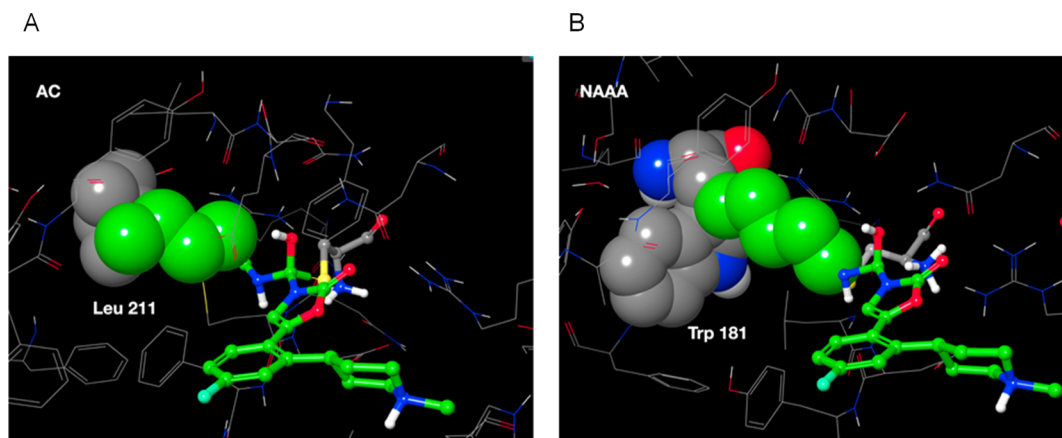


Figure 9. Putative docking poses of compound **32b** in *hAC* (PDB code: 6MHM) (A) and in *hNAAA* (PDB code: 6DXX) (B).

Table 6. PK Properties of **32b** after Intravenous (3 mg/kg) and Oral Administration (10 mg/kg) in C57BL/6 Mice

parameters ^a	(3 mg/kg, i.v.)	(10 mg/kg, p.o.)
t_{\max} (min)		30
C_{\max} (ng/mL)		278
$t_{1/2}$ (min)	119	147
Cl (mL/min/kg)	72	155
V_{dss} (mL/kg)	12 426	32 877
AUC (min \times ng/mL)	31 978	42 525
F (%)		40

^aPK parameters were calculated using PK solutions.

Å). It is conceivable that the electron-withdrawing nature of the fluorophenyl might promote the strength of the pi–pi interaction.

Analysis of **32b** in the anti-target *hNAAA* suggests that the binding site of the two enzymes share over 90% similarity in their amino acid composition. However, when compound **32b** is docked into *hNAAA*,⁶⁹ the resultant equivalent pose has a very low score. Careful examination of the docking poses (modeling details in Experimental Section) show that there is a critical difference between *hAC* and *hNAAA* around residue 182 in the binding site. While *hAC* has Leu at position 182, the equivalent position is occupied by much larger Trp181 in *hNAAA*. The *n*-pentyl side-chain on the compound **32b** easily fits in the wider pocket of *hAC* (Figure 9A), but it causes steric clashes, as seen in the Figure 9B, in the case of *hNAAA* because of the much bulkier Trp181 side-chain. We believe this to be one of key reasons for selectivity observed in **32b** that might be further exploited in future drug design programs.

Because of the overall property profile of **32b**, this compound was selected for additional pharmacological studies with the aim of testing its ability to inhibit *hAC* in intact cells. In particular, we examined the effects of compound **32b** treatment using human neuroblastoma SH-SY5Y cells, which are a well-characterized and widely used in vitro cell model.^{70,71} Notably, Kyriakou and co-workers recently established and characterized a stable *AC* knockdown human neuroblastoma SH-SY5Y cell line, as a human in vitro cell model for studying the effects of *AC* deficiency.⁷² Human neuroblastoma SH-SY5Y cells were incubated in the presence of **32b** at different concentrations for 3 h (1, 2.5, 5, and 10 μM , Figure 6) and in the presence of **32b** (10 μM) at different incubation times (1, 3, and 6 h, Figure 7). *hAC* activity was measured and SL levels were identified and quantified with a liquid chromatography/mass spectrometry (LC/MS)-based activity assay, as previously described.^{55,56,61} We indeed demonstrated that **32b** is effectively able to engage *hAC* in the complex cellular environment under our experimental conditions, causing the expected changes in the cellular levels of SL. Treatment of SH-SY5Y cell cultures with **32b** caused a concentration (Figure 6A) and time-dependent reduction of *hAC* activity (Figure 7A). After 3 h incubation, we observed an intracellular accumulation of various Cer species, including Cer (d18:0/16:0) and Cer (d18:1/16:0) (Figure 6B,C), and a corresponding decrease in So levels in a concentration-dependent manner (Figure 6D). Conversely, no major variations were observed in the levels of SM (d18:1/16:0) (Figure 6E) and HexCer (d18:1/16:0) (Figure 6F). The effect of **32b** (10 μM) on the inhibition of *hAC* activity and the intracellular SL levels is reported in Figure 7A–F. Specifically, we observed that **32b** inhibits *hAC* in SH-SY5Y cells leading to an increased Cer (d18:0/16:0) and Cer (d18:1/16:0) (Figure

7B,C) and decreased So levels (Figure 7D), which persisted up to 6 h. No major variations were observed in the levels of SM (d18:1/16:0) (Figure 7E) and HexCer (d18:1/16:0) (Figure 7F).

Finally, we then took **32b** for pharmacokinetic (PK) studies in C57BL/6 mice, following intravenous (i.v.) and oral administration (p.o.). The relevant PK parameters are reported in Table 6. Values of plasma clearance (Cl_p), volume of distribution (V_{dss}), and plasma elimination half-life ($t_{1/2}$) were calculated after i.v. administration of **32b** at 3 mg/kg. Cl_p was relatively low (72 mL/min/kg) with acceptable plasma $t_{1/2}$ (119 min) and high V_{dss} (12426 mL/kg), indicating that **32b** is well distributed out of the circulating mouse plasma compartment. Compound **32b** is an orally bioavailable *hAC* inhibitor at 10 mg/kg (oral bioavailability, $F = 40\%$) and is rapidly adsorbed in the plasma compartment ($t_{\max} = 30$ min), with a maximal plasma concentration (C_{\max}) of 278 ng/mL and acceptable plasma $t_{1/2}$ (147 min). Moreover, **32b** shows significant exposures in mouse plasma, after both i.v. and p.o. doses (AUC = 31978 and 42525 min \times ng/mL, respectively).

Taking into account its overall profile, **32b** was selected for further development studies aimed to elucidate the potential therapeutic applications of *AC* inhibition in cellular and in vivo model systems of relevant SL-mediated disorders, which will be described elsewhere in due course.

CONCLUSIONS

Although *hAC* inhibition has been the focus of intense discovery in the last decade, only a very limited number of valuable candidates for in vivo experiments are available. The scope of this work was directed to solve this limitation. The design and synthesis of a series of substituted oxazol-2-one-3-carboxamide derivatives were presented, resulting in the identification of two initial hits, **8a** and **12a** as a novel and versatile class of *hAC* inhibitors. Preliminary results of the hit expansion around these new scaffolds in the three main Regions A, B, and C contributed to the definition of the pharmacophore necessary for target inhibition and directed the strategies for chemical optimization. Our medicinal chemistry efforts around the most promising 5-substituted oxazol-2-one-3-carboxamide series led to the identification of 5-[4-fluoro-2-(1-methyl-4-piperidyl)phenyl]-2-oxo-*N*-pentyl-oxazole-3-carboxamide (**32b**) as an optimized *hAC* inhibitor, structurally distinct from previous reported inhibitors, with good drug-like properties. Furthermore, **32b** showed target engagement in human neuroblastoma SH-SY5Y cells and desirable PK properties in mice, with good $F\%$ and significant exposures in plasma, after intravenous and oral administrations. Compound **32b** is a valuable lead that increases the arsenal of suitable *hAC*-targeting molecules, which can directly probe the link of *hAC* function to distinct physiological processes and investigate how the inhibition of its activity can provide health benefits under severe pathological conditions. The identification of novel *hAC*-modulating compounds, targeting active Cys143 with optimal drug-like properties, remains a challenging task and can be only achieved by a critical and balanced modulation of different parameters, whose objectives often clash during the chemical optimization process. Utilizing the recently reported crystal structures, we were able to dock our covalent inhibitors into the reactive site highlighting the basis for selectivity observed with **32b** for *hAC* compared to *hNAAA*. In addition, the modeling that was undertaken can guide future optimization of this lead series accelerating the field

of research and contributing to the identification of additional novel and efficacious *hAC* inhibitors.

EXPERIMENTAL SECTION

Chemicals, Materials, and Methods. Solvents and reagents were obtained from commercial suppliers and were used without further purification. Automated column chromatography purifications were done using a Teledyne ISCO apparatus (CombiFlash Rf) with prepacked silica gel or neutral alumina columns of different sizes (from 4 g until 120 g). Mixtures of increasing polarity of Cy and EtOAc or dichloromethane (DCM) and MeOH were used as eluents. Thin-layer chromatography (TLC) analyses were performed using Supelco silica gel on TLC Al foils 0.2 mm with a fluorescence indicator 254 nm. NMR experiments of all the intermediates and final compounds were run on a Bruker AVANCE III 400 system (400.13 MHz for ^1H , and 100.62 MHz for ^{13}C), equipped with a BBI probe and Z-gradient coil. Spectra were acquired at 300 K using DMSO- d_6 or CDCl_3 as solvents. Chemical shifts for ^1H and ^{13}C spectra were recorded in parts per million (ppm) using the residual nondeuterated solvent as the internal standard (for DMSO- d_6 : 2.50 ppm, ^1H ; 39.52 ppm, ^{13}C ; for CDCl_3 : 7.26 ppm, ^1H and 77.16 ppm, ^{13}C). Data are reported as follows: chemical shift (ppm), multiplicity (indicated as: bs, broad singlet; s, singlet; d, doublet; t, triplet; q, quartet; p, quintet; sx, sextet; m, multiplet; and combinations thereof), coupling constants (J) in Hertz (Hz), and integrated intensity. Quantitative ^1H NMR analyses of the freshly prepared 10 mM DMSO- d_6 stock solutions (used for biological screenings) of the final compounds were performed using the PULCON method (pulse length-based concentration determination, Bruker software, topspin 3.0. References: (a) Wider, G.; Reires, L. *J. Am. Chem. Soc.* **2006**, *128* (8), 2571–2576; (b) Burton, I. W.; Quilliam, M. A.; Valter, J. A. *Anal. Chem.* **2005**, *77*, 3123–3131). UPLC/MS analyses of all the intermediates and final compounds were performed on a Waters Acquity UPLC/MS system consisting of single quadrupole detection (SQD) mass spectrometry (MS) equipped with an electrospray ionization (ESI) interface and a photodiode array (PDA) detector. The PDA range was 210–400 nm. Analyses were performed on an Acquity UPLC BEH C18 column (50 \times 2.1 mm ID, particle size 1.7 μm) with a VanGuard BEH C18 pre-column (5 \times 2.1 mm ID, particle size 1.7 μm). The mobile phase was 10 mM NH_4OAc in H_2O at pH 5 adjusted with AcOH (A) and 10 mM NH_4OAc in $\text{CH}_3\text{CN}/\text{H}_2\text{O}$ (95:5) at pH 5 (B). ESI in both positive and negative modes was used in the mass scan range 100–650 Da. Analyses were performed with *method A*, *B*, *C*, or *D*. *Method A*: Gradient: 5–95% B over 2.5 min. Flow rate 0.5 mL/min. Temperature 40 $^\circ\text{C}$. *Method B*: Gradient: 50–100% B over 2.5 min. Flow rate 0.5 mL/min. Temperature 40 $^\circ\text{C}$. *Method C*: Gradient: 0–100% B over 2.5 min. Flow rate 0.5 mL/min. Temperature 40 $^\circ\text{C}$. *Method D*: Isocratic 55% B over 5 min. Flow rate 0.5 mL/min. Temperature 40 $^\circ\text{C}$. UPLC/MS analyses of freshly prepared 10 mM DMSO- d_6 stock solutions (used for biological screenings) of the final compounds were performed with *method E* or *method F*. DMSO- d_6 stock solution (10 μL , 10 mM) was diluted 20-fold or 100-fold with a 1:1 $\text{CH}_3\text{CN}/\text{H}_2\text{O}$ solution and directly analyzed. An Acquity UPLC BEH C18 (100 \times 2.1 mm ID, particle size 1.7 μm) with a VanGuard BEH C18 pre-column (5 \times 2.1 mm ID, particle size 1.7 μm). The mobile phase was either 10 mM NH_4OAc in H_2O at pH 5 adjusted with AcOH (A) and 10 mM NH_4OAc in $\text{CH}_3\text{CN}/\text{H}_2\text{O}$ (95:5) at pH 5 (B). ESI in positive and negative modes was applied in the mass scan range 100–650 Da. *Method E*: Gradient: 10–90% B over 6 min. Flow rate 0.5 mL/min. Temperature 40 $^\circ\text{C}$. *Method F*: Gradient: 50–100% B over 6 min. Flow rate 0.5 mL/min. Temperature 40 $^\circ\text{C}$. The detection wavelength (λ) was set at 215 nm for relative purity determination. R_f of the final compounds under *method E* or *F* UPLC/MS analytical conditions are reported in Table S3. Optical rotations were measured on a Rudolf Research Analytical Autopol II Automatic polarimeter using a sodium lamp (589 nm) as the light source, concentrations are expressed in g/100 mL using CHCl_3 as a solvent and a 1 dm cell. Accurate mass measurements were performed on a Synapt G2 Quadrupole-ToF Instrument (Waters, USA), equipped with an ESI ion source; the

compounds were diluted to 50 μM in $\text{CH}_3\text{CN}/\text{H}_2\text{O}$ and analyzed. Leucine Enkephalin (2 ng/mL) was used as the lock mass reference compound for spectra recalibration. All final compounds displayed $\geq 95\%$ purity as determined by NMR and UPLC/MS analysis.

General Procedure for the Synthesis of 4-Substituted-oxazol-2-ones (Procedure A). To a mixture of the appropriate α -hydroxy ketone (1.0 equiv) and KNCO (2.0 equiv) in *i*-PrOH (0.2 M) was added dropwise AcOH (2.0 equiv) with stirring. The resulting suspension was heated at 70 $^\circ\text{C}$ for 3 h, then poured into an ice/ H_2O bath, and extracted with DCM or EtOAc. The organic phase was dried over Na_2SO_4 and concentrated under reduced pressure. The crude was purified by column chromatography (SiO_2), eluting with Cy/EtOAc or used as crude in the next step without further purification.

General Procedure for the Synthesis of 5-Substituted-oxazol-2-ones (Procedure B). Step 1: to a stirred solution of the appropriate α -bromoketone (1.0 equiv) and TZD (1.2 equiv) in DMF (0.1–1 M) was added K_2CO_3 (1.5 equiv). The resulting mixture was stirred at rt for 1–2 h and then poured into an ice/ H_2O bath. In some cases, the resulting solid was filtered off and washed with H_2O . In other cases, the aq phase was extracted with EtOAc, and the organic layer was washed with 5% aq LiCl and brine and dried over Na_2SO_4 . After evaporation of the solvent, the crude was purified by flash chromatography (SiO_2) eluting with Cy/EtOAc or used as a crude in the next step without further purification, as indicated in each case. Step 2: the corresponding intermediate from step 1 was dissolved in THF (0.1 M) and treated with LiOH (4.0 equiv) or *t*-BuOK (2.0–4.0 equiv) as indicated in each case. The resulting mixture was stirred at rt for 30–60 min and then poured into a cold aq AcOH solution (5.0–10.0 equiv). In some cases, the resulting solid was filtered off, washed with H_2O , and used in the next step without further purification. Alternatively, the aq phase was extracted with EtOAc and the organic phase was dried over Na_2SO_4 . After evaporation of the solvent, the crude was purified by flash chromatography (SiO_2 or Al_2O_3) eluting with Cy/EtOAc or DCM/MeOH or DCM/EtOH or used as a crude in the next step without further purification, as indicated in each case.

General Procedure for the Synthesis of 5-Phenyl-oxazolidin-2-ones (Procedure C). To a solution of (S) or (R)-2-amino-1-phenylethanol (1.0 equiv) in DCM (0.1 M) was added imidazole (0.5 equiv) followed by the addition of CDI (1.1 equiv). The reaction mixture was stirred at rt 16 h, then washed with H_2O , and dried over Na_2SO_4 . After evaporation of the solvent, the crude was purified by flash chromatography (SiO_2) eluting with DCM/MeOH, as indicated in each case.

General Procedure for the Synthesis of Carboxamides (Procedure D). *Method A*: to a stirred solution of the appropriate oxazol-2-one, or oxazolidin-2-one, (1.0 equiv) in CH_3CN , or pyridine, or DMF (0.2 M) were added DMAP (0.1–1.1 equiv), or Et_3N (4.0 equiv), and the appropriate isocyanate (1.1–2.0 equiv). The resulting solution was stirred at rt (or at 50 $^\circ\text{C}$, as indicated in each case) for 3–16 h, then diluted with EtOAc, washed with sat. aq NH_4Cl solution and brine, and dried over Na_2SO_4 . After evaporation of the solvent, the crude was purified by column chromatography (SiO_2 or Al_2O_3), eluting with Cy/EtOAc or DCM/MeOH, as indicated in each case. *Method B*: To a stirred solution of Boc_2O (2.0 equiv) in CH_3CN (0.4 M) were added DMAP (2.0 equiv) and the appropriate amine (1.1–2.0 equiv). The resulting solution was stirred at rt for 10 min then the appropriate oxazol-2-one derivative (1.0 equiv) was added, and the mixture was stirred at rt for 1–3 h. After evaporation of the solvent, the crude was purified by flash chromatography (SiO_2) eluting with Cy/EtOAc or DCM/MeOH, as indicated in each case. *Method C*: To a stirred solution of triphosgene (0.33 equiv) in dry DCM (0.2 M), a solution of the appropriate amine (1.0 equiv) and Et_3N , or DIPEA, (2.0 equiv) in DCM (0.2 M) was added at -15°C . The resulting mixture was stirred at rt for 30 min under a N_2 atmosphere and then added to a solution of the appropriate oxazol-2-one (0.33 equiv) and Et_3N , or DIPEA, (1.0 equiv) in DCM (0.2 M). The reaction mixture was stirred under a N_2 atmosphere at rt for 3–12 h, then diluted with DCM, washed with sat. aq NH_4Cl solution and brine, and dried over Na_2SO_4 . After evaporation of the solvent, the crude was purified by column chromatography

(SiO₂), eluting with Cy/EtOAc, or DCM/MeOH, as indicated in each case.

General Procedure for Palladium-Catalyzed Cross-Coupling Reaction (Procedure E). To a solution of the appropriate phenyl bromide (1.0 equiv) in dry 1,4-dioxane (0.1 M, previously degassed under a nitrogen atmosphere), **19** (1.1 equiv) was added followed by the addition of Pd(PPh₃)₄ (0.05 equiv) and Na₂CO₃ (2.2 equiv, 2 M aq solution). The suspension was stirred at reflux on, cooled to rt, and then diluted with EtOAc and filtered through a pad of celite. The filtrate was concentrated under reduced pressure, diluted with EtOAc, washed with sat. aq NH₄Cl solution and brine, and dried over Na₂SO₄. After evaporation of the solvent, the crude was purified by flash chromatography (SiO₂), eluting with Cy/EtOAc, as indicated in each case.

General Procedure for Catalytic Hydrogenation Reaction (Procedure F). *Method A:* To a suspension of the appropriate unsaturated intermediate (1.0 equiv) in EtOH (0.1 M) were added 10% Pd/C (0.1 equiv) and cyclohexene (20.0 equiv), and the mixture was stirred at 60 °C until disappearance of the starting material, as indicated by UPLC/MS analysis. The suspension was filtered through a pad of celite, and the filtrate was quickly evaporated under reduced pressure. The crude was purified by flash chromatography (SiO₂), eluting with Cy/EtOAc or used in the next step without further purification, as indicated in each case. *Method B:* To a suspension of the appropriate unsaturated intermediate (1.0 equiv) in MeOH (0.1 M) were added 20% Pd(OH)₂ on carbon (10% wt) and HCO₂NH₄ (7.0 equiv), and the mixture was stirred at 60 °C for 4 h. The suspension was filtered through a pad of celite, and the filtrate was quickly evaporated under reduced pressure. The crude was purified by flash chromatography (SiO₂), eluting with Cy/EtOAc, or used in the next step without further purification, as indicated in each case.

General Procedure for N-Boc Removal (Procedure G). To a suspension of the appropriate *N*-Boc protected intermediate (1.0 equiv) in 1,4-dioxane (0.1 M) was added HCl (30.0 equiv, 4 M in 1,4-dioxane), and the reaction mixture was stirred at rt for 2 h. After evaporation of the solvent, the crude was triturated with Et₂O, or used as a crude, in the next step without further purification.

General Procedure for Reductive Amination Reaction (Procedure H). To a solution of the appropriate substituted piperidine intermediate (1.0 equiv) in CH₃CN (0.1 M) were added 37% aq solutions of HCHO (2.0–5.0 equiv), AcOH (2.0 equiv), and NaBH(OAc)₃ (3.0 equiv). The mixture was stirred at rt for 1 h. Then, the reaction mixture was poured into a saturated aqueous NaHCO₃ solution and extracted with EtOAc. The organic phase was washed with brine and dried over Na₂SO₄. After evaporation of the solvent, the crude was purified by flash chromatography (SiO₂) eluting with DCM/MeOH, or used as a crude, in the next step without further purification, as indicated in each case.

Synthesis of 4-Phenyl-3H-oxazol-2-one (7a). Compound **7a** was prepared according to general procedure A using **6a** (1.360 g, 10.00 mmol). The crude was purified by column chromatography (SiO₂), eluting with Cy/EtOAc (4:1) to afford **7a** as a yellow solid (0.858 g, 53%). ¹H NMR (400 MHz, DMSO-*d*₆): δ 11.34 (bs, 1H), 7.68 (d, *J* = 1.2 Hz, 1H), 7.62–7.53 (m, 2H), 7.49–7.40 (m, 2H), 7.39–7.29 (m, 1H). UPLC/MS (*method A*): *R*_t 1.48 min. MS (ES): C₉H₇NO₂ requires, 161; found, 162 [M + H]⁺, 160 [M – H][–].

Synthesis of 5-Methyl-4-phenyl-3H-oxazol-2-one (7b). Compound **7b** was prepared according to general procedure A using **6b** (0.350 g, 2.33 mmol). The crude was used in the next step without further purification. ¹H NMR (400 MHz, CDCl₃): δ 9.39 (bs, 1H), 7.48–7.41 (m, 2H), 7.40–7.32 (m, 3H), 2.32 (s, 3H). UPLC/MS (*method A*): *R*_t 1.84 min. MS (ES): C₁₀H₉NO₂ requires, 175; found, 176 [M + H]⁺, 174 [M – H][–].

Synthesis of 4-(4-Chlorophenyl)-3H-oxazol-2-one (7c). Compound **7c** was prepared according to general procedure A using **6c** (0.241 g, 1.41 mmol). The crude was purified by column chromatography (SiO₂), eluting with Cy/EtOAc (9:1), to afford **7c** as a yellow solid (0.10 g, 36%). ¹H NMR (400 MHz, CDCl₃): δ 9.61 (bs, 1H), 7.42 (d, *J* = 8.5 Hz, 2H), 7.33 (d, *J* = 8.5 Hz, 2H), 7.11–7.08

(m, 1H). UPLC/MS (*method A*): *R*_t 1.71 min. MS (ES): C₉H₆ClNO₂ requires, 195; found, 196 [M + H]⁺, 194 [M – H][–].

Synthesis of 2-Oxo-4-phenyl-N-(4-phenylbutyl)oxazole-3-carboxamide (8a). Compound **8a** was prepared according to general procedure D (*method A*) using **7a** (0.161 g, 1.00 mmol), DMAP (0.012 g, 0.10 mmol), and 4-phenylbutyl isocyanate (0.350 g, 2.00 mmol) in CH₃CN. The crude was purified by column chromatography (SiO₂), eluting with Cy/EtOAc (9:1), to afford **8a** as a white solid (0.243 g, 72%). ¹H NMR (400 MHz, CDCl₃): δ 8.10 (bs, 1H), 7.56–7.34 (m, 5H), 7.34–7.27 (m, overlapped with CDCl₃ signal, 2H), 7.26–7.11 (m, 3H), 6.75 (s, 1H), 3.42–3.26 (m, 2H), 2.63 (t, *J* = 7.2 Hz, 2H), 1.78–1.60 (m, 4H). ¹³C NMR (101 MHz, CDCl₃): δ 154.57, 148.99, 142.09, 129.36, 129.00, 128.85, 128.53, 128.50, 128.14, 127.43, 125.99 (2C), 40.28, 35.57, 29.12, 28.68. UPLC/MS (*method A*): *R*_t 2.55 min. MS (ES): C₂₀H₂₀N₂O₃ requires, 336; found, 337 [M + H]⁺. HRMS: C₂₀H₂₀N₂O₃ [M + H]⁺ calcd 337.1552; measured, 337.1549, Δppm –0.9.

Synthesis of 2-Oxo-N-pentyl-4-phenyl-oxazole-3-carboxamide (8b). Compound **8b** was prepared according to general procedure D (*method A*) using **7a** (0.161 g, 1.00 mmol), DMAP (0.012 g, 0.10 mmol), and *n*-pentyl isocyanate (0.170 g, 1.50 mmol) in CH₃CN. The crude was purified by column chromatography (SiO₂), eluting with Cy/EtOAc (9:1), to afford **8b** as yellow oil (0.225 g, 82%). ¹H NMR (400 MHz, CDCl₃): δ 8.09 (bs, 1H), 7.45–7.32 (m, 5H), 6.74 (s, 1H), 3.34–3.23 (m, 2H), 1.64–1.49 (m, overlapped with a H₂O signal, 2H), 1.40–1.23 (m, 4H), 0.91 (t, *J* = 6.8 Hz, 3H). ¹³C NMR (101 MHz, CDCl₃): δ 154.57, 148.94, 129.33, 128.97, 128.85, 128.12, 127.45, 125.80, 40.45, 29.16, 29.08, 22.42, 14.09. UPLC/MS (*method A*): *R*_t 2.40 min. MS (ES): C₁₅H₁₈N₂O₃ requires, 274; found, 275 [M + H]⁺. HRMS: C₁₅H₁₈N₂O₃Na [M + Na]⁺ calcd 297.1215; measured, 297.1210, Δppm –1.7.

Synthesis of 5-Methyl-2-oxo-4-phenyl-N-(4-phenylbutyl)oxazole-3-carboxamide (8c). Compound **8c** was prepared according to general procedure D (*method A*) using **7b** (0.130 g, 0.74 mmol), DMAP (0.099 g, 0.81 mmol), and 4-phenylbutyl isocyanate (0.142 g, 0.81 mmol) in pyridine. The crude was purified by column chromatography (SiO₂), eluting with Cy/EtOAc (4:1), to afford **8c** as a white solid (0.040 g, 15%). ¹H NMR (400 MHz, CDCl₃): δ 8.09 (t, *J* = 4.4 Hz, 1H), 7.42–7.37 (m, 3H), 7.33–7.24 (m, overlapped with CDCl₃ signal, 4H), 7.21–7.12 (m, 3H), 3.34–3.23 (m, 2H), 2.61 (t, *J* = 7.4 Hz, 2H), 2.05 (s, 3H), 1.71–1.56 (m, overlapped with H₂O signal, 4H). ¹³C NMR (101 MHz, CDCl₃): δ 149.26, 142.13, 135.35, 131.21, 129.77, 129.14, 128.87, 128.53, 128.47, 128.11, 126.59, 125.95, 40.16, 35.58, 29.16, 28.69, 10.19. UPLC/MS (*method A*): *R*_t 2.71 min. MS (ES): C₂₁H₂₂N₂O₃ requires, 350; found, 351 [M + H]⁺. HRMS: C₂₁H₂₂N₂O₃Na [M + Na]⁺ calcd 373.1528; measured, 373.1523, Δppm –1.3.

Synthesis of 4-(4-Chlorophenyl)-2-oxo-N-(4-phenylbutyl)oxazole-3-carboxamide (8d). Compound **8d** was prepared according to general procedure D (*method A*) using **7c** (0.100 g, 0.51 mmol), DMAP (0.068 g, 0.56 mmol), and 4-phenylbutyl isocyanate (0.098 g, 0.56 mmol) in pyridine. The crude was purified by column chromatography (SiO₂), eluting with Cy/EtOAc (9:5), to afford **8d** as yellow oil (0.040 g, 21%). ¹H NMR (400 MHz, CDCl₃): δ 8.10 (t, *J* = 5.2 Hz, 1H), 7.40–7.34 (m, 2H), 7.32–7.26 (m, overlapped with CDCl₃ signal, 4H), 7.22–7.12 (m, 3H), 6.75 (s, 1H), 3.41–3.23 (m, 2H), 2.63 (t, *J* = 7.3 Hz, 2H), 1.90–1.49 (m, 4H). ¹³C NMR (101 MHz, CDCl₃): δ 154.33, 148.93, 142.02, 135.54, 130.32, 128.50 (2C), 128.43 (3C), 126.00, 125.88, 40.29, 35.54, 29.07, 28.65. UPLC/MS (*method A*): *R*_t 2.71 min. MS (ES): C₂₀H₁₉ClN₂O₃ requires, 370; found, 371 [M + H]⁺. HRMS: C₂₀H₁₉ClN₂O₃ [M + Na]⁺ calcd 393.0982; measured, 393.0973, Δppm –2.3.

Synthesis of 3-Phenacylthiazolidine-2,4-dione (10a). Compound **10a** was prepared according to general procedure B, Step 1, using **9a** (1.990 g, 10.00 mmol). The crude was used in Step 2 without further purification. UPLC/MS (*method A*): *R*_t 1.69 min. MS (ES): C₁₁H₉NO₃S requires, 235; found, 234 [M – H][–].

Synthesis of 3-(1-Methyl-2-oxo-2-phenyl-ethyl)thiazolidine-2,4-dione (10b). Compound **10b** was prepared according to general procedure B, Step 1, using **9b** (0.500 g, 2.35 mmol). The crude was

purified by column chromatography (SiO₂), eluting with Cy/EtOAc (4:1), to afford **10b** as a white solid (0.550 g, 94%). ¹H NMR (400 MHz, CDCl₃): δ 7.75–7.68 (m, 2H), 7.58–7.52 (m, 1H), 7.47–7.41 (m, 2H), 5.55 (q, *J* = 7.0 Hz, 1H), 3.90 (d, *J* = 17.5 Hz, 1H), 3.82 (d, *J* = 17.5 Hz, 1H), 1.65 (d, *J* = 7.0 Hz, 3H). UPLC/MS (*method A*): *R*_t 1.83 min. MS (ES): C₁₂H₁₁NO₃S requires, 249; found, 250 [M + H]⁺.

Synthesis of 3-[2-(4-Chlorophenyl)-2-oxo-ethyl]thiazolidine-2,4-dione (10c). Compound **10c** was prepared according to general procedure B, Step 1, using **9c** (1.170 g, 5.00 mmol). The crude was used in Step 2 without further purification. UPLC/MS (*method A*): *R*_t 2.01 min. MS (ES): C₁₁H₈ClNO₃S requires, 269; found, 268 [M – H][–].

Synthesis of 3-[2-(4-Fluorophenyl)-2-oxo-ethyl]thiazolidine-2,4-dione (10d). Compound **10d** was prepared according to general procedure B, Step 1, using **9d** (2.170 g, 10.00 mmol). The crude was used in Step 2 without further purification. UPLC/MS (*method A*): *R*_t 1.81 min. MS (ES): C₁₁H₈FNO₃S requires, 253; found, 254 [M + H]⁺, 252 [M – H][–].

Synthesis of 3-[2-(4-Methoxyphenyl)-2-oxo-ethyl]thiazolidine-2,4-dione (10e). Compound **10e** was prepared according to general procedure B, Step 1, using **9e** (2.290 g, 10.00 mmol). The crude was used in Step 2 without further purification. ¹H NMR (400 MHz, DMSO-*d*₆): δ 8.13–7.92 (m, 2H), 7.14–7.05 (m, 2H), 5.06 (s, 2H), 4.39 (s, 2H), 3.87 (s, 3H). UPLC/MS (*method A*): *R*_t 1.78 min. MS (ES): C₁₂H₁₁NO₄S requires, 265; found, 266 [M + H]⁺, 264 [M – H][–].

Synthesis of 3-[2-(3-Methoxyphenyl)-2-oxo-ethyl]thiazolidine-2,4-dione (10f). Compound **10f** was prepared according to general procedure B, Step 1, using **9f** (1.260 g, 5.50 mmol). The crude was used in Step 2 without further purification. UPLC/MS (*method A*): *R*_t 1.83 min. MS (ES): C₁₂H₁₁NO₄S requires, 265; found, 266 [M + H]⁺, 264 [M – H][–].

Synthesis 3-[2-(2-Methoxyphenyl)-2-oxo-ethyl]thiazolidine-2,4-dione (10g). Compound **10g** was prepared according to general procedure B, Step 1, using **9g** (0.500 g, 2.18 mmol). The crude was used in Step 2 without further purification. UPLC/MS (*method A*): *R*_t 1.85 min. MS (ES): C₁₂H₁₁NO₄S requires, 265; found, 266 [M + H]⁺, 264 [M – H][–].

Synthesis of 3-[2-(4-Fluoro-3-methoxy-phenyl)-2-oxo-ethyl]thiazolidine-2,4-dione (10h). Compound **10h** was prepared according to general procedure B, Step 1, using **9h** (0.250 g, 1.01 mmol). The crude was used in Step 2 without further purification. UPLC/MS (*method A*): *R*_t 1.85 min. MS (ES): C₁₂H₁₀FNO₄S requires, 283; found, 284 [M + H]⁺, 282 [M – H][–].

Synthesis of 3-[2-Oxo-2-(2-pyridyl)ethyl]thiazolidine-2,4-dione (10i). Compound **10i** was prepared according to general procedure B, Step 1, using **9i** (0.400 g, 2.00 mmol). The crude was used in Step 2 without further purification. UPLC/MS (*method A*): *R*_t 1.38 min. MS (ES): C₁₀H₈N₂O₃S requires, 236; found, 237 [M + H]⁺.

Synthesis of 3-[2-Oxo-2-(3-pyridyl)ethyl]thiazolidine-2,4-dione (10j). Compound **10j** was prepared according to general procedure B, Step 1, using **9j** (2.000 g, 10.00 mmol). The crude was used in Step 2 without further purification. UPLC/MS (*method A*): *R*_t 1.21 min. MS (ES): C₁₀H₈N₂O₃S requires, 236; found, 237 [M + H]⁺.

Synthesis of 3-[2-Oxo-2-(4-pyridyl)ethyl]thiazolidine-2,4-dione (10k). Compound **10k** was prepared according to general procedure B, Step 1, using **9k** (1.000 g, 5.00 mmol). The crude was used in Step 2 without further purification. UPLC/MS (*method A*): *R*_t 1.15 min. MS (ES): C₁₀H₈N₂O₃S requires, 236; found, 237 [M + H]⁺.

Synthesis of 3-(2-Oxo-2-pyrazin-2-yl-ethyl)thiazolidine-2,4-dione (10l). Compound **10l** was prepared according to general procedure B, Step 1, using **9l** (0.600 g, 2.99 mmol). The crude was used in Step 2 without further purification. UPLC/MS (*method A*): *R*_t 1.25 min. MS (ES): C₉H₇N₃O₃S requires, 237; found, 238 [M + H]⁺.

Synthesis of 3-(2-Oxo-2-quinoxalin-2-yl-ethyl)thiazolidine-2,4-dione (10m). Compound **10m** was prepared according to general procedure B, Step 1, using **9m** (0.200 g, 0.80 mmol). The crude was used in Step 2 without further purification. UPLC/MS (*method A*): *R*_t 1.76 min. MS (ES): C₁₃H₉N₃O₃S requires, 287; found, 288 [M + H]⁺.

Synthesis of 3-[2-(1-Methylindazol-3-yl)-2-oxo-ethyl]thiazolidine-2,4-dione (10n). Compound **10n** was prepared according to general procedure B, Step 1, using **9n** (0.120 g, 0.47 mmol). The crude was used in Step 2 without further purification. UPLC/MS

(*method D*): *R*_t 1.08 min. MS (ES): C₁₃H₁₁N₃O₃S requires, 289; found, 290 [M + H]⁺, 288 [M – H][–].

Synthesis of 3-(2-Oxo-2-thiazol-2-yl-ethyl)thiazolidine-2,4-dione (10o). Compound **10o** was prepared according to general procedure B, Step 1, using **9o** (0.500 g, 2.43 mmol). The crude was used in Step 2 without further purification. UPLC/MS (*method A*): *R*_t 1.47 min. MS (ES): C₈H₆N₂O₃S₂ requires, 242; found, 243 [M + H]⁺, 241 [M – H][–].

Synthesis of 3-(2-Oxo-2-thiazol-4-yl-ethyl)thiazolidine-2,4-dione (10p). Compound **10p** was prepared according to general procedure B, Step 1, using **9p** (0.130 g, 0.63 mmol). The crude was used in Step 2 without further purification. UPLC/MS (*method A*): *R*_t 1.27 min. MS (ES): C₈H₆N₂O₃S₂ requires, 242; found, 243 [M + H]⁺, 241 [M – H][–].

Synthesis of tert-Butyl 4-[2-(2,4-Dioxothiazolidin-3-yl)acetyl]piperidine-1-carboxylate (10q). Compound **10q** was prepared according to general procedure B, Step 1, using **9q** (0.310 g, 1.00 mmol). The crude was used in Step 2 without further purification. ¹H NMR (400 MHz, CDCl₃): δ 4.46 (s, 2H), 4.17–4.06 (m, 2H), 4.03 (s, 2H), 2.89–2.77 (m, 2H), 2.61 (tt, *J* = 11.2, 3.8 Hz, 1H), 1.92–1.81 (m, 2H), 1.61 (qd, *J* = 11.9, 4.3 Hz, 1H), 1.45 (s, 9H). UPLC/MS (*method A*): *R*_t 1.98 min. MS (ES): C₁₅H₂₂N₂O₅S requires, 342; found, 343 [M + H]⁺.

Synthesis of 5-Phenyl-3H-oxazol-2-one (11a). Compound **11a** was prepared using **10a** (2.350 g, 10.00 mmol) and LiOH (0.960 g, 40.00 mmol), according to general procedure B, Step 2. After aq. work-up, the resulting solid was collected by filtration to afford **11a** as a white solid (1.20 g, 74%). ¹H NMR (400 MHz, DMSO-*d*₆): δ 10.83 (bs, 1H), 7.53–7.46 (m, 3H), 7.44–7.36 (m, 2H), 7.31–7.23 (m, 1H). ¹³C NMR (101 MHz, DMSO-*d*₆): δ 155.16, 138.51, 128.82, 128.80, 127.90, 127.43, 122.30, 122.27, 109.05. UPLC/MS (*method A*): *R*_t 1.50 min. MS (ES): C₉H₇NO₂ requires, 161; found, 162 [M + H]⁺, 160 [M – H][–]. HRMS: C₉H₈NO₂ [M + H]⁺ calcd 162.0555; measured, 162.0546, Δppm –5.0.

Synthesis of 4-Methyl-5-phenyl-3H-oxazol-2-one (11b). Compound **11b** was prepared using **10b** (0.150 g, 0.60 mmol) and *t*-BuOK (0.130 g, 1.20 mmol), according to general procedure B, Step 2. The crude was purified by column chromatography (Al₂O₃), eluting with DCM/EtOH (9:1 to 6:4), to afford **11b** as a white solid (0.010 g, 10%). ¹H NMR (400 MHz, CDCl₃): δ 9.30 (bs, 1H), 7.50–7.45 (m, 2H), 7.43–7.37 (m, 2H), 7.32–7.26 (m, overlapped with CDCl₃ signal, 1H), 2.31 (s, 3H). UPLC/MS (*method A*): *R*_t 1.61 min. MS (ES): C₁₀H₉NO₂ requires, 175; found, 176 [M + H]⁺, 174 [M – H][–].

Synthesis of 5-(4-Chlorophenyl)-3H-oxazol-2-one (11c). Compound **11c** was prepared using **10c** (1.345 g, 5.00 mmol) and LiOH (0.479 g, 20.00 mmol), according to general procedure B, Step 2. After aq work-up, the resulting solid was collected by filtration to afford **11c** as a pink solid (0.975 g, quant.). ¹H NMR (400 MHz, DMSO-*d*₆): δ 10.82 (bs, 1H), 7.55 (s, 1H), 7.53–7.43 (m, 4H). UPLC/MS (*method A*): *R*_t 1.79 min. MS (ES): C₉H₆ClNO₂ requires, 195; found, 196 [M + H]⁺, 194 [M – H][–].

Synthesis of 5-(4-Fluorophenyl)-3H-oxazol-2-one (11d). Compound **11d** was prepared using **10d** (2.530 g, 10.00 mmol) and LiOH (0.958 g, 40.00 mmol), according to general procedure B, Step 2. After aq work-up, the resulting solid was collected by filtration to afford **11d** as a white solid (0.300 g, 17%). ¹H NMR (400 MHz, DMSO-*d*₆): δ 10.84 (bs, 1H), 7.59–7.49 (m, 2H), 7.46 (s, 1H), 7.30–7.20 (m, 2H). UPLC/MS (*method A*): *R*_t 1.60 min. MS (ES): C₉H₆FNO₂ requires, 179; found, 180 [M + H]⁺, 178 [M – H][–].

Synthesis of 5-(4-Methoxyphenyl)-3H-oxazol-2-one (11e). Compound **11e** was prepared using **10e** (2.650 g, 10.00 mmol) and LiOH (0.958 g, 40.00 mmol), according to general procedure B, Step 2. After aq work-up, the resulting solid was collected by filtration to afford **11e** as a white solid (1.040 g, 54%). ¹H NMR (400 MHz, DMSO-*d*₆): δ 10.62 (bs, 1H), 7.48–7.39 (m, 2H), 7.30 (s, 1H), 7.03–6.91 (m, 2H), 3.77 (s, 3H). UPLC/MS (*method A*): *R*_t 1.55 min. MS (ES): C₁₀H₉NO₃ requires, 191; found, 192 [M + H]⁺, 190 [M – H][–].

Synthesis of 5-(3-Methoxyphenyl)-3H-oxazol-2-one (11f). Compound **11f** was prepared using **10f** (1.458 g, 5.50 mmol) and LiOH (0.527 g, 22.00 mmol), according to general procedure B, Step 2. After aq work-up, the resulting solid was collected by filtration to afford **11f** as a white solid (0.627 g, 60%). ¹H NMR (400 MHz, DMSO-*d*₆): δ 10.85

(bs, 1H), 7.52 (s, 1H), 7.31 (t, $J = 8.0$ Hz, 1H), 7.19–6.95 (m, 2H), 6.85 (ddd, $J = 8.4, 2.6, 0.9$ Hz, 1H), 3.78 (s, 3H). UPLC/MS (*method A*): R_t 1.59 min. MS (ES): $C_{10}H_9NO_3$ requires, 191; found, 192 $[M + H]^+$, 190 $[M - H]^-$.

Synthesis of 5-(2-Methoxyphenyl)-3H-oxazol-2-one (11g). Compound **11g** was prepared using **10g** (0.578 g, 2.18 mmol) and LiOH (0.210 g, 8.72 mmol), according to general procedure B, Step 2. After aq work-up, the resulting solid was collected by filtration to afford **11g** as a white solid (0.250 g, 60%). 1H NMR (400 MHz, $CDCl_3$): δ 9.56 (bs, 1H), 7.66 (dd, $J = 7.7, 1.6$ Hz, 1H), 7.31–7.21 (m, overlapped with $CDCl_3$ signal, 1H), 7.11 (d, $J = 1.9$ Hz, 1H), 7.02 (t, $J = 7.6$ Hz, 1H), 6.93 (d, $J = 8.3$ Hz, 1H), 3.93 (s, 3H). UPLC/MS (*method A*): R_t 1.65 min. MS (ES): $C_{10}H_9NO_3$ requires, 191; found, 192 $[M + H]^+$, 190 $[M - H]^-$.

Synthesis of 5-(4-Fluoro-3-methoxy-phenyl)-3H-oxazol-2-one (11h). Compound **11h** was prepared using **10h** (0.286 g, 1.01 mmol) and LiOH (0.097 g, 4.04 mmol), according to general procedure B, Step 2. The crude was purified by flash chromatography (SiO_2), eluting with DCM/MeOH (95:5), to afford **11h** as a yellow solid (0.055 g, 26%). 1H NMR (400 MHz, $CDCl_3$): δ 8.67 (bs, 1H), 7.13–7.04 (m, 2H), 7.04–6.97 (m, 1H), 6.78 (s, 1H), 3.93 (s, 3H). UPLC/MS (*method A*): R_t 1.61 min. MS (ES): $C_{10}H_8FNO_3$ requires, 209; found, 210 $[M + H]^+$, 208 $[M - H]^-$.

Synthesis of 5-(2-Pyridyl)-3H-oxazol-2-one (11i). Compound **11i** was prepared using **10i** (0.472 g, 2.00 mmol) and LiOH (0.192 g, 8.00 mmol), according to general procedure B, Step 2. After aq work-up, the resulting solid was collected by filtration to afford **11i** as an orange solid (0.308 g, 93%). 1H NMR (400 MHz, $DMSO-d_6$): δ 8.56–8.49 (m, 1H), 7.82 (td, $J = 7.8, 1.8$ Hz, 1H), 7.55 (s, 1H), 7.47–7.42 (m, 1H), 7.34–7.19 (m, 1H). UPLC/MS (*method A*): R_t 1.02 min. MS (ES): $C_8H_6N_2O_2$ requires, 162; found, 163 $[M + H]^+$, 161 $[M - H]^-$.

Synthesis of 5-(3-Pyridyl)-3H-oxazol-2-one (11j). Compound **11j** was prepared using **10j** (2.360 g, 10.00 mmol) and LiOH (0.958 g, 40.00 mmol), according to general procedure B, Step 2. The crude was purified by flash chromatography (SiO_2), eluting with DCM/MeOH (95:5), to afford **11j** as an orange solid (0.375 g, 23%). 1H NMR (400 MHz, $CDCl_3$): δ 8.78–8.74 (m, 1H), 8.55 (dd, $J = 4.9, 1.7$ Hz, 1H), 7.79 (dt, $J = 8.0, 2.0$ Hz, 1H), 7.34 (ddd, $J = 8.2, 5.0, 0.8$ Hz, 1H), 6.93 (d, $J = 2.1$ Hz, 1H). UPLC/MS (*method A*): R_t 1.00 min. MS (ES): $C_8H_6N_2O_2$ requires, 162; found, 163 $[M + H]^+$, 161 $[M - H]^-$.

Synthesis of 5-(4-Pyridyl)-3H-oxazol-2-one (11k). Compound **11k** was prepared using **10k** (1.180 g, 5.00 mmol) and LiOH (0.479 g, 20.00 mmol), according to general procedure B, Step 2. The crude was purified by flash chromatography (SiO_2), eluting with DCM/MeOH (95:5), to afford **11k** as an orange solid (0.122 g, 15%). 1H NMR (400 MHz, $DMSO-d_6$): δ 11.18 (bs, 1H), 8.60–8.52 (m, 2H), 7.85 (s, 1H), 7.49–7.40 (m, 2H). UPLC/MS (*method A*): R_t 0.83 min. MS (ES): $C_8H_6N_2O_2$ requires, 162; found, 163 $[M + H]^+$, 161 $[M - H]^-$.

Synthesis of 5-Pyrazin-2-yl-3H-oxazol-2-one (11l). Compound **11l** was prepared using **10l** (0.709 g, 2.99 mmol) and LiOH (0.958 g, 40.00 mmol), according to general procedure B, Step 2. The crude was purified by flash chromatography (SiO_2), eluting with DCM/MeOH (95:5), to afford **11l** as a brown solid (0.030 g, 6%). UPLC/MS (*method A*): R_t 0.86 min. MS (ES): $C_7H_5N_3O_2$ requires, 163; found, 162 $[M - H]^-$. 1H NMR (400 MHz, $CDCl_3$): δ 8.94–8.88 (m, 1H), 8.64–8.60 (m, 1H), 8.55–8.52 (m, 1H), 8.27–7.87 (m, 1H).

Synthesis of 5-Quinoxalin-2-yl-3H-oxazol-2-one (11m). Compound **11m** was prepared using **10m** (0.230 g, 0.80 mmol) and LiOH (0.077 g, 3.20 mmol), according to general procedure B, Step 2. After aq work-up, the resulting solid was collected by filtration to afford **11m** as an orange solid (0.158 g, 93%). 1H NMR (400 MHz, $DMSO-d_6$): δ 11.46 (bs, 1H), 9.17 (s, 1H), 8.18 (d, $J = 2.3$ Hz, 1H), 8.12–7.99 (m, 2H), 7.90–7.65 (m, 2H). UPLC/MS (*method A*): R_t 1.29 min. MS (ES): $C_{11}H_7N_3O_2$ requires, 213; found, 214 $[M + H]^+$, 212 $[M - H]^-$.

Synthesis of 5-(1-Methylindazol-3-yl)-3H-oxazol-2-one (11n). Compound **11n** was prepared using **10n** (0.136 g, 0.47 mmol) and LiOH (0.045 g, 1.88 mmol), according to general procedure B, Step 2. The crude was purified by flash chromatography (SiO_2), eluting with DCM/MeOH (8:2), to afford **11n** as a yellow solid (0.050 g, 49%). 1H NMR (400 MHz, $DMSO-d_6$): δ 10.97 (bs, 1H), 7.97–7.92 (m, 1H),

7.70–7.64 (m, 1H), 7.59 (d, $J = 2.2$ Hz, 1H), 7.49–7.43 (m, 1H), 7.25–7.19 (m, 1H), 4.06 (s, 3H). UPLC/MS (*method D*): R_t 0.49 min. MS (ES): $C_{11}H_9N_3O_2$ requires, 215; found, 216 $[M + H]^+$, 214 $[M - H]^-$.

Synthesis of 5-Thiazol-2-yl-3H-oxazol-2-one (11o). Compound **11o** was prepared using **10o** (0.588 g, 2.43 mmol) and LiOH (0.233 g, 9.72 mmol), according to general procedure B, Step 2. After aq work-up, the resulting solid was collected by filtration to afford **11o** as a yellow solid (0.200 g, 49%). 1H NMR (400 MHz, $DMSO-d_6$): δ 11.29 (bs, 1H), 7.86 (d, $J = 3.2$ Hz, 1H), 7.73 (d, $J = 3.2$ Hz, 1H), 7.72–7.68 (m, 1H). UPLC/MS (*method A*): R_t 1.09 min. MS (ES): $C_6H_4N_2O_2S$ requires, 168; found, 169 $[M + H]^+$, 167 $[M - H]^-$.

Synthesis of 5-Thiazol-4-yl-3H-oxazol-2-one (11p). Compound **11p** was prepared using **10p** (0.152 g, 0.63 mmol) and LiOH (0.060 g, 2.52 mmol), according to general procedure B, Step 2. After aq work-up, the resulting solid was collected by filtration to afford **11p** as a brown solid (0.100 g, 94%). 1H NMR (400 MHz, $DMSO-d_6$): δ 10.92 (bs, 1H), 9.16 (d, $J = 1.9$ Hz, 1H), 7.68 (d, $J = 1.9$ Hz, 1H), 7.32 (s, 1H). UPLC/MS (*method A*): R_t 1.09 min. MS (ES): $C_6H_4N_2O_2S$ requires, 168; found, 169 $[M + H]^+$, 167 $[M - H]^-$.

Synthesis of tert-Butyl 4-(2-Oxo-3H-oxazol-5-yl)piperidine-1-carboxylate (11q). Compound **11q** was prepared using **10q** (0.300 g, 0.88 mmol) and *t*-BuOK (0.197 g, 1.75 mmol) in THF, according to general procedure B, Step 2. The crude was purified by column chromatography (SiO_2), eluting with DCM/EtOAc (3:7 to 0:10), to afford **11q** as a pale yellow solid (0.091 g, 38%). 1H NMR (400 MHz, $DMSO-d_6$): δ 10.27 (bs, 1H), 6.58 (d, $J = 1.4$ Hz, 1H), 4.02–3.79 (m, 2H), 2.97–2.68 (m, 2H), 2.63–2.52 (m, overlapped with $DMSO$ signal, 1H), 1.86–1.73 (m, 2H), 1.39 (s, 9H), 1.28 (qd, $J = 12.1, 4.3$ Hz, 2H). UPLC/MS (*method A*): R_t 1.72 min. MS (ES): $C_{13}H_{20}N_2O_4$ requires, 268; found, 267 $[M - H]^-$.

Synthesis of 2-Oxo-5-phenyl-N-(4-phenylbutyl)oxazole-3-carboxamide (12a). Compound **12a** was prepared according to general procedure D (*method A*) using **11a** (0.161 g, 1.00 mmol), DMAP (0.012 g, 0.10 mmol), and 4-phenylbutyl isocyanate (0.350 g, 2.00 mmol) in CH_3CN . The crude was purified by column chromatography (SiO_2), eluting with Cy/EtOAc (9:1), to afford **12a** as a white solid (0.276 g, 82%). 1H NMR (400 MHz, $CDCl_3$): δ 7.95 (t, $J = 5.7$ Hz, 1H), 7.57–7.49 (m, 2H), 7.46 (s, 1H), 7.45–7.32 (m, 3H), 7.32–7.25 (m, overlapped with $CDCl_3$ signal, 2H), 7.22–7.15 (m, 3H), 3.49–3.35 (m, 2H), 2.67 (t, $J = 7.2$ Hz, 2H), 1.79–1.60 (m, 4H). ^{13}C NMR (101 MHz, $CDCl_3$): δ 152.83, 148.59, 142.01, 139.77, 129.29, 129.12 (2C), 128.53, 126.41, 126.03, 123.72, 106.08, 40.44, 35.58, 29.21, 28.65. UPLC/MS (*method A*): R_t 2.74 min. MS (ES): $C_{20}H_{20}N_2O_3$ requires, 336; found, 337 $[M + H]^+$. HRMS: $C_{20}H_{20}N_2O_3Na$ $[M + Na]^+$ calcd 359.1372; measured, 359.1366, Δ ppm -0.6 .

Synthesis of 2-Oxo-N-pentyl-5-phenyl-oxazole-3-carboxamide (12b). Compound **12b** was prepared according to general procedure D (*method B*) using **11a** (0.100 g, 0.62 mmol) and *n*-pentyl amine (0.059 g, 0.68 mmol). The crude was purified by column chromatography (SiO_2), eluting with Cy/EtOAc (9:1), to afford **12b** as a white solid (0.107 g, 63%). 1H NMR (400 MHz, $CDCl_3$): δ 7.94 (bs, 1H), 7.56–7.49 (m, 2H), 7.47 (s, 1H), 7.45–7.38 (m, 2H), 7.38–7.32 (m, 1H), 3.45–3.33 (m, 2H), 1.68–1.51 (m, overlapped with H_2O signal, 2H), 1.43–1.29 (m, 4H), 0.99–0.86 (m, 3H). ^{13}C NMR (101 MHz, $CDCl_3$): δ 152.52, 148.24, 139.39, 128.92, 128.77, 126.11, 123.37, 105.79, 40.29, 28.96, 28.73, 22.11, 13.75. UPLC/MS (*method A*): R_t 2.62 min. MS (ES): $C_{15}H_{18}N_2O_3$ requires, 274; found, 275 $[M + H]^+$, 160 $[M - CONH(CH_2)_4CH_3]^-$. HRMS: $C_{15}H_{18}N_2O_3Na$ $[M + Na]^+$ calcd 297.1215; measured, 297.1207, Δ ppm -2.7 .

Synthesis of N-(2-Ethoxyethyl)-2-oxo-5-phenyl-oxazole-3-carboxamide (12c). Compound **12c** was prepared according to general procedure D (*method B*) using **11a** (0.161 g, 1.00 mmol) and 2-ethoxyethyl amine (0.178 g, 2.00 mmol). The crude was purified by column chromatography (SiO_2), eluting with Cy/EtOAc (8:2), to afford **12c** as a white solid (0.222 g, 80%). 1H NMR (400 MHz, $CDCl_3$): δ 8.21 (bs, 1H), 7.56–7.49 (m, 2H), 7.46 (s, 1H), 7.45–7.38 (m, 2H), 7.38–7.32 (m, 1H), 3.62–3.59 (m, 4H), 3.54 (q, $J = 7.0$ Hz, 2H), 1.23 (t, $J = 7.0$ Hz, 3H). ^{13}C NMR (101 MHz, $CDCl_3$): δ 152.66, 148.72, 139.77, 129.27, 129.10, 126.41, 123.71, 106.03, 68.63, 66.78,

40.56, 15.23. UPLC/MS (*method A*): R_t 2.19 min. MS (ES): $C_{14}H_{16}N_2O_4$ requires, 276; found, 277 $[M + H]^+$, 275 $[M - H]^-$, 160 $[M - CONH(CH_2)_2OCH_2CH_3]^-$. HRMS: $C_{14}H_{16}N_2O_4$ $[M + H]^+$ calcd 277.1188; measured, 277.1187, Δ ppm -0.4 .

Synthesis of *N*-(3-Methoxypropyl)-2-oxo-5-phenyl-oxazole-3-carboxamide (12d). Compound 12d was prepared according to general procedure D (*method B*) using 11a (0.100 g, 0.62 mmol) and 3-methoxypropyl amine (0.061 g, 0.68 mmol). The crude was purified by column chromatography (SiO_2), eluting with DCM/MeOH (8:2), to afford 12d as a white solid (0.082 g, 48%). 1H NMR (400 MHz, $CDCl_3$): δ 8.24 (bs, 1H), 7.56–7.49 (m, 2H), 7.46 (s, 1H), 7.45–7.38 (m, 2H), 7.38–7.32 (m, 1H), 3.56–3.47 (m, 4H), 3.38 (s, 3H), 1.89 (p, $J = 6.2$ Hz, 2H). ^{13}C NMR (101 MHz, $CDCl_3$): δ 152.71, 148.59, 129.24, 129.11, 128.44, 126.48, 123.71, 106.13, 70.86, 58.94, 38.70, 29.29. UPLC/MS (*method A*): R_t 2.11 min. MS (ES): $C_{14}H_{16}N_2O_4$ requires, 276; found, 277 $[M + H]^+$, 160 $[M - CONH(CH_2)_3OCH_3]^-$. HRMS: $C_{14}H_{16}N_2O_4$ $[M + H]^+$ calcd 277.1188; measured, 277.1183, Δ ppm -1.8 .

Synthesis of *N*-isobutyl-2-oxo-5-phenyl-oxazole-3-carboxamide (12e). Compound 12e was prepared according to general procedure D (*method C*) using 11a (0.050 g, 0.31 mmol), 2-methylpropan-1-amine (0.069 g, 0.94 mmol), and DIPEA (0.243 g, 1.88 mmol). The crude was purified by column chromatography (SiO_2), eluting with Cy/EtOAc (95:5), to afford 12e as a white solid (0.061 g, 76%). 1H NMR (400 MHz, $CDCl_3$): δ 8.01 (t, $J = 6.0$ Hz, 1H), 7.55–7.49 (m, 2H), 7.47 (s, 1H), 7.45–7.38 (m, 2H), 7.38–7.32 (m, 1H), 3.23 (t, $J = 6.4$ Hz, 2H), 1.97–1.82 (m, 1H), 0.98 (d, $J = 6.7$ Hz, 6H). ^{13}C NMR (101 MHz, $CDCl_3$): δ 152.87, 148.69, 139.71, 129.24, 129.08, 126.43, 123.69, 106.14, 47.87, 28.61, 20.10. UPLC/MS (*method A*): R_t 2.42 min. MS (ES): $C_{14}H_{16}N_2O_3$ requires, 260; found, 261 $[M + H]^+$, 160 $[M - CONHCH_2CH(CH_3)]^-$. HRMS: $C_{14}H_{16}N_2O_3Na$ $[M + Na]^+$ calcd 283.1059; measured, 283.1049, Δ ppm -3.5 .

Synthesis of (\pm)-2-Oxo-5-phenyl-*N*-s-butyl-oxazole-3-carboxamide (12f). Compound 12f was prepared according to general procedure D (*method B*) using 11a (0.161 g, 1.00 mmol) and butan-2-amine (0.110 g, 1.50 mmol). The crude was purified by column chromatography (SiO_2), eluting with Cy/EtOAc (95:5), to afford 12f as a white solid (0.062 g, 24%). 1H NMR (400 MHz, $CDCl_3$): δ 7.78 (d, $J = 7.5$ Hz, 1H), 7.58–7.49 (m, 2H), 7.46 (s, 1H), 7.45–7.38 (m, 2H), 7.38–7.32 (m, 1H), 4.02–3.85 (m, 1H), 1.60 (q, $J = 7.3$ Hz, overlapped with H_2O signal, 2H), 1.25 (d, $J = 6.6$ Hz, 3H), 0.97 (t, $J = 7.4$ Hz, 3H). ^{13}C NMR (101 MHz, $CDCl_3$): δ 152.86, 148.00, 139.67, 129.24, 129.11, 126.48, 123.71, 106.13, 48.44, 29.63, 20.50, 10.40. UPLC/MS (*method A*): R_t 2.44 min. MS (ES): $C_{14}H_{16}N_2O_3$ requires, 260; found, 261 $[M + H]^+$. HRMS: $C_{14}H_{16}N_2O_3Na$ $[M + Na]^+$ calcd 283.1059; measured, 283.1059, Δ ppm 0.0.

Synthesis of 2-Oxo-*N*,5-diphenyl-oxazole-3-carboxamide (12g). Compound 12g was prepared according to general procedure D (*method A*) using 11a (0.050 g, 0.31 mmol), Et_3N (0.125 g, 1.24 mmol), and phenyl isocyanate (0.046 g, 0.34 mmol) in CH_3CN . The crude was purified by column chromatography (SiO_2), eluting with Cy/EtOAc (95:5), to afford 12g as a white solid (0.068 g, 78%). 1H NMR (400 MHz, $CDCl_3$): δ 9.95 (bs, 1H), 7.63–7.52 (m, 5H), 7.49–7.34 (m, 5H), 7.22–7.15 (m, 1H). ^{13}C NMR (101 MHz, $CDCl_3$): δ 152.87, 145.86, 140.24, 136.43, 129.54, 129.39, 129.18, 126.17, 125.23, 123.85, 120.41, 105.83. UPLC/MS (*method B*): R_t 2.48 min. MS (ES): $C_{16}H_{12}N_2O_3$ requires, 280; found, 160 $[M - CONHPh]^-$. HRMS: $C_{16}H_{13}N_2O_2$ $[M + H]^+$ calcd 281.0923; measured, 281.0926, Δ ppm 0.

Synthesis of 4-Methyl-2-oxo-5-phenyl-*N*-(4-phenylbutyl)oxazole-3-carboxamide (12h). Compound 12h was prepared according to general procedure D (*method A*) using 11b (0.010 g, 0.057 mmol), DMAP (0.008 g, 0.06 mmol), and 4-phenylbutyl isocyanate (0.011 g, 0.06 mmol) in CH_3CN . The crude was purified by column chromatography (Al_2O_3), eluting with Cy, to afford 12h as a white solid (0.007 g, 35%). 1H NMR (400 MHz, $CDCl_3$): δ 8.33 (t, $J = 5.3$ Hz, 1H), 7.52–7.47 (m, 2H), 7.47–7.41 (m, 2H), 7.40–7.34 (m, 1H), 7.32–7.26 (m, 2H, overlapped with $CDCl_3$ signal), 7.22–7.15 (m, 3H), 3.38 (td, $J = 6.8, 5.6$ Hz, 2H), 2.67 (t, $J = 7.3$ Hz, 2H), 2.58 (s, 3H), 1.78–1.56 (m, overlapped with H_2O signal, 4H). ^{13}C NMR (101 MHz, $CDCl_3$): δ 154.02, 150.34, 142.12, 135.72, 128.92, 128.86, 128.56,

128.51, 127.12, 126.68, 126.00, 119.54, 40.17, 35.61, 29.16, 28.74, 12.16. UPLC/MS (*method B*): R_t 1.97 min. MS (ES): $C_{21}H_{22}N_2O_3$ requires, 350; found, 351 $[M + H]^+$, 174 $[M - CONH(CH_2)_4Ph]^-$. HRMS: $C_{21}H_{22}N_2O_3$ $[M + H]^+$ calcd 351.1709; measured, 351.1714, Δ ppm 1.4.

Synthesis of 5-(4-Chlorophenyl)-2-oxo-*N*-(4-phenylbutyl)oxazole-3-carboxamide (12i). Compound 12i was prepared according to general procedure D (*method A*) using 11c (0.100 g, 0.51 mmol), DMAP (0.006 g, 0.05 mmol), and 4-phenylbutyl isocyanate (0.135 g, 0.77 mmol) in CH_3CN . The precipitate was collected by filtration to afford 12i as a white solid (0.055 g, 29%). 1H NMR (400 MHz, $CDCl_3$): δ 7.91 (t, $J = 5.9$ Hz, 1H), 7.50–7.42 (m, 3H), 7.41–7.36 (m, 2H), 7.33–7.24 (m, overlapped with $CDCl_3$ signal, 2H), 7.22–7.15 (m, 3H), 3.51–3.34 (m, 2H), 2.67 (t, $J = 7.2$ Hz, 2H), 1.78–1.61 (m, 4H). ^{13}C NMR (101 MHz, $CDCl_3$): δ 152.61, 148.43, 141.98, 138.81, 135.18, 129.45, 128.53 (2C), 126.04, 124.96, 124.91, 106.51, 40.48, 35.57, 29.19, 28.63. UPLC/MS (*method B*): R_t 2.08 min. MS (ES): $C_{20}H_{19}ClN_2O_3$ requires, 370; found, 369 $[M - H]^-$ and 194 $[M - CONH(CH_2)_4Ph]^-$. HRMS: $C_{20}H_{19}ClN_2O_3$ $[M + H]^+$ calcd 371.1184; measured, 371.1168, Δ ppm 1.6.

Synthesis of 5-(4-Fluorophenyl)-2-oxo-*N*-(4-phenylbutyl)oxazole-3-carboxamide (12j). Compound 12j was prepared according to general procedure D (*method A*) using 11d (0.150 g, 0.84 mmol), DMAP (0.112 g, 0.92 mmol), and 4-phenylbutyl isocyanate (0.161 g, 0.92 mmol) in pyridine. The crude was purified by column chromatography (SiO_2), eluting with Cy/EtOAc (8:2), to afford 12j as a white solid (0.180 g, 59%). 1H NMR (400 MHz, $CDCl_3$): δ 7.92 (t, $J = 5.9$ Hz, 1H), 7.54–7.46 (m, 2H), 7.41 (s, 1H), 7.32–7.24 (m, overlapped with $CDCl_3$ signal, 2H), 7.23–7.15 (m, 3H), 7.15–7.08 (m, 2H), 3.46–3.37 (m, 2H), 2.67 (t, $J = 7.2$ Hz, 2H), 1.78–1.61 (m, 4H). ^{13}C NMR (101 MHz, $CDCl_3$): δ 163.16 (d, $J_{C-F} = 250.4$ Hz), 152.70, 148.51, 141.99, 138.97, 128.52 (2C), 125.77 (d, $J_{C-F} = 8.2$ Hz, $\times 2$), 122.69, 116.38 (d, $J_{C-F} = 22.1$ Hz), 105.78, 40.45, 35.56, 29.19, 28.63. UPLC/MS (*method A*): R_t 2.76 min. MS (ES): $C_{20}H_{19}FN_2O_3$ requires, 354; found, 353 $[M - H]^-$ and 178 $[M - CONH(CH_2)_4Ph]^-$. HRMS: $C_{20}H_{19}FN_2O_3$ $[M + H]^+$ calcd 355.1458; measured, 355.1451, Δ ppm 1.1.

Synthesis of 5-(4-Methoxyphenyl)-2-oxo-*N*-(4-phenylbutyl)oxazole-3-carboxamide (12k). Compound 12k was prepared according to general procedure D (*method A*) using 11e (0.150 g, 0.84 mmol), DMAP (0.105 g, 0.86 mmol), and 4-phenylbutyl isocyanate (0.150 g, 0.86 mmol) in pyridine. The crude was purified by column chromatography (SiO_2), eluting with Cy/EtOAc (8:2), to afford 12k as a yellow solid (0.187 g, 65%). 1H NMR (400 MHz, $CDCl_3$): δ 7.95 (t, $J = 5.9$ Hz, 1H), 7.48–7.41 (m, 2H), 7.32 (s, 1H), 7.31–7.24 (m, overlapped with $CDCl_3$ signal, 2H), 7.22–7.14 (m, 3H), 6.98–6.89 (m, 2H), 3.84 (s, 3H), 3.47–3.35 (m, 2H), 2.67 (t, $J = 7.3$ Hz, 2H), 1.78–1.60 (m, 4H). ^{13}C NMR (101 MHz, $CDCl_3$): δ 160.46, 152.91, 148.71, 142.02, 139.86, 128.53, 128.50, 126.00, 125.34, 119.05, 114.59, 104.39, 55.51, 40.38, 35.56, 29.20, 28.62. UPLC/MS (*method A*): R_t 2.72 min. MS (ES): $C_{21}H_{22}N_2O_4$ requires, 366; found, 190 $[M - CONH(CH_2)_4Ph]^-$. HRMS: $C_{21}H_{22}N_2O_4$ $[M + H]^+$ calcd 367.1658; measured, 367.1646, Δ ppm -1.2 .

Synthesis of 5-(3-Methoxyphenyl)-2-oxo-*N*-(4-phenylbutyl)oxazole-3-carboxamide (12l). Compound 12l was prepared according to general procedure D (*method A*) using 11f (0.191 g, 1.00 mmol), DMAP (0.012 g, 0.10 mmol), and 4-phenylbutyl isocyanate (0.350 g, 2.00 mmol) in CH_3CN . The precipitate was collected by filtration to afford 12l as a white solid (0.150 g, 41%). 1H NMR (400 MHz, $CDCl_3$): δ 7.94 (t, $J = 5.8$ Hz, 1H), 7.46 (s, 1H), 7.36–7.24 (m, overlapped with $CDCl_3$ signal, 3H), 7.22–7.15 (m, 3H), 7.11 (dt, $J = 7.7, 1.2$ Hz, 1H), 7.06–7.02 (m, 1H), 6.92–6.87 (m, 1H), 3.84 (s, 3H), 3.45–3.38 (m, 2H), 2.67 (t, $J = 7.3$ Hz, 2H), 1.78–1.60 (m, 4H). ^{13}C NMR (101 MHz, $CDCl_3$): δ 160.15, 152.77, 148.55, 142.01, 139.63, 130.27, 128.54, 127.61, 126.03, 116.12, 115.34, 108.94, 106.35, 104.88, 55.54, 40.45, 35.58, 29.21, 28.65. UPLC/MS (*method A*): R_t 2.73 min. MS (ES): $C_{21}H_{22}N_2O_4$ requires, 366; found, 367 $[M + H]^+$, 190 $[M - CONH(CH_2)_4Ph]^-$. HRMS: $C_{21}H_{22}N_2O_4$ $[M + H]^+$ calcd 367.1658; measured, 367.1654, Δ ppm -1.1 .

Synthesis of 5-(2-Methoxyphenyl)-2-oxo-N-(4-phenylbutyl)-oxazole-3-carboxamide (12m). Compound **12m** was prepared according to general procedure D (*method A*) using **11g** (0.120 g, 0.63 mmol), DMAP (0.084 g, 0.69 mmol), and 4-phenylbutyl isocyanate (0.121 g, 0.69 mmol) in pyridine. The crude was purified by column chromatography (SiO₂), eluting with Cy/EtOAc (8:2), to afford **12m** as a yellow solid (0.060 g, 26%). ¹H NMR (400 MHz, CDCl₃): δ 8.01 (t, *J* = 5.2 Hz, 1H), 7.65 (s, 1H), 7.63 (dd, *J* = 7.8, 1.6 Hz, 1H), 7.35–7.25 (m, overlapped with CDCl₃ signal, 3H), 7.23–7.12 (m, 3H), 7.03 (td, *J* = 7.7, 0.8 Hz, 1H), 6.99–6.93 (m, 1H), 3.95 (s, 3H), 3.46–3.37 (m, 2H), 2.67 (t, *J* = 7.3 Hz, 2H), 1.78–1.60 (m, 4H). ¹³C NMR (101 MHz, CDCl₃): δ 155.98, 152.63, 148.84, 142.05, 136.36, 129.69, 128.55, 128.51, 126.00, 125.53, 120.93, 115.43, 110.73, 110.35, 55.59, 40.38, 35.59, 29.23, 28.66. UPLC/MS (*method A*): *R*_t 2.79 min. MS (ES): C₂₁H₂₂N₂O₄ requires, 366; found, 367 [M + H]⁺, 190 [M–CONH(CH₂)₄Ph][–]. HRMS: C₂₁H₂₂N₂O₄ [M + H]⁺ calcd 367.1658; measured, 367.1655, Δppm –1.0.

Synthesis of 5-(4-Fluoro-3-methoxy-phenyl)-2-oxo-N-(4-phenylbutyl)oxazole-3-carboxamide (12n). Compound **12n** was prepared according to general procedure D (*method A*) using **11h** (0.055 g, 0.26 mmol), DMAP (0.035 g, 0.29 mmol), and 4-phenylbutyl isocyanate (0.051 g, 0.29 mmol) in pyridine. The crude was purified by column chromatography (SiO₂), eluting with DCM/MeOH (9:1), and then was triturated with pentane to afford **12n** as a white solid (0.045 g, 45%). ¹H NMR (400 MHz, CDCl₃): δ 7.91 (t, *J* = 5.2 Hz, 1H), 7.41 (s, 1H), 7.32–7.24 (m, overlapped with CDCl₃ signal, 2H), 7.23–7.15 (m, 3H), 7.15–7.03 (m, 3H), 3.93 (s, 3H), 3.47–3.37 (m, 2H), 2.67 (t, *J* = 7.0 Hz, 2H), 1.77–1.60 (m, 4H). ¹³C NMR (101 MHz, CDCl₃): δ 154.13, 152.89 (d, *J*_{C–F} = 250.1 Hz), 152.65, 148.47, 141.99, 138.98, 128.53 (2C), 126.04, 122.93 (d, *J*_{C–F} = 3.9 Hz), 116.91 (d, *J*_{C–F} = 19.5 Hz), 116.51 (d, *J*_{C–F} = 7.1 Hz), 108.86, 105.92, 56.47, 40.46, 35.56, 29.18, 28.64. UPLC/MS (*method A*): *R*_t 2.70 min. MS (ES): C₂₁H₂₁FN₂O₄ requires, 384; found, 385 [M + H]⁺, 208 [M–CONH(CH₂)₄Ph][–]. HRMS: C₂₁H₂₁FN₂O₄ [M + H]⁺ calcd 385.1564; measured, 385.1566, Δppm 0.5.

Synthesis of 2-Oxo-N-(4-phenylbutyl)-5-(2-pyridyl)oxazole-3-carboxamide (12o). Compound **12o** was prepared according to general procedure D (*method A*) using **11i** (0.280 g, 1.73 mmol), DMAP (0.232 g, 1.90 mmol), and 4-phenylbutyl isocyanate (0.333 g, 1.90 mmol) in pyridine. The crude was purified by column chromatography (SiO₂), eluting with DCM/MeOH (9:1), to afford **12o** as a white solid (0.058 g, 10%). ¹H NMR (400 MHz, CDCl₃): δ 8.60 (ddd, *J* = 4.8, 1.7, 0.9 Hz, 1H), 7.92 (t, *J* = 4.8 Hz, 1H), 7.86 (s, 1H), 7.76 (td, *J* = 7.8, 1.7 Hz, 1H), 7.55–7.48 (m, 1H), 7.31–7.22 (m, overlapped with CDCl₃ signal, 3H), 7.21–7.15 (m, 3H), 3.48–3.36 (m, 2H), 2.67 (t, *J* = 7.2 Hz, 2H), 1.79–1.60 (m, 4H). ¹³C NMR (101 MHz, CDCl₃): δ 152.66, 150.17, 148.31, 145.92, 142.01, 139.13, 137.10, 128.54 (2C), 126.03, 123.56, 118.81, 109.78, 40.50, 35.57, 29.18, 28.64. UPLC/MS (*method A*): *R*_t 2.38 min. MS (ES): C₁₉H₁₉N₃O₃ requires, 337; found, 338 [M + H]⁺, 161 [M–CONH(CH₂)₄Ph][–]. HRMS: C₁₉H₁₉N₃O₃ [M + H]⁺ calcd 338.1505; measured, 338.1497, Δppm –2.4.

Synthesis of 2-Oxo-N-(4-phenylbutyl)-5-(3-pyridyl)oxazole-3-carboxamide (12p). Compound **12p** was prepared according to general procedure D (*method A*) using **11j** (0.200 g, 1.23 mmol), DMAP (0.165 g, 1.35 mmol), and 4-phenylbutyl isocyanate (0.236 g, 1.35 mmol) in pyridine. The crude was purified by column chromatography (SiO₂), eluting with DCM/MeOH (9:1), to afford **12p** as a white solid (0.187 g, 45%). ¹H NMR (400 MHz, CDCl₃): δ 8.85–8.79 (m, 1H), 8.60 (dd, *J* = 4.9, 1.5 Hz, 1H), 7.89 (t, *J* = 5.0 Hz, 1H), 7.83 (dt, *J* = 8.0, 1.8 Hz, 1H), 7.59 (s, 1H), 7.39 (ddd, *J* = 8.0, 4.9, 0.7 Hz, 1H), 7.32–7.24 (m, overlapped with CDCl₃ signal, 2H), 7.22–7.15 (m, 3H), 3.51–3.35 (m, 2H), 2.67 (t, *J* = 7.2 Hz, 2H), 1.92–1.60 (m, overlapped with H₂O signal, 4H). ¹³C NMR (101 MHz, CDCl₃): δ 152.52, 149.90, 148.26, 144.99, 141.97, 137.06, 131.08, 128.55 (2C), 126.07, 123.89, 122.98, 107.73, 40.54, 35.57, 29.17, 28.62. UPLC/MS (*method A*): *R*_t 2.34 min. MS (ES): C₁₉H₁₉N₃O₃ requires, 337; found, 338 [M + H]⁺, 161 [M–CONH(CH₂)₄Ph][–]. HRMS: C₁₉H₁₉N₃O₃ [M + H]⁺ calcd 338.1505; measured, 338.1497, Δppm –2.4.

Synthesis of 2-Oxo-N-(4-phenylbutyl)-5-(4-pyridyl)oxazole-3-carboxamide Hydrochloride (12q). Compound **12q** was prepared

according to general procedure D (*method A*) using **11k** (0.120 g, 0.74 mmol), DMAP (0.099 g, 0.81 mmol), and 4-phenylbutyl isocyanate (0.142 g, 0.81 mmol) in pyridine. The crude was purified by column chromatography (SiO₂), eluting with DCM/MeOH (9:1), to afford the free base of **12q**. The free base of **12q** was then dissolved in 1.0 mL of 1,4-dioxane and 4.0 M HCl solution (3.7 mL, 14.8 mmol, 20.0 equiv) was added. The evaporation of solvents afforded **12q** as a white solid (0.120 g, 43%). ¹H NMR (400 MHz, DMSO-*d*₆): δ 8.84–8.78 (m, 2H), 8.72 (s, 1H), 8.08 (t, *J* = 5.9 Hz, 1H), 8.03–7.97 (m, 2H), 7.32–7.24 (m, 2H), 7.22–7.12 (m, 3H), 3.43–3.24 (m, overlapped with H₂O signal, 2H), 2.61 (t, *J* = 7.2 Hz, 2H), 1.68–1.49 (m, 4H). ¹³C NMR (101 MHz, DMSO): δ 151.14, 147.38, 144.25, 141.99, 134.41, 128.28, 128.22, 125.67, 118.87, 116.84, 40.35 (overlapped with DMSO signal), 34.70, 28.51, 28.05. UPLC/MS (*method A*): *R*_t 2.26 min. MS (ES): C₁₉H₁₉N₃O₃ requires, 337; found, 338 [M + H]⁺, 161 [M–CONH(CH₂)₄Ph][–]. HRMS: C₁₉H₁₉N₃O₃ [M + H]⁺ calcd 338.1505; measured, 338.1503, Δppm –0.6.

Synthesis of 2-Oxo-N-(4-phenylbutyl)-5-pyrazin-2-yl-oxazole-3-carboxamide (12r). Compound **12r** was prepared according to general procedure D (*method A*) using **11l** (0.027 g, 0.16 mmol), DMAP (0.022 g, 0.18 mmol), and 4-phenylbutyl isocyanate (0.033 g, 0.18 mmol) in pyridine. The crude was purified by column chromatography (SiO₂), eluting with DCM/MeOH (9:1), to afford **12r** as a white solid (0.045 g, 83%). ¹H NMR (400 MHz, CDCl₃): δ 8.83–8.77 (m, 1H), 8.59–8.50 (m, 2H), 7.92 (s, 1H), 7.89 (bs, 1H), 7.33–7.24 (m, overlapped with CDCl₃ signal, 2H), 7.22–7.15 (m, 3H), 3.49–3.38 (m, 2H), 2.67 (t, *J* = 7.2 Hz, 2H), 1.80–1.58 (m, 4H). ¹³C NMR (101 MHz, CDCl₃): δ 152.28, 147.97, 144.62, 144.40, 141.91, 140.07, 136.89, 128.50 (2C), 126.02, 111.67, 40.55, 35.52, 29.11, 28.58. UPLC/MS (*method A*): *R*_t 2.28 min. MS (ES): C₁₈H₁₈N₄O₃ requires, 338; found, 339 [M + H]⁺, 162 [M–CONH(CH₂)₄Ph][–]. HRMS: C₁₈H₁₈N₄O₃ [M + H]⁺ calcd 339.1457; measured, 339.1455, Δppm –0.6.

2-Oxo-N-(4-phenylbutyl)-5-quinoxalin-2-yl-oxazole-3-carboxamide (12s). Compound **12s** was prepared according to general procedure D (*method A*) using **11m** (0.081 g, 0.38 mmol), DMAP (0.051 g, 0.42 mmol), and 4-phenylbutyl isocyanate (0.074 g, 0.42 mmol) in pyridine. The crude was purified by column chromatography (SiO₂), eluting with DCM/MeOH (9:1), to afford **12s** as a white solid (0.063 g, 43%). ¹H NMR (400 MHz, CDCl₃): δ 9.08 (s, 1H), 8.16–8.06 (m, 3H), 7.93 (t, *J* = 5.3 Hz, 1H), 7.86–7.74 (m, 2H), 7.32–7.25 (m, overlapped with CDCl₃ signal, 2H), 7.23–7.15 (m, 3H), 3.45–3.40 (m, 2H), 2.68 (t, *J* = 7.2 Hz, 2H), 1.80–1.63 (m, 4H). ¹³C NMR (101 MHz, CDCl₃): δ 152.37, 148.02, 142.23, 142.10, 141.96, 140.84, 140.49, 137.53, 131.23, 130.65, 129.61, 129.48, 128.56 (2C), 126.08, 112.35, 40.64, 35.57, 29.15, 28.64. UPLC/MS (*method A*): *R*_t 2.49 min. MS (ES): C₂₂H₂₀N₄O₃ requires, 388; found, 389 [M + H]⁺, 212 [M–CONH(CH₂)₄Ph][–]. HRMS: C₂₂H₂₀N₄O₃ [M + H]⁺ calcd 389.1614; measured, 389.1611, Δppm –0.8.

Synthesis of 5-(1-Methylindazol-3-yl)-2-oxo-N-(4-phenylbutyl)-oxazole-3-carboxamide (12t). Compound **12t** was prepared according to general procedure D (*method A*) using **11n** (0.041 g, 0.19 mmol), DMAP (0.026 g, 0.21 mmol), and 4-phenylbutyl isocyanate (0.037 g, 0.21 mmol) in pyridine. The crude was purified by column chromatography (SiO₂), eluting with DCM/MeOH (9:1), and, then, triturated with pentane to afford **12t** as a white solid (0.040 g, 54%). ¹H NMR (400 MHz, CDCl₃): δ 7.99 (t, *J* = 5.2 Hz, 1H), 7.91 (d, *J* = 8.2 Hz, 1H), 7.65 (s, 1H), 7.50–7.40 (m, 2H), 7.34–7.23 (m, overlapped with CDCl₃ signal, 3H), 7.23–7.14 (m, 3H), 4.12 (s, 3H), 3.50–3.38 (m, 2H), 2.67 (t, *J* = 7.2 Hz, 2H), 1.80–1.59 (m, 4H). ¹³C NMR (101 MHz, CDCl₃): δ 152.64, 148.56, 142.02, 140.96, 135.22, 131.42, 128.55, 128.52, 127.27, 126.02, 122.10, 120.94, 120.82, 109.62, 107.28, 40.47, 36.07, 35.58, 29.20, 28.66. UPLC/MS (*method A*): *R*_t 2.63 min. MS (ES): C₂₂H₂₂N₄O₃ requires, 390; found, 391 [M + H]⁺, 214 [M–CONH(CH₂)₄Ph][–].

Synthesis of 2-Oxo-N-(4-phenylbutyl)-5-thiazol-2-yl-oxazole-3-carboxamide (12u). Compound **12u** was prepared according to general procedure D (*method A*) using **11o** (0.100 g, 0.59 mmol), DMAP (0.079 g, 0.65 mmol), and 4-phenylbutyl isocyanate (0.114 g, 0.65 mmol) in pyridine. The crude was purified by column chromatography (SiO₂), eluting with Cy/EtOAc (8:2), to afford **12u**

as a white solid (0.150 g, 73%). ^1H NMR (400 MHz CDCl_3): δ 7.89 (d, $J = 3.2$ Hz, 1H), 7.86 (t, $J = 5.4$ Hz, 1H), 7.80 (s, 1H), 7.42 (d, $J = 3.2$ Hz, 1H), 7.34–7.24 (m, overlapped with CDCl_3 signal, 2H), 7.23–7.12 (m, 3H), 3.47–3.35 (m, 2H), 2.66 (t, $J = 7.2$ Hz, 2H), 1.77–1.60 (m, overlapped with H_2O signal, 4H). ^{13}C NMR (101 MHz, CDCl_3): δ 151.81, 147.95, 144.46, 144.42, 141.94, 140.61, 128.53 (2C), 126.05, 119.74, 109.26, 40.58, 35.54, 29.11, 28.61. UPLC/MS (method A): R_t 2.41 min. MS (ES): $\text{C}_{17}\text{H}_{17}\text{N}_3\text{O}_3\text{S}$ requires, 343; found, 344 $[\text{M} + \text{H}]^+$, 167 $[\text{M} - \text{CONH}(\text{CH}_2)_4\text{Ph}]^-$. HRMS: $\text{C}_{17}\text{H}_{17}\text{N}_3\text{O}_3\text{S}$ $[\text{M} + \text{H}]^+$ calcd 344.1069; measured, 344.1054, $\Delta\text{ppm} -4.4$.

Synthesis of 2-Oxo-N-(4-phenylbutyl)-5-thiazol-4-yl-oxazole-3-carboxamide (12v). Compound 12v was prepared according to general procedure D (method A) using 11p (0.120 g, 0.71 mmol), DMAP (0.100 g, 0.78 mmol), and 4-phenylbutyl isocyanate (0.140 g, 0.78 mmol) in pyridine. The crude was purified by column chromatography (SiO_2), eluting with Cy/EtOAc (8:2), to afford 12v as a white solid (0.122 g, 50%). ^1H NMR (400 MHz, CDCl_3): δ 7.90 (d, $J = 3.2$ Hz, 1H), 7.86 (t, $J = 4.8$ Hz, 1H), 7.83 (s, 1H), 7.42 (d, $J = 3.2$ Hz, 1H), 7.33–7.25 (m, overlapped with CDCl_3 signal, 2H), 7.22–7.15 (m, 3H), 3.47–3.36 (m, 2H), 2.66 (t, $J = 7.2$ Hz, 2H), 1.76–1.59 (m, 4H). ^{13}C NMR (101 MHz, CDCl_3): δ 153.82, 151.80, 147.15, 144.36, 141.94, 138.47, 128.57 (2C), 126.05, 119.76, 109.41, 40.59, 35.55, 29.12, 28.62. UPLC/MS (method A): R_t 2.41 min. MS (ES): $\text{C}_{17}\text{H}_{17}\text{N}_3\text{O}_3\text{S}$ requires, 343; found, 344 $[\text{M} + \text{H}]^+$, 167 $[\text{M} - \text{CONH}(\text{CH}_2)_4\text{Ph}]^-$. HRMS: $\text{C}_{17}\text{H}_{17}\text{N}_3\text{O}_3\text{S}$ $[\text{M} + \text{H}]^+$ calcd 344.1069; measured, 344.1061, $\Delta\text{ppm} -2.3$.

Synthesis of tert-Butyl 4-[2-Oxo-3-(4-phenylbutylcarbamoyl)-oxazol-5-yl]piperidine-1-carboxylate (12w). Compound 12w was prepared according to general procedure D (method A) using 11q (0.090 g, 0.34 mmol), DMAP (0.045 g, 0.37 mmol), and 4-phenylbutyl isocyanate (0.065 g, 0.37 mmol) in CH_3CN . The crude was purified by column chromatography (SiO_2), eluting with Cy/EtOAc (65:35), to afford 12w as a white solid (0.025 g, 17%). ^1H NMR (400 MHz, CDCl_3): δ 7.88 (t, $J = 5.7$ Hz, 1H), 7.32–7.26 (m, overlapped with CDCl_3 signal, 2H), 7.21–7.12 (m, 3H), 6.87 (d, $J = 1.4$ Hz, 1H), 4.23–4.05 (m, 2H), 3.37 (q, $J = 6.5$ Hz, 2H), 2.90–2.75 (m, 2H), 2.65 (t, $J = 7.3$ Hz, 2H), 2.62–2.53 (m, 1H), 1.95–1.85 (m, 2H), 1.77–1.49 (m, 6H), 1.46 (s, 9H). UPLC/MS (method B): R_t 1.91 min. MS (ES): $\text{C}_{24}\text{H}_{33}\text{N}_3\text{O}_3$ requires, 443; found, 444 $[\text{M} + \text{H}]^+$.

Synthesis of 2-Oxo-N-(4-phenylbutyl)-5-(4-piperidyl)oxazole-3-carboxamide Hydrochloride (12x). Compound 12x was prepared according to general procedure G using 12w (0.025 g, 0.06 mmol). The crude was used in the next step without further purification. ^1H NMR (400 MHz, $\text{DMSO}-d_6$): δ 8.79 (bs, 2H), 7.98 (t, $J = 5.9$ Hz, 1H), 7.30–7.23 (m, 2H), 7.22–7.12 (m, 4H), 3.33–3.17 (m, overlapped with H_2O signal, 4H), 2.94 (td, $J = 12.2$, 3.1 Hz, 2H), 2.88–2.77 (m, 1H), 2.59 (t, $J = 7.3$ Hz, 2H), 2.04–1.94 (m, 2H), 1.78–1.64 (m, 2H), 1.62–1.44 (m, 4H). UPLC/MS (method A): R_t 1.89 min. MS (ES): $\text{C}_{19}\text{H}_{25}\text{N}_3\text{O}_3$ requires, 343; found, 344 $[\text{M} + \text{H}]^+$.

Synthesis of 5-(1-Methyl-4-piperidyl)-2-oxo-N-(4-phenylbutyl)-oxazole-3-carboxamide (12y). Compound 12y was prepared according to general procedure H using 12x (0.022 g, 0.06 mmol) and 37% aq solution of HCHO (0.023 g, 0.022 mL, 0.29 mmol). The crude was purified by column chromatography (SiO_2), eluting with DCM/MeOH (88:12), to afford 12y as a white solid (0.007 g, 34%). ^1H NMR (400 MHz, $\text{DMSO}-d_6$): δ 7.97 (t, $J = 5.9$ Hz, 1H), 7.30–7.23 (m, 2H), 7.21–7.13 (m, 3H), 7.05 (d, $J = 1.5$ Hz, 1H), 3.26 (q, $J = 6.4$ Hz, 2H), 2.74 (dt, $J = 11.7$, 3.6 Hz, 2H), 2.58 (t, $J = 7.3$ Hz, 2H), 2.44–2.33 (m, 1H), 2.15 (s, 3H), 1.91 (td, $J = 11.6$, 2.5 Hz, 2H), 1.84–1.74 (m, 2H), 1.63–1.42 (m, 6H). ^{13}C NMR (101 MHz, $\text{DMSO}-d_6$): δ 152.30, 148.08, 144.06, 142.00, 128.27, 128.21, 125.65, 106.25, 54.32 (2C), 46.06, 39.77 (overlapped with DMSO signal), 34.69, 31.87, 28.58, 28.09. UPLC/MS (method A): R_t 1.90 min. MS (ES): $\text{C}_{20}\text{H}_{27}\text{N}_3\text{O}_3$ requires, 357; found, 358 $[\text{M} + \text{H}]^+$. HRMS: $\text{C}_{20}\text{H}_{27}\text{N}_3\text{O}_3$ $[\text{M} + \text{H}]^+$ calcd 358.2131; measured, 358.2121, $\Delta\text{ppm} -2.8$.

Synthesis of N-Methyl-2-oxo-5-phenyl-N-(4-phenylbutyl)-oxazole-3-carboxamide (13a). Compound 13a was prepared according to general procedure D (method C) using 11a (0.155 g, 0.96 mmol, 1.0 equiv), N-methyl-4-phenylbutylamine hydrochloride (0.061 g, 0.32 mmol, 0.33 equiv), and DIPEA (0.496 g, 0.668 mL, 3.84

mmol, 4.0 equiv). The crude was purified by column chromatography (SiO_2), eluting with Cy/EtOAc (91:9), to afford 13a as yellow oil (0.109 g, 98%). ^1H NMR (400 MHz, $\text{DMSO}-d_6$): δ 7.82 (s, 1H), 7.62–7.56 (m, 2H), 7.50–7.42 (m, 2H), 7.40–7.32 (m, 1H), 7.30–7.23 (m, 2H), 7.22–7.14 (m, 3H), 3.46–3.37 (m, 2H), 3.00 (s, 3H), 2.65–2.56 (m, 2H), 1.65–1.51 (m, 4H). ^{13}C NMR (101 MHz, $\text{DMSO}-d_6$): δ 150.11, 149.58, 141.88, 139.14, 128.93, 128.52, 128.23 (2C), 126.66, 125.67, 122.99, 110.18, 49.52, 36.47, 34.69, 27.69 ($\times 2$). UPLC/MS (method B): R_t 1.56 min. MS (ES): $\text{C}_{21}\text{H}_{22}\text{N}_2\text{O}_3$ requires, 350; found, 351 $[\text{M} + \text{H}]^+$. HRMS: $\text{C}_{21}\text{H}_{22}\text{N}_2\text{O}_3$ $[\text{M} + \text{H}]^+$ calcd 351.1704; measured, 351.1709, $\Delta\text{ppm} -1.4$.

Synthesis of 4-Phenylbutyl-2-oxo-5-phenyl-oxazole-3-carboxylate (13b). Compound 13b was prepared according to general procedure D (method C) using 11a (0.160 g, 1.00 mmol), 4-phenyl-1-butanol (0.050 g, 0.051 mL, 0.33 mmol, 0.33 equiv), and DIPEA (0.260 g, 0.350 mL, 2.01 mmol). The crude was purified by column chromatography (SiO_2), eluting with Cy/EtOAc (94:6), to afford 13b as a white solid (0.059 g, 53%). ^1H NMR (400 MHz, CDCl_3): δ 7.58–7.50 (m, 2H), 7.49–7.37 (m, 3H), 7.33–7.24 (m, overlapped with CDCl_3 signal, 2H), 7.24–7.14 (m, 4H), 4.42 (t, $J = 6.1$ Hz, 2H), 2.70 (t, $J = 7.1$ Hz, 2H), 1.90–1.71 (m, 4H). ^{13}C NMR (101 MHz, CDCl_3): δ 149.39, 148.73, 141.80, 140.13, 129.56, 129.12, 128.57 (2C), 126.26, 126.12, 123.91, 105.95, 68.52, 35.43, 28.16, 27.45. UPLC/MS (method B): R_t 2.48 min. MS (ES): $\text{C}_{20}\text{H}_{19}\text{NO}_4$ requires, 337; found, 338 $[\text{M} + \text{H}]^+$. HRMS: $\text{C}_{20}\text{H}_{19}\text{NO}_4\text{Na}$ $[\text{M} + \text{Na}]^+$ calcd 360.1212; measured, 360.1207, $\Delta\text{ppm} -1.4$.

Synthesis of 5-Phenyl-3-(6-phenylhexanoyl)oxazol-2-one (13c). To a solution of 6-phenylhexanoic acid (0.086 g, 0.45 mmol, 1.2 equiv) in dry DCM (7.5 mL, 0.06 M) was added slowly SOCl_2 (0.169 g, 0.104 mL, 0.53 mmol, 1.5 equiv) at 0 °C. The mixture was stirred at rt for 6 h and then, the solvent was evaporated. The residue was taken up in dry THF (1.0 mL) and added dropwise over 10 min to a solution of 11a (0.060 g, 0.37 mmol, 1.0 equiv) and Et_3N (0.163 g, 0.225 mL, 1.61 mmol, 4.3 equiv) in dry THF (0.37 M) at 0 °C. The reaction mixture was stirred, and then, sat. aq NH_4Cl was added and extracted with DCM. The combined organic layers were dried over Na_2SO_4 . After the evaporation of the solvent, the crude was purified by column chromatography (SiO_2), eluting with Cy/EtOAc (97:3), to afford 13c as a white solid (0.069 g, 55%). ^1H NMR (400 MHz, $\text{DMSO}-d_6$): δ 8.06 (s, 1H), 7.71–7.63 (m, 2H), 7.50–7.42 (m, 2H), 7.42–7.35 (m, 1H), 7.30–7.23 (m, 2H), 7.22–7.13 (m, 3H), 2.94 (t, $J = 7.3$ Hz, 2H), 2.58 (t, $J = 7.7$ Hz, 2H), 1.71–1.52 (m, 4H), 1.44–1.30 (m, 2H). ^{13}C NMR (101 MHz, $\text{DMSO}-d_6$): δ 170.12, 150.51, 142.16, 139.35, 128.98, 128.96, 128.25, 128.19, 126.25, 125.59, 123.49, 106.70, 34.97, 34.65, 30.70, 27.97, 23.06. UPLC/MS (method B): R_t 2.16 min. MS (ES): $\text{C}_{21}\text{H}_{21}\text{NO}_3$ requires, 335; found, 336 $[\text{M} + \text{H}]^+$, 334 $[\text{M} - \text{H}]^-$. HRMS: $\text{C}_{21}\text{H}_{21}\text{NO}_3\text{Na}$ $[\text{M} + \text{Na}]^+$ calcd 358.1419; measured, 358.1416, $\Delta\text{ppm} -0.8$.

Synthesis of (4S)-(+)-2-Oxo-4-phenyl-N-(4-phenylbutyl)-oxazolidine-3-carboxamide (15a). Compound 15a was prepared according to general procedure D (method A) at 50 °C using 14a (0.250 g, 1.53 mmol), DMAP (0.206 g, 0.17 mmol), and 4-phenylbutyl isocyanate (0.279 g, 1.70 mmol) in DMF. The crude was purified by column chromatography (SiO_2), eluting with Cy/EtOAc (85:15), to afford 15a as a white solid (0.420 g, 81%). ^1H NMR (400 MHz, CDCl_3): δ 7.81 (bs, 1H), 7.42–7.23 (m, overlapped with CDCl_3 signal, 7H), 7.21–7.10 (m, 3H), 5.43 (dd, $J = 8.9$, 3.8 Hz, 1H), 4.71 (t, $J = 8.9$ Hz, 1H), 4.28 (dd, $J = 8.8$, 3.8 Hz, 1H), 3.37–3.12 (m, 2H), 2.61 (t, $J = 7.5$ Hz, 2H), 1.70–1.44 (m, overlapped with H_2O signal, 4H). ^{13}C NMR (101 MHz, CDCl_3): δ 156.01, 151.05, 142.17, 139.70, 129.32, 128.80, 128.50, 128.45, 125.95, 125.91, 70.47, 57.72, 40.05, 35.56, 29.31, 28.65. $[\alpha]_D^{30} +71.8$ (c 0.1, CHCl_3). UPLC/MS (method A): R_t 2.48 min. MS (ES): $\text{C}_{20}\text{H}_{22}\text{N}_2\text{O}_3$ requires, 338; found, 339 $[\text{M} + \text{H}]^+$. HRMS: $\text{C}_{20}\text{H}_{22}\text{N}_2\text{O}_3$ $[\text{M} + \text{H}]^+$ calcd 339.1709; measured, 339.1697, $\Delta\text{ppm} -1.2$.

Synthesis of (4R)-(–)-2-Oxo-4-phenyl-N-(4-phenylbutyl)-oxazolidine-3-carboxamide (15b). Compound 15b was prepared according to general procedure D (method A) using 14b (0.326 g, 2.00 mmol), DMAP (0.268 g, 2.20 mmol), and 4-phenylbutyl isocyanate (0.385 g, 2.20 mmol) in pyridine. The crude was purified by column

chromatography (SiO₂), eluting with Cy/EtOAc (85:15), to afford **15b** as a white solid (0.320 g, 47%). ¹H NMR (400 MHz, CDCl₃): δ 7.81 (bs, 1H), 7.42–7.23 (m, overlapped with CDCl₃ signal, 7H), 7.21–7.10 (m, 3H), 5.43 (dd, *J* = 8.9, 3.8 Hz, 1H), 4.71 (t, *J* = 8.9 Hz, 1H), 4.28 (dd, *J* = 8.8, 3.8 Hz, 1H), 3.37–3.12 (m, 2H), 2.61 (t, *J* = 7.5 Hz, 2H), 1.70–1.44 (m, overlapped with H₂O signal, 4H). ¹³C NMR (101 MHz, CDCl₃): δ 155.92, 150.96, 142.08, 139.65, 129.20, 128.67, 128.41, 128.35, 125.85, 125.82, 70.36, 57.59, 39.92, 35.45, 29.21, 28.55. [α]_D³⁰ –39.8 (c 0.1, CHCl₃). UPLC/MS (method A): *R*_t 2.48 min. MS (ES): C₂₀H₂₂N₂O₃ requires, 338; found, 339 [M + H]⁺. HRMS: C₂₀H₂₂N₂O₃ [M + H]⁺ calcd 339.1709; measured, 339.1714, Δppm 0.5.

Synthesis of (5S)-(+)-5-Phenylloxazolidin-2-one (17a). Compound **17a** was prepared according to general procedure C using **16a** (0.100 g, 0.73 mmol). The crude was purified by column chromatography (SiO₂), eluting with DCM/MeOH (8:2), to afford **17a** as a white solid (0.103 g, 86%). ¹H NMR (400 MHz, CDCl₃): δ 7.49–7.31 (m, 5H), 5.72–5.49 (m, 2H), 3.98 (t, *J* = 8.6 Hz, 1H), 3.58–3.51 (m, 1H). [α]_D³⁰ +28.3 (c 0.6, EtOH), consistent with data reported in the literature (lit.⁷³ [α]_D³⁰ +26.1 (c 0.88, EtOH)). UPLC/MS (method A): *R*_t 1.41 min. MS (ES): C₉H₉NO₂ requires, 163; found, 164 [M + H]⁺.

Synthesis of (5R)-(–)-5-Phenylloxazolidin-2-one (17b). Compound **17b** was prepared according to general procedure C using **16b** (0.100 g, 0.73 mmol). The crude was purified by column chromatography (SiO₂), eluting with DCM/MeOH (9:1), to afford **17b** as a whitish solid (0.109 g, 92%). ¹H NMR (400 MHz, CDCl₃): δ 7.49–7.31 (m, 5H), 5.63 (t, *J* = 8.1 Hz, 1H), 5.35 (bs, 1H), 4.02–3.95 (m, 1H), 3.58–3.51 (m, 1H). [α]_D³⁰ –26.0 (c 0.5, EtOH), consistent with data reported in the literature (lit.⁷⁴ [α]_D²² –24.6° (c 0.045, EtOH)). UPLC/MS (method A): *R*_t 1.41 min. MS (ES): C₉H₉NO₂ requires, 163; found, 164 [M + H]⁺.

Synthesis of (5S)-(–)-2-Oxo-5-phenyl-N-(4-phenylbutyl)-oxazolidin-3-carboxamide (18a). Compound **18a** was prepared according to general procedure D (method A) at 50 °C using compound **17a** (0.103 g, 0.63 mmol), DMAP (0.084 g, 0.69 mmol), and 4-phenylbutyl isocyanate (0.122 g, 0.69 mmol) in DMF. The crude was purified by column chromatography (SiO₂), eluting with DCM/MeOH (97:3), to afford **18a** as colorless oil (0.146 g, 68%). ¹H NMR (400 MHz, CDCl₃): δ 7.80 (bs, 1H), 7.47–7.39 (m, 3H), 7.39–7.34 (m, 2H), 7.31–7.24 (m, overlapped with CDCl₃ signal, 2H), 7.22–7.14 (m, 3H), 5.58 (t, *J* = 8.3 Hz, 1H), 4.43 (dd, *J* = 10.5, 8.9 Hz, 1H), 3.96 (dd, *J* = 10.5, 7.7 Hz, 1H), 3.40–3.26 (m, 2H), 2.65 (t, *J* = 7.4 Hz, 2H), 1.77–1.57 (m, 4H). ¹³C NMR (101 MHz, CDCl₃): δ 155.35, 151.61, 142.17, 137.15, 129.54, 129.24, 128.55, 128.49, 125.96, 125.89, 75.45, 49.86, 40.18, 35.62, 29.38, 28.71. [α]_D³⁰ –8.70 (c 0.1, CHCl₃). UPLC/MS (method B): *R*_t 1.50 min. MS (ES): C₂₀H₂₂N₂O₃ requires, 338; found, 339 [M + H]⁺. HRMS: C₂₀H₂₂N₂O₃ [M + H]⁺ calcd 339.1709; measured, 339.1703, Δppm –1.8.

Synthesis of (5R)-(+)-2-Oxo-5-phenyl-N-(4-phenylbutyl)-oxazolidin-3-carboxamide (18b). Compound **18b** was prepared according to general procedure D (method A) using **17b** (0.109 g, 0.67 mmol), DMAP (0.084 g, 0.74 mmol), and 4-phenylbutyl isocyanate (0.130 g, 0.74 mmol) in pyridine. The crude was purified by column chromatography (SiO₂), eluting with Cy/EtOAc (9:1), to afford **18b** as colorless oil (0.180 g, 79%). ¹H NMR (400 MHz, CDCl₃): δ 7.80 (bs, 1H), 7.47–7.39 (m, 3H), 7.39–7.34 (m, 2H), 7.31–7.24 (m, overlapped with CDCl₃ signal, 2H), 7.22–7.14 (m, 3H), 5.58 (t, *J* = 8.3 Hz, 1H), 4.43 (dd, *J* = 10.5, 8.9 Hz, 1H), 3.96 (dd, *J* = 10.5, 7.7 Hz, 1H), 3.40–3.26 (m, 2H), 2.65 (t, *J* = 7.4 Hz, 2H), 1.77–1.57 (m, 4H). ¹³C NMR (101 MHz, CDCl₃): δ 155.35, 151.61, 142.17, 137.15, 129.54, 129.24, 128.55, 128.49, 125.96, 125.89, 75.45, 49.86, 40.18, 35.62, 29.38, 28.71. [α]_D³⁰ +18.9 (c 0.1, CHCl₃). UPLC/MS (method B): *R*_t 1.50 min. MS (ES): C₂₀H₂₂N₂O₃ requires, 338; found, 339 [M + H]⁺. HRMS: C₂₀H₂₂N₂O₃ [M + H]⁺ calcd 339.1709; measured, 339.1704, Δppm –1.5.

Synthesis of tert-Butyl 4-(3-Acetylphenyl)-3,6-dihydro-2H-pyridine-1-carboxylate (21a). Compound **21a** was prepared according to general procedure E using **20a** (0.500 g, 2.50 mmol) and **19** (0.850 g, 2.75 mmol). The crude was purified by column chromatography (SiO₂), eluting with Cy/EtOAc (8:2), to afford **21a** as yellowish oil (0.580 g, 77%). ¹H NMR (400 MHz, CDCl₃): δ 7.99–7.94 (m, 1H),

7.87–7.81 (m, 1H), 7.60–7.54 (m, 1H), 7.43 (t, *J* = 7.7 Hz, 1H), 6.15–6.08 (m, 1H), 4.12–4.07 (m, 2H), 3.66 (t, *J* = 5.7 Hz, 2H), 2.62 (s, 3H), 2.59–2.52 (m, 2H), 1.50 (s, 9H). UPLC/MS (method A): *R*_t 2.42 min. MS (ES): C₁₈H₂₃NO₃ requires, 301; found, 302 [M + H]⁺.

Synthesis of tert-Butyl 4-(5-Acetyl-2-fluoro-phenyl)-3,6-dihydro-2H-pyridine-1-carboxylate (21b). Compound **21b** was prepared according to general procedure E using **20b** (1.000 g, 4.61 mmol) and **19** (1.568 g, 5.07 mmol). The crude was purified by column chromatography (SiO₂), eluting with Cy/EtOAc (9:1), to afford **20b** as colorless oil (1.280 g, 87%). ¹H NMR (400 MHz, CDCl₃): δ 7.91–7.81 (m, 2H), 7.11 (dd, *J* = 10.4, 8.5 Hz, 1H), 6.04–5.94 (m, 1H), 4.11–4.06 (m, 2H), 3.63 (t, *J* = 5.7 Hz, 2H), 2.59 (s, 3H), 2.54–2.49 (m, 2H), 1.50 (s, 9H). UPLC/MS (method A): *R*_t 2.56 min. MS (ES): C₁₈H₂₂FNO₃ requires, 319; found, 320 [M + H]⁺.

Synthesis of tert-Butyl 4-(3-Acetylphenyl)piperidine-1-carboxylate (22a). Compound **22a** was prepared according to general procedure F (method A) using **21a** (0.510 g, 1.69 mmol). The crude was used in the next step without further purification. ¹H NMR (400 MHz, CDCl₃): δ 7.88–7.76 (m, 2H), 7.44–7.38 (m, 2H), 4.32–4.21 (m, 2H), 2.81 (td, *J* = 13.0, 2.7 Hz, 2H), 2.72 (tt, *J* = 12.1, 3.7 Hz, 1H), 2.60 (s, 3H), 1.89–1.78 (m, 2H), 1.65 (qd, *J* = 12.7, 4.5 Hz, 2H), 1.49 (s, 9H). UPLC/MS (method A): *R*_t 2.43 min. MS (ES): C₁₈H₂₅NO₃ requires, 303; found, 304 [M + H]⁺.

Synthesis of tert-Butyl 4-(5-Acetyl-2-fluoro-phenyl)piperidine-1-carboxylate (22b). Compound **22b** was prepared according to general procedure F (method A) using **21b** (1.000 g, 3.13 mmol). The crude was purified by column chromatography (SiO₂), eluting with Cy/EtOAc (9:1), to afford **21b** as colorless oil (0.650 g, 65%). ¹H NMR (400 MHz, CDCl₃): δ 7.87–7.84 (m, 1H), 7.84–7.78 (m, 1H), 7.09 (dd, *J* = 9.9, 8.5 Hz, 1H), 4.34–4.22 (m, 2H), 3.02 (tt, *J* = 12.1, 3.6 Hz, 1H), 2.83 (td, *J* = 13.2, 2.7 Hz, 2H), 2.58 (s, 3H), 1.86–1.78 (m, 2H), 1.68 (qd, *J* = 12.6, 4.1 Hz, 2H), 1.48 (s, 9H). UPLC/MS (method A): *R*_t 2.54 min. MS (ES): C₁₈H₂₄FNO₃ requires, 321; found, 322 [M + H]⁺.

Synthesis of tert-Butyl 4-[3-(2-Bromoacetyl)phenyl]piperidine-1-carboxylate (22c). To a solution of **22a** (0.370 g, 1.22 mmol, 1.0 equiv) in dry THF (12 mL, 0.1 M), Et₃N (0.494 g, 0.68 mmol, 4.88 mmol, 4.0 equiv) was added at 0 °C under a N₂ atmosphere. After 30 min, TMSOTf (0.425 g, 0.35 mL, 1.92 mmol, 1.5 equiv) was added dropwise at –78 °C. The mixture was stirred at –50 °C for 4 h and then quenched with cold 5% aq NaHCO₃ solution and extracted with cold EtOAc (3 times). The combined organic layer was dried over Na₂SO₄. After evaporation of the solvent, the crude was dissolved in dry THF (12 mL, 0.1 M) and NBS (0.230 g, 1.28 mmol, 1.0 equiv) was added at –40 °C, and the mixture was stirred at –20 °C for additional 30 min. The reaction was diluted with H₂O and extracted with EtOAc. The combined organic layer was washed with brine and dried over Na₂SO₄. After evaporation of the solvent, **22c** was used in the next step without further purification. UPLC/MS (method A): *R*_t 2.66 min. MS (ES): C₁₈H₂₄BrNO₃ requires, 381; found, 382 [M + H]⁺.

Synthesis of tert-Butyl 4-[5-(2-Bromoacetyl)-2-fluoro-phenyl]piperidine-1-carboxylate (22d). To a solution of **22b** (0.450 g, 1.40 mmol, 1.0 equiv) in dry THF (14 mL, 0.1 M), Et₃N (0.570 g, 0.780 mL, 5.60 mmol, 4.0 equiv) was added at 0 °C under a N₂ atmosphere. After 30 min, TMSOTf (0.470 g, 0.380 mL, 2.10 mmol, 1.5 equiv) was added dropwise at –78 °C. The mixture was stirred at –50 °C for 4 h. Then, the mixture was quenched with cold 5% aq NaHCO₃ solution and extracted with cold EtOAc (3 times). The combined organic layer was dried over Na₂SO₄ and the solvent was removed under vacuum. The crude was dissolved in dry THF (14 mL, 0.1 M) and NBS (0.230 g, 1.28 mmol, 1.0 equiv) was added at –40 °C, and the mixture was stirred at –20 °C for an additional 30 min. The reaction was diluted with H₂O and extracted with EtOAc. The combined organic layer was washed with brine and dried over Na₂SO₄. After evaporation of the solvent, **22d** was used as the crude in the next step without further purification. UPLC/MS (method B): *R*_t 1.68 min. MS (ES): C₁₈H₂₃BrFNO₃ requires, 399; found, 400 [M + H]⁺.

Synthesis of tert-Butyl 4-[3-[2-(2,4-Dioxothiazolidin-3-yl)acetyl]phenyl]piperidine-1-carboxylate (23a). Compound **23a** was prepared according to general procedure B, Step 1, using **22c** (0.466 g, 1.22 mmol). The crude was used in Step 2 without further purification.

UPLC/MS (*method A*): R_t 2.46 min. MS (ES): $C_{21}H_{26}N_2O_5S$ requires, 418; found, 419 $[M + H]^+$, 417 $[M - H]^-$.

Synthesis of tert-Butyl 4-[5-[2-(2,4-Dioxothiazolidin-3-yl)acetyl]-2-fluoro-phenyl]piperidine-1-carboxylate (23b). Compound 23b was prepared according to general procedure B, Step 1, using 22d (0.560 g, 1.40 mmol, 1.0 equiv). The crude was purified by column chromatography (SiO_2), eluting with Cy/EtOAc (9:1), to afford 23b as a white solid (0.570 g, 93%). 1H NMR (600 MHz, $CDCl_3$): δ 7.87–7.80 (m, 2H), 7.15 (dd, $J = 9.8, 8.4$ Hz, 1H), 5.00 (s, 2H), 4.32–4.24 (m, 2H), 4.10 (s, 2H), 3.04 (tt, $J = 12.2, 3.5$ Hz, 1H), 2.83 (td, $J = 13.1, 2.6$ Hz, 2H), 1.86–1.78 (m, 2H), 1.67 (qd, $J = 12.8, 4.4$ Hz, 2H), 1.48 (s, 9H). UPLC/MS (*method A*): R_t 2.50 min. MS (ES): $C_{21}H_{25}FN_2O_5S$ requires, 436; found, 437 $[M + H]^+$.

Synthesis of tert-Butyl 4-[3-(2-Oxo-3H-oxazol-5-yl)phenyl]piperidine-1-carboxylate (24a). Compound 24a was prepared using 23a (0.509 g, 1.22 mmol) and LiOH (0.117 g, 4.88 mmol), according to general procedure B, Step 2. The crude was purified by flash chromatography (SiO_2), eluting with Cy/EtOAc (9:1), to afford 24a as colorless oil (0.120 g, 29%). 1H NMR (400 MHz, $CDCl_3$): δ 7.43–7.39 (m, 2H), 7.34–7.31 (m, 1H), 7.29–7.24 (m, overlapped with $CDCl_3$ signal, 1H), 6.95 (s, 1H), 4.29–4.19 (m, 2H), 2.94 (tt, $J = 11.8, 3.3$ Hz, 1H), 2.84–2.73 (m, 2H), 1.83–1.75 (m, 2H), 1.70–1.60 (m, overlapped with H_2O signal, 2H), 1.48 (s, 9H). UPLC/MS (*method A*): R_t 2.83 min. MS (ES): $C_{19}H_{24}N_2O_4$ requires, 344; found, 345 $[M + H]^+$.

Synthesis of tert-Butyl 4-[2-Fluoro-5-(2-oxo-3H-oxazol-5-yl)phenyl]piperidine-1-carboxylate (24b). Compound 24b was prepared using 23b (0.560 g, 1.30 mmol) and *t*-BuOK (0.586 g, 5.22 mmol, 4.0 equiv), according to general procedure B, Step 2. The crude was purified by flash chromatography (SiO_2), eluting with Cy/EtOAc (6:4), to afford 24b as an orange solid (0.340 g, 72%). 1H NMR (600 MHz, $CDCl_3$): δ 9.22–9.12 (m, 1H), 7.36–7.29 (m, 2H), 7.04 (dd, $J = 9.9, 8.5$ Hz, 1H), 6.79–6.76 (m, 1H), 4.35–4.20 (m, 2H), 3.01 (tt, $J = 12.2, 3.5$ Hz, 1H), 2.87–2.76 (m, 2H), 1.84–1.75 (m, 2H), 1.66 (qd, $J = 12.7, 4.4$ Hz, 2H), 1.48 (s, 9H). UPLC/MS (*method A*): R_t 2.30 min. MS (ES): $C_{19}H_{23}FN_2O_4$ requires, 362; found, 363 $[M + H]^+$, 361 $[M - H]^-$.

Synthesis of 5-[4-Fluoro-3-(4-piperidyl)phenyl]-3H-oxazol-2-one Hydrochloride (24c). Compound 24c was prepared according to general procedure G using 24b (0.150 g, 0.41 mmol). The crude was used in the next step without further purification. UPLC/MS (*method A*): R_t 1.22 min. MS (ES): $C_{14}H_{13}FN_2O_2$ requires, 262; found, 263 $[M + H]^+$, 261 $[M - H]^-$.

Synthesis of 5-[4-Fluoro-3-(1-methyl-4-piperidyl)phenyl]-3H-oxazol-2-one (24d). Compound 24d was prepared according to general procedure H using 24c (0.123 g, 0.41 mmol) and 37% aq. solution of HCHO (0.066 g, 0.061 mL, 0.82 mmol). The crude was purified by trituration with Et_2O to afford 24d as a white solid (0.080 g, 71%). 1H NMR (400 MHz, $CDCl_3$): δ 7.48–7.41 (m, 1H), 7.38–7.31 (m, 1H), 7.08–6.99 (m, 1H), 6.91 (s, 1H), 3.48–3.36 (m, 2H), 3.10–2.98 (m, 1H), 2.67 (s, 3H), 2.66–2.53 (m, 2H), 2.37–2.20 (m, 2H), 2.02–1.91 (m, 2H). UPLC/MS (*method A*): R_t 1.23 min. MS (ES): $C_{15}H_{17}FN_2O_2$ requires, 276; found, 277 $[M + H]^+$, 275 $[M - H]^-$.

Synthesis of tert-Butyl 4-[3-[2-Oxo-3-(4-phenylbutyl)carbamoyl]-oxazol-5-yl]phenylpiperidine-1-carboxylate (25a). Compound 25a was prepared according to general procedure D (*method A*) using 24a (0.120 g, 0.35 mmol), DMAP (0.047 g, 0.39 mmol) and 4-phenylbutyl isocyanate (0.068 g, 0.067 mL, 0.39 mmol) in pyridine. The crude was purified by column chromatography (SiO_2), eluting with Cy/EtOAc (9:1), to afford 25a as yellowish oil (0.125 g, 69%). UPLC/MS (*method B*): R_t 2.46 min. MS (ES): $C_{30}H_{37}N_3O_3$ requires, 519; found, 520 $[M + H]^+$.

Synthesis of 2-Oxo-N-(4-phenylbutyl)-5-[3-(4-piperidyl)phenyl]-oxazole-3-carboxamide Hydrochloride (25b). Compound 25b was prepared according to general procedure G using 25a (0.125 g, 0.24 mmol). The crude was purified by trituration with Et_2O to afford 25b as a white solid (0.046 g, 46%). 1H NMR (400 MHz, $DMSO-d_6$): δ 8.66 (bs, 2H), 8.12 (t, $J = 5.9$ Hz, 1H), 7.57 (s, 1H), 7.52–7.45 (m, 2H), 7.39–7.32 (m, 2H), 7.31–7.24 (m, 2H), 7.24–7.11 (m, 3H), 3.43–3.26 (m, overlapped with H_2O signal, 4H), 3.24–3.13 (m, 1H), 3.09–2.90 (m, 1H), 2.61 (t, $J = 7.2$ Hz, 2H), 1.95–1.77 (m, 4H), 1.68–1.48

(m, 4H). UPLC/MS (*method B*): R_t 1.72 min. MS (ES): $C_{25}H_{29}N_3O_3$ requires, 419; found, 420 $[M + H]^+$, 418 $[M - H]^-$.

Synthesis of 5-[3-(1-Methyl-4-piperidyl)phenyl]-2-oxo-N-(4-phenylbutyl)oxazole-3-carboxamide (25c). Compound 25c was prepared according to general procedure H using 25b (0.046 g, 0.01 mmol) and 37% aq. solution of HCHO (0.016 g, 0.015 mL, 0.19 mmol). The crude was purified by trituration with Et_2O to afford 25c as a white solid (0.025 g, 60%). 1H NMR (400 MHz, $CDCl_3$): δ 7.99 (t, $J = 5.9$ Hz, 1H), 7.48–7.37 (m, 3H), 7.34–7.22 (m, overlapped with $CDCl_3$ signal, 4H), 7.25–7.16 (m, 3H), 3.48–3.39 (m, 2H), 3.11–2.98 (m, 2H), 2.80 (tt, $J = 11.9, 3.8$ Hz, 1H), 2.67 (t, $J = 7.2$ Hz, 2H), 2.38 (s, 3H), 2.23–2.09 (m, 2H), 2.03–1.87 (m, 2H), 1.86–1.78 (m, 2H), 1.78–1.60 (m, overlapped with H_2O signal, 4H). ^{13}C NMR (101 MHz, $CDCl_3$): δ 152.89, 148.67, 144.41, 141.99, 139.54, 130.49, 129.13, 128.53 (2C), 127.01, 126.68, 126.04, 125.01, 108.93, 56.16, 46.11, 40.44, 38.30, 35.57, 32.89, 29.22, 28.65. UPLC/MS (*method B*): R_t 1.10 min. MS (ES): $C_{26}H_{31}N_3O_3$ requires, 433; found, 434 $[M + H]^+$, 257 $[M - CONH(CH_2)_4Ph]^-$. HRMS: $C_{26}H_{31}N_3O_3$ $[M + H]^+$ calcd 434.2444; measured, 434.2450, Δ ppm 1.4.

Synthesis of 5-[4-Fluoro-3-(1-methyl-4-piperidyl)phenyl]-2-oxo-N-(4-phenylbutyl)oxazole-3-carboxamide (25d). Compound 25d was prepared according to general procedure D (*method A*) using 24d (0.075 g, 0.27 mmol), DMAP (0.037 g, 0.30 mmol), and 4-phenylbutyl isocyanate (0.095 g, 0.092 mL, 0.54 mmol) in pyridine at 50 °C. The crude was purified by column chromatography (SiO_2), eluting with DCM/MeOH (92:8), to afford 25d as a white solid (0.030 g, 25%). 1H NMR (400 MHz, $CDCl_3$): δ 7.92 (t, $J = 5.8$ Hz, 1H), 7.41 (dd, $J = 6.9, 2.3$ Hz, 1H), 7.38 (s, 1H), 7.34 (ddd, $J = 8.5, 4.8, 2.3$ Hz, 1H), 7.31–7.26 (m, overlapped with $CDCl_3$ signal, 2H), 7.22–7.13 (m, 3H), 7.06 (dd, $J = 9.9, 8.5$ Hz, 1H), 3.45–3.36 (m, 2H), 3.14–3.00 (m, 2H), 2.94–2.81 (m, 1H), 2.66 (t, $J = 7.2$ Hz, 2H), 2.40 (s, 3H), 2.26–2.13 (m, 2H), 2.01–1.80 (m, 4H), 1.77–1.60 (m, 4H). ^{13}C NMR (101 MHz, $CDCl_3$): δ 152.70, 148.52, 142.02, 139.03, 128.56, 128.53, 126.03, 123.38, 122.98, 116.42 (d, $J_{C-F} = 24.2$ Hz), 105.90, 55.80, 45.60, 40.46, 35.57, 34.37, 30.85, 29.20, 28.64. UPLC/MS (*method A*): R_t 2.30 min. MS (ES): $C_{26}H_{30}FN_3O_3$ requires, 451; found, 452 $[M + H]^+$, 275 $[M - CONH(CH_2)_4Ph]^-$. HRMS: $C_{26}H_{30}FN_3O_3$ $[M + H]^+$ calcd 452.2349; measured, 452.2340, Δ ppm –2.0.

Synthesis of 5-[4-Fluoro-3-(1-methyl-4-piperidyl)phenyl]-2-oxo-N-pentyl-oxazole-3-carboxamide (25e). Compound 25e was prepared according to general procedure D (*method A*), using 24d (0.070 g, 0.25 mmol), Et_3N (0.050 g, 0.070 mL, 0.05 mmol) and pentyl isocyanate (0.034 g, 0.038 mL, 0.30 mmol) in CH_3CN at 50 °C. The crude was purified by column chromatography (SiO_2), eluting with DCM/MeOH (9:1), to afford 25e as a white solid (0.035 g, 36%). 1H NMR (400 MHz, $DMSO-d_6$): δ 8.09 (s, 1H), 8.01 (t, $J = 5.8$ Hz, 1H), 7.68–7.62 (m, 1H), 7.55–7.49 (m, 1H), 7.23 (dd, $J = 10.3, 8.7$ Hz, 1H), 3.33–3.22 (m, overlapped with H_2O signal, 2H), 3.02–2.89 (m, 2H), 2.79 (tt, $J = 11.7, 3.5$ Hz, 1H), 2.28 (s, 3H), 2.20–2.02 (m, 2H), 1.82 (qd, $J = 12.4, 3.3$ Hz, 2H), 1.75–1.66 (m, 2H), 1.53 (p, $J = 7.2$ Hz, 2H), 1.37–1.21 (m, 4H), 0.88 (t, $J = 6.8$ Hz, 3H). ^{13}C NMR (101 MHz, $DMSO-d_6$): δ 159.96 (d, $J_{C-F} = 246.6$ Hz), 151.80, 147.92, 142.44, 137.69, 132.80, 123.23, 123.15 (d, $J_{C-F} = 3.1$ Hz), 116.08 (d, $J = 24.1$ Hz), 107.61, 54.89, 44.95, 40.11 (overlapped with $DMSO$ signal), 33.82, 30.38, 28.61, 28.34, 21.76, 13.85. UPLC/MS (*method A*): R_t 2.12 min. MS (ES): $C_{21}H_{28}FN_3O_3$ requires, 389; found, 390 $[M + H]^+$, 275 $[M - CONH(CH_2)_4CH_3]^-$. HRMS: $C_{21}H_{28}FN_3O_3$ $[M + H]^+$ calcd 390.2193; measured, 390.2195, Δ ppm 0.5.

Synthesis of 5-[4-Fluoro-3-(1-methyl-4-piperidyl)phenyl]-N-isobutyl-2-oxo-oxazole-3-carboxamide (25f). Compound 25f was prepared according to general procedure D (*method C*) using 24d (0.035 g, 0.13 mmol), 2-methylpropan-1-amine (0.028 g, 0.030 mL, 0.39 mmol), and Et_3N (0.079 g, 0.109 mL, 0.78 mmol). The crude was purified by column chromatography (SiO_2), eluting with DCM/MeOH (9:1), to afford 25f as a white solid (0.040 g, 82%). 1H NMR (400 MHz, $CDCl_3$): δ 7.98 (t, $J = 4.9$ Hz, 1H), 7.45–7.41 (m, 1H), 7.41 (s, 1H), 7.35 (ddd, $J = 8.6, 4.8, 2.2$ Hz, 1H), 7.07 (dd, $J = 10.0, 8.5$ Hz, 1H), 3.23 (t, $J = 6.4$ Hz, 2H), 3.20–3.11 (m, 2H), 2.92 (tt, $J = 11.5, 2.9$ Hz, 1H), 2.47 (s, 3H), 2.40–2.25 (m, 2H), 2.11–1.96 (m, 2H), 1.95–1.82 (m, 3H), 0.98 (d, $J = 6.7$ Hz, 6H). ^{13}C NMR (101 MHz, $CDCl_3$): δ 161.07

(d, J_{C-F} = 249.2 Hz), 152.75, 148.63, 139.04, 133.22 (d, J = 15.4 Hz), 123.45, 123.40, 122.93 (d, J_{C-F} = 3.5 Hz), 116.38 (d, J_{C-F} = 24.2 Hz), 105.86 (d, J_{C-F} = 2.1 Hz), 55.93, 47.89, 45.88, 34.56, 31.19, 28.61, 20.11. UPLC/MS (method A): R_t 1.96 min. MS (ES): $C_{20}H_{26}FN_3O_3$ requires, 375; found, 376 $[M + H]^+$, 275 $[M - CONHCH_2CH(CH_3)_2]^-$. HRMS: $C_{20}H_{26}FN_3O_3$ $[M + H]^+$ calcd 376.2036 measured 376.2028, Δ ppm -2.1.

Synthesis of tert-Butyl 4-(2-Acetyl-5-fluoro-phenyl)-3,6-dihydro-2H-pyridine-1-carboxylate (27). Compound 27 was prepared according to general procedure E using 26 (2.000 g, 9.22 mmol) and 19 (3.990 g, 12.90 mmol). The crude was purified by column chromatography (SiO₂), eluting with Cy/EtOAc (9:1), to afford 27 as colorless oil (2.530 g, 85%). ¹H NMR (400 MHz, CDCl₃): δ 7.60 (dd, J = 8.6, 5.7 Hz, 1H), 7.05–6.99 (m, 1H), 6.92 (dd, J = 9.5, 2.6 Hz, 1H), 5.60–5.51 (m, 1H), 4.02 (q, J = 2.8 Hz, 2H), 3.65 (t, J = 5.6 Hz, 2H), 2.46 (s, 3H), 2.40–2.32 (m, 2H), 1.49 (s, 9H). UPLC/MS (method B): R_t 1.40 min. MS (ES): $C_{18}H_{22}FNO_3$ requires, 319; found, 320 $[M + H]^+$.

Synthesis of tert-Butyl 4-(2-Acetyl-5-fluoro-phenyl)piperidine-1-carboxylate (28). Compound 28 was prepared according to general procedure F (method B) using 27 (1.500 g, 4.70 mmol). The crude was purified by column chromatography (SiO₂), eluting with Cy/EtOAc (9:1), to afford 28 as colorless oil (1.040 g, 69%). ¹H NMR (400 MHz, CDCl₃): δ 7.65 (dd, J = 8.6, 5.9 Hz, 1H), 7.05 (dd, J = 10.6, 2.6 Hz, 1H), 6.98–6.92 (m, 1H), 4.31–4.16 (m, 2H), 3.43 (dddd, J = 10.0, 8.6, 3.7, 1.6 Hz, 1H), 2.81 (t, J = 12.8 Hz, 2H), 2.58 (s, 3H), 1.85–1.75 (m, 2H), 1.61–1.52 (m, overlapped with H₂O signal, 2H), 1.48 (s, 9H). UPLC/MS (method B): R_t 1.51 min. MS (ES): $C_{18}H_{24}FNO_3$ requires, 321; found, 322 $[M + H]^+$.

Synthesis of tert-Butyl 4-[2-(2-Bromoacetyl)-5-fluoro-phenyl]piperidine-1-carboxylate (29). To a solution of 28 (0.410 g, 1.28 mmol, 1.0 equiv) in dry THF (13 mL, 0.1 M), and Et₃N (0.516 g, 0.710 mL, 5.10 mmol, 4.0 equiv) was added at 0 °C under a N₂ atmosphere. After 30 min, TMSOTf (0.425 g, 0.346 mL, 1.92 mmol, 1.5 equiv) was added dropwise at -78 °C. The mixture was stirred at -50 °C for 4 h. Then, the mixture was quenched with cold 5% aq NaHCO₃ solution and extracted with cold EtOAc (3 times). The combined organic layer was washed with brine and dried over Na₂SO₄. After evaporation of the solvent, the crude was dissolved in dry THF (13 mL, 0.1 M), NBS (0.227 g, 1.28 mmol, 1.0 equiv) was added at -40 °C, and the mixture was stirred at -20 °C for additional 30 min. The reaction was diluted with H₂O and extracted with EtOAc. The combined organic layer was washed with brine and dried over Na₂SO₄. After evaporation of the solvent, the crude of 29 was used in the next step without further purification. UPLC/MS (method B): R_t 1.70 min. MS (ES): $C_{18}H_{23}BrFNO_3$ requires, 399; found, 400 $[M + H]^+$, 398 $[M - H]^-$.

Synthesis of tert-Butyl 4-[2-(2,4-Dioxothiazolidin-3-yl)acetyl]-5-fluoro-phenylpiperidine-1-carboxylate (30). Compound 30 was prepared according to general procedure B, Step 1, using 29 (0.512 g, 1.28 mmol). The crude was purified by column chromatography (SiO₂), eluting with Cy/EtOAc (8:2), to afford 30 as colorless oil (0.366 g, 66%). ¹H NMR (400 MHz, CDCl₃): δ 7.67 (dd, J = 8.7, 5.6 Hz, 1H), 7.10 (dd, J = 10.5, 2.6 Hz, 1H), 7.05–6.98 (m, 1H), 4.85 (s, 2H), 4.27–4.16 (m, 2H), 4.10 (s, 2H), 3.36–3.25 (m, 1H), 2.81 (td, J = 13.4, 13.0, 2.5 Hz, 2H), 1.84–1.74 (m, 2H), 1.58–1.51 (m, overlapped with H₂O signal, 2H), 1.47 (s, 9H). UPLC/MS (method B): R_t 1.42 min. MS (ES): $C_{21}H_{23}FN_2O_5S$ requires, 436; found, 437 $[M + H]^+$, 435 $[M - H]^-$.

Synthesis of tert-Butyl 4-[5-Fluoro-2-(2-oxo-3H-oxazol-5-yl)-phenyl]piperidine-1-carboxylate (31a). Compound 31a was prepared using 30 (0.366 g, 0.84 mmol) and *t*-BuOK (0.376 g, 3.35 mmol), according to general procedure B, Step 2. The crude was purified by flash chromatography (SiO₂), eluting with DCM/MeOH (95:5), to afford 31a as yellow foam (0.204 g, 67%). ¹H NMR (400 MHz, CDCl₃): δ 9.14 (bs, 1H), 7.39 (dd, J = 8.6, 5.8 Hz, 1H), 7.02 (dd, J = 10.3, 2.6 Hz, 1H), 6.99–6.92 (m, 1H), 6.59 (d, J = 1.9 Hz, 1H), 4.41–4.14 (m, 2H), 3.05–2.90 (m, 1H), 2.89–2.70 (m, 2H), 1.84–1.75 (m, 2H), 1.71–1.53 (m, overlapped with H₂O signal, 2H), 1.48 (s, 9H). UPLC/MS (method A): R_t 2.25 min. MS (ES): $C_{19}H_{23}FN_2O_4$ requires, 362; found, 363 $[M + H]^+$, 361 $[M - H]^-$.

Synthesis of 5-[4-Fluoro-2-(4-piperidyl)phenyl]-3H-oxazol-2-one Hydrochloride (31b). Compound 31b was prepared according to general procedure G using 31a (0.150 g, 0.41 mmol). The crude was used in the next step without further purification. UPLC/MS (method A): R_t 1.27 min. MS (ES): $C_{14}H_{15}FN_2O_2$ requires, 262; found, 263 $[M + H]^+$, 261 $[M - H]^-$.

Synthesis of 5-[4-Fluoro-2-(1-methyl-4-piperidyl)phenyl]-3H-oxazol-2-one (31c). Compound 31c was prepared according to general procedure H using 31b (0.123 g, 0.41 mmol) and 37% aq solution of HCHO (0.165 g, 0.150 mL, 2.05 mmol). The crude was used in the next step without further purification. ¹H NMR (400 MHz, DMSO-*d*₆): δ 10.85 (bs, 1H), 7.43 (dd, J = 8.7, 6.1 Hz, 1H), 7.21 (dd, J = 10.8, 2.7 Hz, 1H), 7.11 (td, J = 8.4, 2.7 Hz, 1H), 7.06 (s, 1H), 2.94–2.84 (m, 2H), 2.83–2.73 (m, 1H), 2.23 (s, 3H), 2.10–1.96 (m, 2H), 1.78–1.62 (m, 4H). ¹³C NMR (101 MHz, DMSO-*d*₆): δ 163.57, 161.12, 155.27, 146.81, 137.06, 130.53, 123.11, 113.52, 113.38, 113.30, 113.17, 55.42, 45.73, 37.72, 32.11. UPLC/MS (method A): R_t 1.27 min. MS (ES): $C_{15}H_{17}FN_2O_2$ requires, 276; found, 277 $[M + H]^+$, 275 $[M - H]^-$. HRMS: $C_{15}H_{18}FN_2O_2$ $[M + H]^+$ calcd 277.1352; measured, 277.1354, Δ ppm 0.7.

Synthesis of 5-[4-Fluoro-2-(1-methyl-4-piperidyl)phenyl]-2-oxo-N-(4-phenylbutyl)oxazole-3-carboxamide (32a). Compound 32a was prepared according to general procedure D (method A) using 31c (0.048 g, 0.174 mmol), DMAP (0.023 g, 0.19 mmol), and 4-phenylbutyl isocyanate (0.033 g, 0.033 mL, 0.19 mmol) in DMF at 50 °C. The crude was purified by column chromatography (SiO₂), eluting with DCM/MeOH (95:5), to afford 32a as a white solid (0.050 g, 62%). ¹H NMR (400 MHz, DMSO-*d*₆): δ 8.06 (t, J = 5.9 Hz, 1H), 7.51 (dd, J = 8.6, 6.0 Hz, 1H), 7.45 (s, 1H), 7.31–7.24 (m, 3H), 7.23–7.11 (m, 4H), 3.36–3.22 (m, overlapped with H₂O signal, 2H), 2.92–2.82 (m, 2H), 2.82–2.71 (m, 1H), 2.61 (t, J = 7.2 Hz, 2H), 2.19 (s, 3H), 1.96 (td, J = 11.1, 3.9 Hz, 2H), 1.79–1.51 (m, 8H). ¹³C NMR (101 MHz, DMSO-*d*₆): δ 163.03 (d, J_{C-F} = 247.8 Hz), 151.80, 148.00, 147.96, 141.98, 137.25, 131.49 (d, J_{C-F} = 8.6 Hz), 128.27, 128.21, 125.65, 121.58 (d, J_{C-F} = 3.2 Hz), 113.76, 113.42 (d, J_{C-F} = 22.3 Hz), 109.67, 55.52 (2C), 46.02, 40.01 (overlapped with DMSO signal), 38.03, 34.71, 32.42 (2C), 28.61, 28.12. UPLC/MS (method A): R_t 2.27 min. MS (ES): $C_{26}H_{30}FN_3O_3$ requires, 451; found, 452 $[M + H]^+$, 275 $[M - CONH(CH_2)_4Ph]^-$. HRMS: $C_{26}H_{30}FN_3O_3$ $[M + H]^+$ calcd 452.2349; measured, 452.2358, Δ ppm 2.0.

Synthesis of 5-[4-Fluoro-2-(1-methyl-4-piperidyl)phenyl]-2-oxo-N-pentyl-oxazole-3-carboxamide (32b). Compound 32b was prepared according to general procedure D (method A) using 31c (0.040 g, 0.14 mmol), DMAP (0.020 g, 0.17 mmol), and *n*-pentyl isocyanate (0.019 g, 0.022 mL, 0.17 mmol) in CH₃CN at 50 °C. The crude was purified by column chromatography (SiO₂), eluting with DCM/MeOH (9:1), to afford 32b as a white solid (0.035 g, 64%). ¹H NMR (400 MHz, DMSO-*d*₆): δ 8.04 (t, J = 5.8 Hz, 1H), 7.51 (dd, J = 8.7, 6.0 Hz, 1H), 7.45 (s, 1H), 7.26 (dd, J = 10.7, 2.7 Hz, 1H), 7.15 (td, J = 8.4, 2.7 Hz, 1H), 3.31–3.23 (m, overlapped with H₂O signal, 2H), 2.90–2.82 (m, 2H), 2.81–2.70 (m, 1H), 2.18 (s, 3H), 1.94 (td, J = 11.0, 3.8 Hz, 2H), 1.78–1.62 (m, 4H), 1.54–1.48 (m, 2H), 1.36–1.25 (m, 4H), 0.88 (t, J = 6.8 Hz, 3H). ¹³C NMR (101 MHz, DMSO-*d*₆): δ 151.85, 148.13, 147.95, 137.28, 131.50 (d, J_{C-F} = 9.0 Hz), 121.60, 113.78, 113.43 (d, J_{C-F} = 23.0 Hz), 109.67, 55.56, 46.08, 40.15 (overlapped with DMSO signal), 38.09, 32.47, 28.61, 28.35, 21.76, 13.85. UPLC/MS (method A): R_t 2.12 min. MS (ES): $C_{21}H_{28}FN_3O_3$ requires, 389; found, 390 $[M + H]^+$, 275 $[M - CONH(CH_2)_4CH_3]^-$. HRMS: $C_{21}H_{28}FN_3O_3$ $[M + H]^+$ calcd 390.2193; measured, 390.2204, Δ ppm 2.8.

Synthesis of 5-[4-Fluoro-2-(1-methyl-4-piperidyl)phenyl]-N-isobutyl-2-oxo-oxazole-3-carboxamide Hydrochloride (32c). Compound 32c was prepared according to general procedure D (method C) using 31c (0.034 g, 0.12 mmol), 2-methylpropan-1-amine (0.027 g, 0.029 mL, 0.37 mmol), and Et₃N (0.075 g, 0.104 mL, 0.74 mmol). The crude was purified by column chromatography (SiO₂), eluting with DCM/MeOH (95:5), to afford the free base of 32c (44%, 0.020 g, 0.053 mmol). The free base of 32c (0.020 g, 0.05 mmol) was then dissolved in 0.5 mL of 1,4-dioxane and 4.0 M HCl solution (0.27 mL, 1.06 mmol, 20.0 equiv) was added. After evaporation of the solvent, the residue was triturated with Et₂O to afford 32c as a white solid (0.009 g,

20%). ^1H NMR (400 MHz, CDCl_3): δ 12.88 (bs, 1H), 7.96 (t, $J = 5.9$ Hz, 1H), 7.39 (dd, $J = 8.6, 5.6$ Hz, 1H), 7.29–7.21 (m, overlapped with CDCl_3 signal, 2H), 7.05–6.97 (m, 1H), 3.67–3.55 (m, 2H), 3.24 (dd, $J = 6.8, 5.9$ Hz, 2H), 3.05 (tt, $J = 12.0, 2.7$ Hz, 2H), 2.91–2.77 (m, 5H), 2.69–2.52 (m, 2H), 2.07–1.97 (m, 2H), 1.96–1.84 (m, 1H), 0.99 (d, $J = 6.7$ Hz, 6H). ^{13}C NMR (101 MHz, CDCl_3): δ 165.58, 152.78, 149.42, 148.51, 144.71, 138.82, 131.80 (d, $J_{\text{C-F}} = 8.7$ Hz), 115.01 (d, $J_{\text{C-F}} = 22.0$ Hz), 114.91, 109.29, 55.10, 47.96, 44.00, 36.67, 29.99, 28.64, 20.11. UPLC/MS (method A): R_t 1.93 min. MS (ES): $\text{C}_{20}\text{H}_{26}\text{FN}_3\text{O}_3$ requires, 375; found, 376 $[\text{M} + \text{H}]^+$, 275 $[\text{M} - \text{CONHCH}_2(\text{CH}_3)_2]^-$. HRMS: $\text{C}_{20}\text{H}_{26}\text{FN}_3\text{O}_3$ $[\text{M} + \text{H}]^+$ calcd 376.2031; measured, 376.2036, $\Delta\text{ppm} -1.3$.

MOLECULAR MODELING AND DOCKING STUDIES

Covalent Docking. To carry out the covalent docking, we used docking modules available in a Schrodinger platform: CovDock in Schrodinger 2018-4 version. These covalent docking tools require that the ligand set must be a series of compounds all of which should react with the receptor at the same site and by the same mechanism. The first step is the regular noncovalent docking of the ligands having the potential to form a covalent bond with the reactive residue of the receptor. Then, the program allows for the different conformations of the side-chain of the reactive residue, which is temporarily mutated to alanine at this stage. The reason for this temporary mutation is only to avoid the bias toward the particular ligand conformation if the side-chain of the reactive residue is present. After the noncovalent docking, the original side-chain of the reactive residue is replaced with the cysteine and the covalent bond is formed. The ligands where the covalent bond lengths between the reactive center of the ligand and the reactive residue of the receptor are longer compared to the standard chemical bonds are discarded. After the bond formation between the potential covalent ligand and the receptor, the complex is minimized using the Prime module of Schrodinger suite. Finally, the docked poses of the covalently linked ligands are to be visualized and rank ordered by energy and the docked score. The reaction site of ligands was determined using a SMART2 search pattern implemented in the covalent docking program. After determining the reactive sites from both the ligands and the receptor, a 12 Å grid box was generated making sure that Cys143 would be in that grid box. The docked poses and the energetics were analyzed and 43 covalent inhibitors were showing good docking poses with lower complex energies and having docking scores ≥ 6.0 . Some of the ligands lacked the proper SMARTS for the reaction and were rejected from the calculations. Docking calculations for hNAAA were carried out under identical conditions using the X-ray structure (PDB code: 6DXX). Compound **32b** did not natively dock into this receptor using the standard CovDock protocol. To understand the binding mode in greater details, each step of the docking run was analyzed and the raw unrefined poses were examined. It was clear that Trp181 was occluding binding of the *n*-pentyl side-chain of compound **32b** leading to a docking score $>10,000$ (indicate no binding affinity to NAAA). The compound was thus modeled using a flexible ligand overlay using the AC docking pose for the purpose of generating a figure.

IN VITRO PHARMACOLOGICAL ASSAY

In Vitro hAC Fluorescent Assay. Cell Culture Conditions and Preparation of the hAC-Enriched Lysate. HEK293 cells stably expressing hAC (HEK293-hAC) were generated in our laboratory using a protocol, as previously described.³⁰ Briefly, hAC (variant 1 coding sequence, NM_177924) cDNA was

purchased from Open Biosystems (clone ID 3923451) and subcloned in the mammalian expression vector pCDNA3.1, containing the neomycin resistance gene. HEK293 cells were transfected with the hAC-pCDNA3.1 construct using a JetPEI reagent (Polyplus Transfection, Illkirch-Graffenstaden, France) and following the manufacturer's instructions. A stable cell line was generated by selection with G418 (1 mg/mL), and cell clones were derived by limited dilution plating. HEK293-hAC were grown in Dulbecco's modified Eagle medium (DMEM) containing 10% fetal bovine serum (FBS), 1% glutamine, 1 mM sodium pyruvate, and 500 $\mu\text{g}/\text{mL}$ G418. Cells were harvested and pellets were stored at -80°C until lysosomal-enriched lysate preparation. Cells were suspended in 20 mM Tris HCl (pH 7.5) with 0.32 M sucrose, sonicated, and centrifuged at $800 \times g$ for 30 min at 4°C . Supernatants were then centrifuged at $12\,000 \times g$ for 30 min at 4°C . Pellets were re-suspended in PBS (pH 7.4) and subjected to three freeze–thaw cycles at -80°C . The suspension was finally centrifuged at $105\,000 \times g$ for 1 h at 4°C , and protein concentration was measured in the supernatant with a bicinchoninic acid based protein assay. This hAC-enriched preparation allowed us to further optimize the enzymatic assay and to use small amounts of lysate (2 $\mu\text{g}/\text{well}$) at the 5 μM substrate (Rbm14-12) around its K_M ($K_M = 5.0 \mu\text{M}$).

Fluorogenic hAC Assay. The assay was performed in Optiplate 96-wells black plates, with each reaction well containing a mixture of 25 mM NaOAc buffer (pH 4.5) and a fixed amount of protein (2 μg) in a volume of 85 μL . After 10 min of pre-incubation with the test compounds (diluted 20 \times from DMSO stock solutions at different concentrations), the fluorogenic probe was added (diluted 40 \times from EtOH stock solution, final concentration 5 μM). After 3 h incubation at 37°C , reactions were stopped with 50 μL of MeOH and 100 μL of a 2.5 mg/mL NaIO_4 fresh solution in 100 mM glycine/NaOH buffer (pH 10.6). The plates were further incubated for 2 h at 37°C in the dark and fluorescence intensities were measured at excitation/emission wavelengths of 355/460 nm. Negative control samples consisted of the same incubation mixture in the absence of protein-enriched extracts. Data were plotted as a function of compound concentrations. IC_{50} values were calculated by nonlinear regression analysis using GraphPad Prism 5 (GraphPad Software Inc., CA, USA) applying a standard slope curve fitting. The reported IC_{50} values are the mean of at least three independent experiments performed in three technical replicates.

KINETIC STUDIES

Michaelis–Menten Analysis. Assay conditions for the kinetic studies were the same as those described for the fluorogenic hAC assay. The enzyme-enriched lysate (2 μg) was incubated with the following concentrations of substrate Rbm14-12: 0.25, 0.5, 1, 2.5, 5, 10, 12.5, 15 μM . Compound **12a** was used at a final concentration of 25 and 100 nM. Initial velocities (V_0) were determined and automatically fitted to the Michaelis–Menten equation to obtain kinetic parameters (K_M and V_{max}). The graph is representative of two independent experiments, each performed in three technical replicates. Graphs and data analysis were performed using GraphPad Prism 5 software (GraphPad Software Inc., CA, USA).

In Vitro hNAAA Fluorescent Assay. Cell Culture and Preparation of the hNAAA-Enriched Lysate. HEK-293 cells stably transfected with the hNAAA coding sequence cloned from a human spleen cDNA library (catalog no. 639124,

Clontech, Mountain View, CA, USA) were used as the enzyme source. Cells were grown in DMEM containing 10% FBS, 1% glutamine, 1 mM sodium pyruvate, and 500 $\mu\text{g}/\text{mL}$ G418. Cells were harvested and pellets were stored at $-80\text{ }^\circ\text{C}$ until lysosomal-enriched lysate preparation. Cells were suspended in 20 mM Tris HCl (pH 7.4) with 0.32 M sucrose, sonicated, and centrifuged at $800 \times g$ for 30 min at $4\text{ }^\circ\text{C}$. Supernatants were then ultracentrifuged at $12\,000 \times g$ for 30 min at $4\text{ }^\circ\text{C}$. Pellets were re-suspended in PBS buffer (pH 7.4) and subjected to three freeze–thaw cycles at $-80\text{ }^\circ\text{C}$. The suspension was finally ultracentrifuged at $105\,000 \times g$ for 1 h at $4\text{ }^\circ\text{C}$, supernatants were collected, protein concentration was measured, and samples aliquoted and stored at $-80\text{ }^\circ\text{C}$ until use.

Fluorogenic hNAAA Assay. The assay was run in 96-well microplates (Black OptiPlate-96 F; PerkinElmer, Massachusetts, USA) in a total reaction volume of 200 μL . hNAAA protein preparation (4.0 μg) was pre-incubated for 30 min with various concentrations of test compounds or vehicle control (DMSO 5%) in 100 mM citrate/phosphate buffer (pH 4.5) containing 3.0 mM dithiothreitol (DTT), 0.1% NP40 0.1%, 0.05% bovine serum albumin, and 150 mM NaCl. *N*-(4-Methyl-2-oxochromen-7-yl)-hexadecanamide (PAMCA) was used as a substrate (2.0 μM) and the reaction carried out for 50 min at $37\text{ }^\circ\text{C}$. Fluorescence was measured with an EnVision 2014 Multilabel Reader (PerkinElmer, Massachusetts, USA) using an excitation wavelength of 355 nm and emission 460 nm. IC_{50} values were calculated by nonlinear regression analysis of $\log[\text{concentration}]/\text{inhibition}$ curves using GraphPad Prism 5 (GraphPad Software Inc., CA, USA) applying a standard slope curve fitting. The values are the mean of at least three independent experiments performed in three technical replicates.

■ CELL CULTURE AND TREATMENTS

SH-SY5Y cells were purchased from Sigma Aldrich (Italy) and cultured in DMEM containing 10% FBS at $37\text{ }^\circ\text{C}$ and 5% CO_2 . Drugs were dissolved in DMSO (10 mM) and diluted in cell culture medium with reduced serum (1%) for cell treatments.

hAC LC/MS-Based Activity Assay. hAC activity measurement was performed as previously described.^{59,61} Total lysates from cells were diluted in assay buffer (100 mM sodium phosphate, 0.1% Nonidet P-40, 150 mM NaCl, 3 mM DTT, 100 mM sodium citrate, pH 4.5). Reactions were started by the addition of 50 μM *N*-lauroyl ceramide (Nu-Chek Prep, Elysian, MN) and carried out for 1 h at $37\text{ }^\circ\text{C}$. Reactions were stopped by the addition of a mixture of $\text{CHCl}_3/\text{MeOH}$ (2:1) spike with 11-lauroleic acid (1.0 nmol, NuChek Prep). The organic phases were collected, dried under N_2 , and analyzed by UPLC/MS (Acquity, Waters) in the negative-ion mode monitoring the reaction product (lauric acid, m/z : 199) using 11-lauroleic acid as the internal standard. Lipids were eluted on an Acquity UPLC BEH C18 column (50 mm length, 2.1 mm ID, 1.7 μm pore size, Waters) column at 0.5 mL/min for 1.5 min with a gradient of CH_3CN and H_2O , both containing 0.25% AcOH and 5 mM NH_4OAc (70–100% CH_3CN in 0.5 min, 100% CH_3CN for 0.5 min, 70% CH_3CN for 0.4 min). The column temperature was $40\text{ }^\circ\text{C}$. ESI was in the negative mode, capillary voltage was 1 kV, and cone voltage was 50 V. N_2 was used as a drying gas at a flow rate of 500 L/h and at a temperature of $400\text{ }^\circ\text{C}$. The $[\text{M} - \text{H}]^-$ ion was monitored in the selected-ion monitoring mode (m/z values: lauric acid 199, 11-lauroleic acid 197.35). Calibration curves were generated with authentic lauric acid (Nu Check Prep).

Lipid Extraction and Ceramide Analysis. Lipid extraction and SL measurements were performed as previously described.^{59,61,75} Lipids were extracted with a $\text{CHCl}_3/\text{MeOH}$ mixture (2:1, 3 mL) spike with internal standards. The organic phase was collected, dried under N_2 , and dissolved in $\text{CHCl}_3/\text{MeOH}$ (1:3) for LC/MS analyses. Ceramides and sphingosine were analyzed by LC/MS/MS, using a Waters Acquity UPLC coupled to a Waters Xevo triple quadrupole mass spectrometer (TQMS) and interfaced with an ESI ion source. Separation was performed on a Waters Acquity BEH C18 1.7 μm column (2.1 \times 50 mm) at $60\text{ }^\circ\text{C}$. A linear gradient of 0.1% HCOOH in $\text{CH}_3\text{CN}/i\text{-PrOH}$ (20:80) as solvent B in 0.1% HCOOH in $\text{CH}_3\text{CN}/\text{H}_2\text{O}$ (20:80) as solvent A and was applied at a flow rate of 0.4 mL/min. The detection of SLs was performed in positive ion mode. Capillary voltage was 3.5 kV and cone voltage was 25 V. The source temperature and desolvation temperatures were set at 120 and $600\text{ }^\circ\text{C}$, respectively. Desolvation gas and cone gas (N_2) flows were 800 and 20 L/h, respectively. Ceramides were identified by comparison of their LC retention times and MS/MS fragmentation patterns with those of authentic standards (Avanti Polar Lipids). Multiple reaction monitoring (MRM) ion chromatograms were used to quantify dihydroceramide (Cer(d18:0/16:0), R_t = 4.6 min, m/z : 540.5 > 522.5), palmitoyl ceramide (Cer(d18:1/16:0), R_t = 4.5 min, m/z : 520.3 > 264.2) sphingosine (So(d18:1), R_t = 2.6 min, m/z : 300.2 > 282.2), sphingomyelin (SM(d18:1/16:0), R_t = 4.2 min, m/z : 703.2 > 184.1) and hexosylceramide (HexCer (d18:1/16:0), 4.3 min, m/z : 682.2 > 264.2). Detection and analysis were controlled by Waters MassLynx software version 4.1. Calibration curves were prepared for every experiment.

Statistics. GraphPad Prism software (GraphPad Software, Inc., USA) was used for statistical analysis. Data were analyzed using the Student *t*-test or 1-way ANOVA followed by Bonferroni post hoc test for multiple comparisons. Differences between groups were considered statistically significant at values of $p < 0.05$. Results are expressed as mean \pm SEM.

■ IN VITRO PHYSICOCHEMICAL AND METABOLIC STABILITY ASSAY

Aqueous Kinetic Solubility Assay. The aqueous kinetic solubility was determined from a 10 mM CH_3CN stock solution of the test compound in PBS at pH 7.4. The study was performed by the incubation of an aliquot of 10 mM CH_3CN stock solution in PBS (pH 7.4) at a target concentration of 250 μM . The incubation was carried out under shaking at $25\text{ }^\circ\text{C}$ for 1 h, followed by centrifugation at $21\,100 \times g$ for 30 min. The supernatant was analyzed by UPLC/MS for the quantification of the dissolved compound (in μM) by UV at a specific wavelength (215 nm). The aqueous kinetic solubility (in μM) was calculated by dividing the peak area of the dissolved test compound (supernatant) by the peak area of the test compound in the reference (250 μM in CH_3CN) and further multiplied by the target concentration and dilution factor. The UPLC/MS analyses were performed on a Waters Acquity UPLC/MS system consisting of SQDMS equipped with an ESI interface and a PDA detector. The PDA range was 210–400 nm. ESI in positive mode was used in the mass scan range 100–650 Da. The analyses were run on an Acquity UPLC BEH C18 column (50 \times 2.1 mm ID, particle size 1.7 μm) with a VanGuard BEH C18 pre-column (5 \times 2.1 mm ID, particle size 1.7 μm), using 10 mM NH_4OAc in H_2O at pH 5 adjusted with AcOH (A) and 10 mM NH_4OAc in $\text{CH}_3\text{CN}/\text{H}_2\text{O}$ (95:5) at pH 5 (B) as the

mobile phase. The values are the mean of at least two independent experiments performed in two technical replicates.

Chemical Stability Assay. Chemical stability of the selected compounds was evaluated under physiological pH conditions (0.01 M PBS, pH 7.4) for up to 8 h. The buffer was added with 10% of CH₃CN. Stock solutions of each compound (10 mM) were freshly prepared in CH₃CN. Each compound was incubated at a final concentration of 1 μM in pre-heated buffer (37 °C). The sample solutions were divided into aliquots in glass vials (preheated at 37 °C) for each time point. The samples were maintained at 37 °C in an UPLC/MS autosampler during the study (no shaking). A reference solution of each compound (final concentration: 1 μM) in preheated CH₃CN was prepared from the stock solutions and maintained at 37 °C in the UPLC/MS autosampler during the study. For each time point, the samples were analyzed directly by LC/MS without any further sample preparation. The samples were analyzed by integrating the corresponding MRM peak areas. The relative compound concentration was calculated by dividing the peak area at each time point by the peak area at $t = 0$ min. The reference solution was analyzed at the beginning ($t = 0$ min) and at the end of the study ($t = 8$ h). The apparent half-life ($t_{1/2}$) of the disappearance of the compound was calculated using the best fitting equation by GraphPad Prism (GraphPad Software, Inc., USA). The analyses were performed on a Waters Acquity UPLC/MS triple quadrupole detection (TQD) system consisting of TQD MS equipped with an ESI interface and a PDA detector. The analyses were run on an Acquity UPLC BEH C18 1.7 μm 2.1 × 50 mm column with a VanGuard BEH C18 1.7 μm pre-column at 40 °C. For each compound, the appropriate mobile phase was chosen. ESI was applied in positive mode. The values are the mean of at least two independent experiments performed in two technical replicates.

In Vitro Plasma Stability Study. Freshly prepared 10 mM CH₃CN stock solution of the test compound was diluted 50-fold with DMSO/H₂O (1:1) and incubated at 37 °C for 2 h with mouse/human plasma added 5% DMSO (preheated at 37 °C for 10 min). The final concentration was 2 μM. At each time point (0, 5, 15, 30, 60, and 120 min), 50 μL of the incubation mixture was diluted with 200 μL of cold CH₃CN spiked with 200 nM of the internal standard, followed by centrifugation at 3300 × *g* for 20 min. The supernatant was further diluted with H₂O (1:1) for analysis. The concentration of the test compound was quantified by LC/MS–MS on a Waters Acquity UPLC/MS TQD system consisting of TQD MS equipped with an ESI interface. The analyses were run on an Acquity UPLC BEH C18 (50 × 2.1 mm ID, particle size 1.7 μm) with a VanGuard BEH C18 pre-column (5 × 2.1 mm ID, particle size 1.7 μm) at 40 °C. For each compound, the appropriate mobile phase was chosen. ESI was applied in positive mode. The response factors, calculated on the basis of the internal standard peak area, were plotted over time. When possible, response versus time profiles were fitted with Prism (GraphPad Software, Inc., USA) to estimate compounds $t_{1/2}$ in the plasma. The values are the mean of at least two independent experiments performed in two technical replicates.

In Vitro Microsomal Stability Study. Freshly prepared 10 mM CH₃CN stock solution of the test compound was pre-incubated at 37 °C for 15 min with mouse/human liver microsomes added 0.1 M Tris-HCl buffer (pH 7.4). The final concentration was 4.6 μM. After pre-incubation, the cofactors (NADPH, G6P, G6PDH, and MgCl₂ pre-dissolved in 0.1 M Tris-HCl) were added to the incubation mixture and the incubation was continued at 37 °C for 1 h. At each time point (0,

5, 15, 30, and 60 min), 30 μL of the incubation mixture was diluted with 200 μL of cold CH₃CN spiked with 200 nM of the internal standard, followed by centrifugation at 3300 *g* for 15 min. The supernatant was further diluted with H₂O (1:1) for analysis. The concentration of the test compound was quantified by LC/MS–MS on a Waters Acquity UPLC/MS TQD system consisting of TQD MS equipped with an ESI interface. The analyses were run on an Acquity UPLC BEH C18 (50 × 2.1 mm ID, particle size 1.7 μm) with a VanGuard BEH C18 pre-column (5 × 2.1 mm ID, particle size 1.7 μm) at 40 °C. For each compound, the appropriate mobile phase was chosen. ESI was applied in positive mode. The percentage of the test compound remaining at each time point relative to $t = 0$ was calculated. The $t_{1/2}$ were determined by a one-phase decay equation using a nonlinear regression of the compound concentration versus time. The values are the mean of at least two independent experiments performed in two technical replicates.

■ ANIMAL MODELS

In Vivo PK Study. C57 B6/J male mice, 8 weeks old (22–24 g), were used (Charles River, Calco). All procedures were performed in accordance with the Ethical Guidelines of European Communities Council (Directive 2010/63/EU of 22 September 2010) and accepted by the Italian Ministry of Health. All efforts were made to minimize animal suffering and to use the minimal number of animals required to produce reliable results, according to the “3Rs rules”. Animals were group-housed in ventilated cages and had free access to food and water. They were maintained under a 12 h light/dark cycle (lights on at 8:00 am) at a controlled temperature (21 ± 1 °C) and relative humidity (55 ± 10%). **32b** was administrated intravenously (i.v.) at 3 mg/kg/5 mL, vehicle: PEG400/Tween 80/saline solution (10/10/80% in volume, respectively) via tail vein injection and via oral administration (p.o.) at 10 mg/kg/10 mL, vehicle: PEG400/Tween 80/saline solution (10/10/80% in volume, respectively) by an oral gavage. **Sample collection.** Samples were collected at 5 min, 15 min, 30 min, 1 h, 2 h, and 4 h (i.v. administration) and at 15 min, 30 min, 1 h, 2 h, 4 h, and 6 h (p.o. administration). $N = 3$ animals per dose time point were treated. Plasma samples were centrifuged at 21,100 *g* for 15 min at 4 °C. An aliquot of each sample was extracted (1:3) with cold CH₃CN containing 200 nM of an appropriate internal standard being a close analogue of compound **32b**. A calibration curve was prepared in blank mouse plasma over a 1 nM–10 μM range. Three quality controls were prepared by spiking compound **32b** in the blank mouse plasma to 20, 200, and 2000 nM as final concentrations. The calibrators and quality controls were extracted (1:3) with the same extraction solution as the plasma samples. The plasma samples, the calibrators, and quality controls were centrifuged at 3270 × *g* for 15 min at 4 °C. The supernatants were further diluted (1:1) with H₂O and analyzed by LC/MS–MS on a Waters Acquity UPLC/MS TQD system consisting of TQD MS equipped with an ESI interface and a PDA detector. ESI was applied in positive mode. Compound-dependent parameters such as MRM transitions and collision energy were developed for compound **32b** and the internal standard. The analyses were run on an Acquity UPLC BEH C18 (50 × 2.1 mm ID, particle size 1.7 μm) with a VanGuard BEH C18 pre-column (5 × 2.1 mm ID, particle size 1.7 μm) at 40 °C. For plasma samples, the mobile phase was H₂O + 0.1% HCOOH (A) and CH₃CN + 0.1% HCOOH (B) at a flow rate = 0.5 mL/min. A linear gradient was applied starting at 20% B with an initial hold for 0.2 min, then 20–100% B in 2 min. All samples

(plasma samples, calibrators, and quality controls) were quantified by a MRM peak area response factor in order to determine the levels of compound **32b** in the plasma. The concentrations versus time were plotted and the profiles were fitted using PK Solutions Excel Application (Summit Research Service, USA) in order to determine the PK parameters.

■ ASSOCIATED CONTENT

SI Supporting Information

The Supporting Information is available free of charge at <https://pubs.acs.org/doi/10.1021/acs.jmedchem.0c01561>.

AC inhibitory activity data and assay methods for selected literature compounds; V_{\max} and K_M determinations; ^1H NMR and ^{13}C NMR spectra of the final compounds; retention times and UPLC analytical methods of the final compounds; and UPLC traces of the final compounds (PDF)

Molecular formula strings (CSV)

■ AUTHOR INFORMATION

Corresponding Authors

Renato Skerlj – *Lysosomal Therapeutics Inc., Cambridge, Massachusetts 02139, United States*; Phone: +1 617 610 8624; Email: renato.skerlj@x4pharma.com

Rita Scarpelli – *Fondazione Istituto Italiano di Tecnologia, I-16163 Genova, Italy; Drug Discovery and Development (D3)-Validation, I-16163 Genova, Italy*; orcid.org/0000-0002-2623-306X; Phone: +39 010 2896233; Email: rita.scarpelli@iit.it

Authors

Samantha Caputo – *Fondazione Istituto Italiano di Tecnologia, I-16163 Genova, Italy; Drug Discovery and Development (D3)-Validation, I-16163 Genova, Italy*

Simona Di Martino – *Fondazione Istituto Italiano di Tecnologia, I-16163 Genova, Italy; Drug Discovery and Development (D3)-Validation, I-16163 Genova, Italy*; orcid.org/0000-0001-5817-751X

Vincenzo Cilibrasi – *Fondazione Istituto Italiano di Tecnologia, I-16163 Genova, Italy; Drug Discovery and Development (D3)-Validation, I-16163 Genova, Italy*

Piero Tardia – *Fondazione Istituto Italiano di Tecnologia, I-16163 Genova, Italy; Drug Discovery and Development (D3)-Validation, I-16163 Genova, Italy*

Marco Mazzonna – *Fondazione Istituto Italiano di Tecnologia, I-16163 Genova, Italy; Drug Discovery and Development (D3)-Validation, I-16163 Genova, Italy*

Debora Russo – *Fondazione Istituto Italiano di Tecnologia, I-16163 Genova, Italy; D3-Pharma Chemistry, I-16163 Genova, Italy*

Ilaria Penna – *Fondazione Istituto Italiano di Tecnologia, I-16163 Genova, Italy; D3-Pharma Chemistry, I-16163 Genova, Italy*

Maria Summa – *Fondazione Istituto Italiano di Tecnologia, I-16163 Genova, Italy; Analytical Chemistry and Translational Pharmacology, I-16163 Genova, Italy*

Sine Mandrup Bertozzi – *Fondazione Istituto Italiano di Tecnologia, I-16163 Genova, Italy; Analytical Chemistry and Translational Pharmacology, I-16163 Genova, Italy*

Natalia Realini – *Fondazione Istituto Italiano di Tecnologia, I-16163 Genova, Italy; Drug Discovery and Development (D3)-Validation, I-16163 Genova, Italy*

Natasha Margaroli – *Fondazione Istituto Italiano di Tecnologia, I-16163 Genova, Italy; Drug Discovery and Development (D3)-Validation, I-16163 Genova, Italy*

Marco Migliore – *Fondazione Istituto Italiano di Tecnologia, I-16163 Genova, Italy; Drug Discovery and Development (D3)-Validation, I-16163 Genova, Italy*

Giuliana Ottonello – *Fondazione Istituto Italiano di Tecnologia, I-16163 Genova, Italy; Analytical Chemistry and Translational Pharmacology, I-16163 Genova, Italy*

Min Liu – *Lysosomal Therapeutics Inc., Cambridge, Massachusetts 02139, United States*

Peter Lansbury – *Lysosomal Therapeutics Inc., Cambridge, Massachusetts 02139, United States*

Andrea Armirotti – *Fondazione Istituto Italiano di Tecnologia, I-16163 Genova, Italy; Analytical Chemistry and Translational Pharmacology, I-16163 Genova, Italy*;

orcid.org/0000-0002-3766-8755

Rosalia Bertorelli – *Fondazione Istituto Italiano di Tecnologia, I-16163 Genova, Italy; Analytical Chemistry and Translational Pharmacology, I-16163 Genova, Italy*

Soumya S. Ray – *Lysosomal Therapeutics Inc., Cambridge, Massachusetts 02139, United States*

Complete contact information is available at:

<https://pubs.acs.org/doi/10.1021/acs.jmedchem.0c01561>

Author Contributions

[¶]S.C. and S.D.M. contributed equally. All the authors have given approval to the final version of the manuscript.

Notes

The authors declare the following competing financial interest(s): All the work in the manuscript was funded by Lysosomal Therapeutics Inc. A Sponsored Research Agreement was signed between Fondazione Istituto Italiano di Tecnologia, Drug Discovery and Development (D3)-Validation and Lysosomal Therapeutics Inc.

■ ACKNOWLEDGMENTS

The authors thank Silvia Venzano, Luca Goldoni and Marina Veronesi for their technical support.

■ ABBREVIATIONS

AC, acid ceramidase; ASM, acid sphingomyelinase; Cer, ceramide; dh-CerDES, dihydro-ceramide desaturase; CerS, ceramide synthase; CerK, ceramide kinase; CerPPase, ceramide phosphate phosphatase; diGalCer, di-galactosylceramide; GAL-Case, β -galactosyl ceramidase; GD, Gaucher's disease; GCase, β -glucosyl ceramidase; GalCer, galactosylceramide; GluCer, glucosylceramide; CGALT, ceramide galactosyl transferase; CGT, ceramide glucosyl transferase; LacCer, lactosylceramide; LSD, lysosomal storage disease; KD, Krabbe's disease; SL, sphingolipid; So, sphingosine; So-1P, sphingosine 1-phosphate; SK, sphingosine kinase; SMase, sphingomyelinase; SPPase, sphingosine phosphate phosphatase; SMS, sphingomyelin synthase; AcOH, acetic acid; Al_2O_3 , alumina; CH_3CN , acetonitrile; NH_4OAc , ammonium acetate; NH_4Cl , ammonium chloride; HCO_2NH_4 , ammonium formate; aq, aqueous; NBS, *N*-bromosuccinimide; CDI, 1,1'-carbonyldiimidazole; CHCl_3 , chloroform; Cy, cyclohexane; celite, diatomaceous earth; DCM, dichloromethane; Et_2O , diethyl ether; DIPEA, *N,N*-diisopropylethylamine; DMAP, 4-(dimethylamino)-pyridine; DMF, *N,N*-dimethylformamide; DMSO, dimethylsulfoxide; Boc_2O , di-*tert*-butyl dicarbonate; equiv, equivalent; EtOH, ethanol; EtOAc,

ethyl acetate; HCHO, formaldehyde; HCOOH, formic acid; HCl, hydrochloric acid; LiCl, lithium chloride; LiOH, lithium hydroxide; MeOH, methanol; N₂, nitrogen; on, overnight; Pd(OH)₂, palladium hydroxide; Pd/C, palladium on carbon; K₂CO₃, potassium carbonate; KNCO, potassium cyanate; *t*-BuOK, potassium *tert*-butoxide; *i*-PrOH, 2-propanol; R_t, retention time; rt, room temperature; sat., saturated; SiO₂, silica gel; NaOAc, sodium acetate; NaHCO₃, sodium bicarbonate; Na₂CO₃, sodium carbonate; NaCl, sodium chloride; Na₂SO₄, sodium sulfate; NaBH(OAc)₃, sodium triacetoxyborohydride; THF, tetrahydrofuran; Pd(PPh₃)₄, tetrakis-(triphenylphosphine) palladium(0); TZD, 2,4-thiazolidine-dione; SOCl₂, thionyl chloride; Et₃N, trimethylamine; TMSOTf, trimethylsilyl trifluoromethanesulfonate; H₂O, water; wt, weight

REFERENCES

- (1) Hannun, Y. A.; Obeid, L. M. Many ceramides. *J. Biol. Chem.* **2011**, *286*, 27855–27862.
- (2) Gomez-Muñoz, A.; Presa, N.; Gomez-Larrauri, A.; Rivera, I.-G.; Trueba, M.; Ordoñez, M. Control of inflammatory responses by ceramide, sphingosine 1-phosphate and ceramide 1-phosphate. *Prog. Lipid Res.* **2016**, *61*, 51–62.
- (3) Hannun, Y. A.; Obeid, L. M. Sphingolipids and their metabolism in physiology and disease. *Nat. Rev. Mol. Cell Biol.* **2018**, *19*, 175–191.
- (4) Kurz, J.; Parnham, M. J.; Geisslinger, G.; Schiffmann, S. Ceramides as novel disease biomarkers. *Trends Mol. Med.* **2019**, *25*, 20–32.
- (5) van Eijk, M.; Ferraz, M. J.; Boot, R. G.; Aerts, J. M. F. G. Lyso-glycosphingolipids: presence and consequences. *Essays Biochem.* **2020**, *64*, 565.
- (6) Sahu, S. K.; Hannun, Y. A.; Yao, N. Emergence of membrane sphingolipids as a potential therapeutic target. *Biochimie* **2019**, *158*, 257–264.
- (7) Coant, N.; Sakamoto, W.; Mao, C.; Hannun, Y. A. Ceramidases, roles in sphingolipid metabolism and in health and disease. *Adv. Biol. Regul.* **2017**, *63*, 122–131.
- (8) Parveen, F.; Bender, D.; Law, S.-H.; Mishra, V. K.; Chen, C.-C.; Ke, L.-Y. Role of ceramidases in sphingolipid metabolism and human diseases. *Cells* **2019**, *8*, 1573–1592.
- (9) García-Barros, M.; Coant, N.; Kawamori, T.; Wada, M.; Snider, A. J.; Truman, J. P.; Wu, B. X.; Furuya, H.; Clarke, C. J.; Bialkowska, A. B.; Ghaleb, A.; Yang, V. W.; Obeid, L. M.; Hannun, Y. A. Role of neutral ceramidase in colon cancer. *FASEB J.* **2016**, *30*, 4159–4171.
- (10) Coant, N.; Hannun, Y. A. Neutral ceramidase: advances in mechanisms, cell regulation, and roles in cancer. *Adv. Biol. Regul.* **2019**, *71*, 141–146.
- (11) Liakath-Ali, K.; Vancollie, V. E.; Lelliott, C. J.; Speak, A. O.; Lafont, D.; Protheroe, H. J.; Ingvorsen, C.; Galli, A.; Green, A.; Gleeson, D.; Ryder, E.; Glover, L.; Vizcay-Barrena, G.; Karp, N. A.; Arends, M. J.; Brenn, T.; Spiegel, S.; Adams, D. J.; Watt, F. M.; van der Weyden, L. Alkaline ceramidase 1 is essential for mammalian skin homeostasis and regulating whole-body energy expenditure. *J. Pathol.* **2016**, *239*, 374–383.
- (12) Sun, W.; Xu, R.; Hu, W.; Jin, J.; Crellin, H. A.; Bielawski, J.; Szulc, Z. M.; Thiers, B. H.; Obeid, L. M.; Mao, C. Upregulation of the human alkaline ceramidase 1 and acid ceramidase mediates calcium-induced differentiation of epidermal keratinocytes. *J. Invest. Dermatol.* **2008**, *128*, 389–397.
- (13) Xu, R.; Wang, K.; Mileva, I.; Hannun, Y. A.; Obeid, L. M.; Mao, C. Alkaline ceramidase 2 and its bioactive product sphingosine are novel regulators of the DNA damage response. *Oncotarget* **2016**, *7*, 18440–18457.
- (14) Hu, W.; Xu, R.; Sun, W.; Szulc, Z. M.; Bielawski, J.; Obeid, L. M.; Mao, C. Alkaline ceramidase 3 (ACER3) hydrolyzes unsaturated long-chain ceramides, and its down-regulation inhibits both cell proliferation and apoptosis. *J. Biol. Chem.* **2010**, *285*, 7964–7976.
- (15) Wang, K.; Xu, R.; Schrandt, J.; Shah, P.; Gong, Y. Z.; Preston, C.; Wang, L.; Yi, J. K.; Lin, C.-L.; Sun, W.; Spyropoulos, D. D.; Rhee, S.; Li, M.; Zhou, J.; Ge, S.; Zhang, G.; Snider, A. J.; Hannun, Y. A.; Obeid, L. M.; Mao, C. Alkaline ceramidase 3 deficiency results in purkinje cell degeneration and cerebellar ataxia due to dyshomeostasis of sphingolipids in the brain. *PLoS Genet.* **2015**, *11*, e1005591–e1005622.
- (16) Edvardson, S.; Yi, J. K.; Jalas, C.; Xu, R.; Webb, B. D.; Snider, J.; Fedick, A.; Kleinman, E.; Treff, N. R.; Mao, C.; Elpeleg, O. Deficiency of the alkaline ceramidase ACER3 manifests in early childhood by progressive leukodystrophy. *J. Med. Genet.* **2016**, *53*, 389–396.
- (17) Bernardo, K.; Hurwitz, R.; Zenk, T.; Desnick, R.; Ferlinz, K.; Schuchman, E.; Sandhoff, K. Purification, characterization, and biosynthesis of human acid ceramidase. *J. Biol. Chem.* **1995**, *270*, 11098–11102.
- (18) Ferlinz, K.; Kopal, G.; Bernardo, K.; Linke, T.; Bär, J.; Breiden, B.; Neumann, U.; Lang, F.; Schuchman, E. H.; Sandhoff, K. Human acid ceramidase. Processing, glycosylation, and lysosomal targeting. *J. Biol. Chem.* **2001**, *276*, 35352–35360.
- (19) Newton, J.; Lima, S.; Maceyka, M.; Spiegel, S. Revisiting the sphingolipid rheostat: Evolving concepts in cancer therapy. *Exp. Cell Res.* **2015**, *333*, 195–200.
- (20) Huang, X.; Withers, B. R.; Dickson, R. C. Sphingolipids and lifespan regulation. *Biochim. Biophys. Acta, Mol. Cell Biol. Lipids* **2014**, *1841*, 657–664.
- (21) Pettus, B. J.; Chalfant, C. E.; Hannun, Y. A. Ceramide in apoptosis: an overview and current perspectives. *Biochim. Biophys. Acta, Mol. Cell Biol. Lipids* **2002**, *1585*, 114–125.
- (22) Morales, A.; Lee, H.; Goñi, F. M.; Kolesnick, R.; Fernandez-Checa, J. C. Sphingolipids and cell death. *Apoptosis* **2007**, *12*, 923–939.
- (23) Zhang, H.; Desai, N. N.; Olivera, A.; Seki, T.; Brooker, G.; Spiegel, S. Sphingosine-1-phosphate, a novel lipid, involved in cellular proliferation. *J. Cell Biol.* **1991**, *114*, 155–167.
- (24) Payne, S. G.; Milstien, S.; Spiegel, S. Sphingosine-1-phosphate: dual messenger functions. *FEBS Lett.* **2002**, *531*, 54–57.
- (25) Spiegel, S.; Milstien, S. Sphingosine-1-phosphate: an enigmatic signalling lipid. *Nat. Rev. Mol. Cell Biol.* **2003**, *4*, 397–407.
- (26) Takabe, K.; Spiegel, S. Export of sphingosine-1-phosphate and cancer progression. *J. Lipid Res.* **2014**, *55*, 1839–1846.
- (27) Schuchman, E. H. Acid ceramidase and the treatment of ceramide diseases: the expanding role of enzyme replacement therapy. *Biochim. Biophys. Acta, Mol. Basis Dis.* **2016**, *1862*, 1459–1471.
- (28) Yu, F. P. S.; Medin, J. A.; Amintas, S.; Levade, T.; Levade, T.; Medin, J. A. Acid ceramidase deficiency: Farber disease and SMA-PME. *Orphanet J. Rare Dis.* **2018**, *13*, 121–140.
- (29) Seelan, R. S.; Qian, C.; Yokomizo, A.; Bostwick, D. G.; Smith, D. I.; Liu, W. Human acid ceramidase is overexpressed but not mutated in prostate cancer. *Genes, Chromosomes Cancer* **2000**, *29*, 137–146.
- (30) Realini, N.; Palese, F.; Pizzirani, D.; Pontis, S.; Basit, A.; Bach, A.; Ganesan, A.; Piomelli, D. Acid ceramidase in melanoma: expression, localization, and effects of pharmacological inhibition. *J. Biol. Chem.* **2016**, *291*, 2422–2434.
- (31) Roh, J.-L.; Park, J. Y.; Kim, E. H.; Jang, H. J. Targeting acid ceramidase sensitizes head and neck cancer to cisplatin. *Eur. J. Cancer* **2016**, *52*, 163–172.
- (32) Klobučar, M.; Grbčić, P.; Pavelić, S. K.; Jonjić, N.; Visentin, S.; Sedić, M. Acid ceramidase inhibition sensitizes human colon cancer cells to oxaliplatin through downregulation of transglutaminase 2 and beta1 integrin/FAK-mediated signalling. *Biochem. Biophys. Res. Commun.* **2018**, *503*, 843–848.
- (33) Doan, N. B.; Alhajala, H.; Al-Gizawiy, M. M.; Mueller, W. M.; Rand, S. D.; Connelly, J. M.; Cochran, E. J.; Chitambar, C. R.; Clark, P.; Kuo, J.; Schmainda, K. M.; Mirza, S. P. Acid ceramidase and its inhibitors: a de novo drug target and a new class of drugs for killing glioblastoma cancer stem cells with high efficiency. *Oncotarget* **2017**, *8*, 112662–112674.
- (34) Mahdy, A. E.; Cheng, J. C.; Li, J.; Elojeimy, S.; Meacham, W. D.; Turner, L. S.; Bai, A.; Gault, C. R.; McPherson, A. S.; Garcia, N.; Beckham, T. H.; Saad, A.; Bielawska, A.; Bielawski, J.; Hannun, Y. A.; Keane, T. E.; Taha, M. I.; Hammouda, H. M.; Norris, J. S.; Liu, X. Acid

ceramidase upregulation in prostate cancer cells confers resistance to radiation: AC inhibition, a potential radiosensitizer. *Mol. Ther.* **2009**, *17*, 430–438.

(35) Saad, A. F.; Meacham, W. D.; Bai, A.; Anelli, V.; Elojeimy, S.; Mahdy, A. E.; Turner, L. S.; Cheng, J.; Bielawska, A.; Bielawski, J.; Keane, T. E.; Obeid, L. M.; Hannun, Y. A.; Norris, J. S.; Liu, X. The functional effects of acid ceramidase overexpression in prostate cancer progression and resistance to chemotherapy. *Cancer Biol. Ther.* **2007**, *6*, 1455–1460.

(36) Huang, Y.; Tanimukai, H.; Liu, F.; Iqbal, K.; Grundke-Iqbal, I.; Gong, C.-X. Elevation of the level and activity of acid ceramidase in Alzheimer's disease brain. *Eur. J. Neurosci.* **2004**, *20*, 3489–3497.

(37) Gieselmann, V. Lysosomal storage diseases. *Biochim. Biophys. Acta, Mol. Basis Dis.* **1995**, *1270*, 103–136.

(38) Ballabio, A.; Gieselmann, V. Lysosomal disorders: From storage to cellular damage. *Biochim. Biophys. Acta, Mol. Cell Res.* **2009**, *1793*, 684–696.

(39) Cox, T. M.; Cachón-González, M. B. The cellular pathology of lysosomal diseases. *J. Pathol.* **2012**, *226*, 241–254.

(40) Stirnemann, J.; Belmatoug, N.; Camou, F.; Serratrice, C.; Froissart, R.; Caillaud, C.; Levade, T.; Astudillo, L.; Serratrice, J.; Brassier, A.; Rose, C.; Billette de Villemeur, T.; Berger, M. A review of gaucher disease pathophysiology, clinical presentation and treatments. *Int. J. Mol. Sci.* **2017**, *18*, 441–471.

(41) Won, J.-S.; Singh, A. K.; Singh, I. Biochemical, cell biological, pathological, and therapeutic aspects of Krabbe's disease. *J. Neurosci. Res.* **2016**, *94*, 990–1006.

(42) Ferraz, M. J.; Marques, M. D.; Verhoek, M.; Strijland, A.; Mirzaian, M.; Scheij, S.; Ouairy, C. M.; Lahav, D.; Wisse, P.; Overkleeft, H. S.; Boot, R. G.; Aerts, J. M. Lysosomal glycosphingolipid catabolism by acid ceramidase: formation of glycosphingoid bases during deficiency of glycosidases. *FEBS Lett.* **2016**, *590*, 716–725.

(43) Li, Y.; Xu, Y.; Benitez, B. A.; Nagree, M. S.; Dearborn, J. T.; Jiang, X.; Guzman, M. A.; Woloszynek, J. C.; Giaramita, A.; Yip, B. K.; Elsbernd, J.; Babcock, M. C.; Lo, M.; Fowler, S. C.; Wozniak, D. F.; Vogler, C. A.; Medin, J. A.; Crawford, B. E.; Sands, M. S. Genetic ablation of acid ceramidase in Krabbe disease confirms the psychosine hypothesis and identifies a new therapeutic target. *Proc. Natl. Acad. Sci. U.S.A.* **2019**, *116*, 20097–20103.

(44) Gebai, A.; Gorelik, A.; Li, Z.; Illes, K.; Nagar, B. Structural basis for the activation of acid ceramidase. *Nat. Commun.* **2018**, *9*, 1621.

(45) Bielawska, A.; Greenberg, M. S.; Perry, D.; Jayadev, S.; Shayman, J. A.; McKay, C.; Hannun, Y. A. (1S,2R)-D-erythro-2-(N-myristoylamino)-1-phenyl-1-propanol as an inhibitor of ceramidase. *J. Biol. Chem.* **1996**, *271*, 12646–12654.

(46) Sugita, M.; Williams, J. T.; Moser, H. W. Ceramidase and ceramide synthesis in human kidney and cerebellum: description of a new alkaline ceramidase. *Biochim. Biophys. Acta, Lipids Lipid Metab.* **1975**, *398*, 125–131.

(47) Grijalvo, S.; Bedia, C.; Triola, G.; Casas, J.; Llebaria, A.; Teixidó, J.; Rabal, O.; Levade, T.; Delgado, A.; Fabriàs, G. Design, synthesis and activity as acid ceramidase inhibitors of 2-oxooctanoyl and N-oleoylethanolamine analogues. *Chem. Phys. Lipids* **2006**, *144*, 69–84.

(48) Raisova, M.; Goltz, G.; Bektas, M.; Bielawska, A.; Riebeling, C.; Hossini, A. M.; Eberle, J.; Hannun, Y. A.; Orfanos, C. E.; Geilen, C. C. Bcl-2 overexpression prevents apoptosis induced by ceramidase inhibitors in malignant melanoma and HaCaT keratinocytes. *FEBS Lett.* **2002**, *516*, 47–52.

(49) Proksch, D.; Klein, J. J.; Arenz, C. Potent inhibition of acid ceramidase by novel B-13 analogues. *J. Lipids* **2011**, *2011*, 971618.

(50) Camacho, L.; Meca-Cortés, O.; Abad, J. L.; Garcia, S.; Rubio, N.; Díaz, A.; Celià-Terrassa, T.; Cingolani, F.; Bermudo, R.; Fernández, P. L.; Blanco, J.; Delgado, A.; Casas, J.; Fabriàs, G.; Thomson, T. M. Acid ceramidase as a therapeutic target in metastatic prostate cancer. *J. Lipid Res.* **2013**, *54*, 1207–1220.

(51) Ordóñez, Y. F.; Abad, J. L.; Aseeri, M.; Casas, J.; Garcia, V.; Casasampere, M.; Schuchman, E. H.; Levade, T.; Delgado, A.; Triola, G.; Fabriàs, G. Activity-based imaging of acid ceramidase in living cells. *J. Am. Chem. Soc.* **2019**, *141*, 7736–7742.

(52) Draper, J. M.; Xia, Z.; Smith, R. A.; Zhuang, Y.; Wang, W.; Smith, C. D. Discovery and evaluation of inhibitors of human ceramidase. *Mol. Cancer Ther.* **2011**, *10*, 2052–2061.

(53) Yildiz-Ozer, M.; Oztopcu-Vatan, P.; Kus, G. The investigation of ceranib-2 on apoptosis and drug interaction with carboplatin in human non small cell lung cancer cells in vitro. *Cytotechnology* **2018**, *70*, 387–396.

(54) Cho, S. M.; Lee, H. K.; Liu, Q.; Wang, M.-W.; Kwon, H. J. A guanidine-based synthetic compound suppresses angiogenesis via inhibition of acid ceramidase. *ACS Chem. Biol.* **2019**, *14*, 11–19.

(55) Realini, N.; Solorzano, C.; Pagliuca, C.; Pizzirani, D.; Armirotti, A.; Luciani, R.; Costi, M. P.; Bandiera, T.; Piomelli, D. Discovery of highly potent acid ceramidase inhibitors with in vitro tumor chemosensitizing activity. *Sci. Rep.* **2013**, *3*, 1035.

(56) Pizzirani, D.; Pagliuca, C.; Realini, N.; Branduardi, D.; Bottegoni, G.; Mor, M.; Bertozzi, F.; Scarpelli, R.; Piomelli, D.; Bandiera, T. Discovery of a new class of highly potent inhibitors of acid ceramidase: synthesis and structure–activity relationship (SAR). *J. Med. Chem.* **2013**, *56*, 3518–3530.

(57) Diamanti, E.; Bottegoni, G.; Goldoni, L.; Realini, N.; Pagliuca, C.; Bertozzi, F.; Piomelli, D.; Pizzirani, D. Pyrazole-based acid ceramidase inhibitors: design, synthesis, and structure–activity relationships. *Synthesis* **2016**, *48*, 2739–2756.

(58) Ortega, J. A.; Arencibia, J. M.; La Sala, G.; Borgogno, M.; Bauer, I.; Bono, L.; Braccia, C.; Armirotti, A.; Girotto, S.; Ganesan, A.; De Vivo, M. Pharmacophore identification and scaffold exploration to discover novel, potent, and chemically stable inhibitors of acid ceramidase in melanoma cells. *J. Med. Chem.* **2017**, *60*, 5800–5815.

(59) Pizzirani, D.; Bach, A.; Realini, N.; Armirotti, A.; Mengatto, L.; Bauer, I.; Girotto, S.; Pagliuca, C.; De Vivo, M.; Summa, M.; Ribeiro, A.; Piomelli, D. Benzoxazolone carboxamides: potent and systemically active inhibitors of intracellular acid ceramidase. *Angew. Chem., Int. Ed.* **2015**, *127*, 495–499.

(60) Bach, A.; Pizzirani, D.; Realini, N.; Vozella, V.; Russo, D.; Penna, I.; Melzig, L.; Scarpelli, R.; Piomelli, D. Benzoxazolone carboxamides as potent acid ceramidase inhibitors: synthesis and structure–activity relationship (SAR) Studies. *J. Med. Chem.* **2015**, *58*, 9258–9272.

(61) Di Martino, S.; Tardia, P.; Cilibrasi, V.; Caputo, S.; Mazzonna, M.; Russo, D.; Penna, I.; Realini, N.; Margaroli, N.; Migliore, M.; Pizzirani, D.; Ottonello, G.; Bertozzi, S. M.; Armirotti, A.; Nguyen, D.; Sun, Y.; Bongarzone, E. R.; Lansbury, P.; Liu, M.; Skerlj, R.; Scarpelli, R. Lead optimization of benzoxazolone carboxamides as orally bioavailable and CNS penetrant acid ceramidase inhibitors. *J. Med. Chem.* **2020**, *63*, 3634–3664.

(62) Wang, Q.; Tan, X.; Zhu, Z.; Dong, X.-Q.; Zhang, X. New synthetic strategy for chiral 2-oxazolidinones derivatives via rhodium-catalyzed asymmetric hydrogenation. *Tetrahedron Lett.* **2016**, *57*, 658–662.

(63) Brown, M. L.; Cheung, M.; Dickerson, S. H.; Gauthier, C.; Harris, P. A.; Hunter, R. N.; Pacofsky, G.; Peel, M. R.; Stafford, J. A. Chemical compounds. WO 2004032882 A2, 2004.

(64) Knölker, H.-J.; Braxmeier, T.; Schlechtingen, G. A Novel method for the synthesis of isocyanates under mild conditions. *Angew. Chem., Int. Ed.* **1995**, *34*, 2497–2500.

(65) Eckert, H.; Forster, B. Triphosgene, a crystalline phosgene substitute. *Angew. Chem., Int. Ed.* **1987**, *26*, 894–895.

(66) Guha, S. K.; Wu, B.; Kim, B. S.; Baik, W.; Koo, S. TMS-OTf-catalyzed α -bromination of carbonyl compounds by N-bromosuccinimide. *Tetrahedron Lett.* **2006**, *47*, 291–293.

(67) Dementiev, A.; Joachimiak, A.; Nguyen, H.; Gorelik, A.; Illes, K.; Shabani, S.; Gelsomino, M.; Ahn, E.-Y. E.; Nagar, B.; Doan, N. Molecular mechanism of inhibition of acid ceramidase by carmofur. *J. Med. Chem.* **2019**, *62*, 987–992.

(68) Ishikawa, M.; Hashimoto, Y. Improvement in aqueous solubility in small molecule drug discovery programs by disruption of molecular planarity and symmetry. *J. Med. Chem.* **2011**, *54*, 1539–1554.

(69) Gorelik, A.; Gebai, A.; Illes, K.; Piomelli, D.; Nagar, B. Molecular mechanism of activation of the immunoregulatory amidase NAAA. *Proc. Natl. Acad. Sci. U.S.A.* **2018**, *115*, E10032–E10040.

(70) Kovalevich, J.; Langford, D. Considerations for the use of SH-SY5Y neuroblastoma cells in neurobiology. *Methods Mol. Biol.* **2013**, *1078*, 9–21.

(71) Xicoy, H.; Wieringa, B.; Martens, G. J. The SH-SY5Y cell line in Parkinson's disease research: a systematic review. *Mol. Neurodegener.* **2017**, *12*, 10–20.

(72) Kyriakou, K.; Lederer, C. W.; Kleanthous, M.; Drousiotou, A.; Malekkou, A. Acid ceramidase depletion impairs neuronal survival and induces morphological defects in neurites associated with altered gene transcription and sphingolipid content. *Int. J. Mol. Sci.* **2020**, *21*, 1607–1631.

(73) Yamanaka, T.; Kondoh, A.; Terada, M. Kinetic resolution of racemic amino alcohols through intermolecular acetalization catalyzed by a chiral Bronsted acid. *J. Am. Chem. Soc.* **2015**, *137*, 1048–1051.

(74) Dinsmore, C. J.; Mercer, S. P. Carboxylation and Mitsunobu reaction of amines to give carbamates: retention vs inversion of configuration is substituent-dependent. *Org. Lett.* **2004**, *6*, 2885–2888.

(75) Basit, A.; Piomelli, D.; Armirotti, A. Rapid evaluation of 25 key sphingolipids and phosphosphingolipids in human plasma by LC-MS/MS. *Anal. Bioanal. Chem.* **2015**, *407*, 5189–5198.